uOttawa

L'Université canadienne
Canada's university

FACULTÉ DES ÉTUDES SUPÉRIEURES ET POSTOCTORALES

uOttawa

L'Université canadienne
Canada's university

FACULTY OF GRADUATE AND POSDOCTORAL STUDIES

Giyora B. Levin

AUTEUR DE LA THÈSE / AUTHOR OF THESIS

Ph.D. (Electrical Engineering)

GRADE / DEGREE

School of Information Technology and Engineering

FACULTÉ, ÉCOLE, DÉPARTEMENT / FACULTY, SCHOOL, DEPARTMENT

Capacity Analysis of Asymptotically Large MIMO Channels

TITRE DE LA THÈSE / TITLE OF THESIS

Sergey Loyka

DIRECTEUR (DIRECTRICE) DE LA THÈSE / THESIS SUPERVISOR

CO-DIRECTEUR (CO-DIRECTRICE) DE LA THÈSE / THESIS CO-SUPERVISOR

EXAMINATEURS (EXAMINATRICES) DE LA THÈSE / THESIS EXAMINERS

Tho Le-Ngoc

Ian D. Marsland

Yongyi Mao

Abbas Yongacoglu

Gary W. Slater

Le Doyen de la Faculté des études supérieures et postdoctorales / Dean of the Faculty of Graduate and Postdoctoral Studies

CAPACITY ANALYSIS OF ASYMPTOTICALLY LARGE MIMO CHANNELS

by

Georgy Levin

The thesis submitted to the
Faculty of Graduate and Postdoctoral Studies
in partial fulfillment of the requirements for the degree of
DOCTOR OF PHILOSOPHY
in Electrical and Computer Engineering

Ottawa-Carleton Institute for Electrical and Computer Engineering,
School of Information Technology and Engineering,
University of Ottawa, Ottawa, Ontario, Canada

Your file Votre référence
ISBN: 978-0-494-48404-3
Our file Notre référence
ISBN: 978-0-494-48404-3

"In the mountains the shortest route is from peak to peak, but for that you must have long legs."

Friedrich Nietzsche, "Thus spoke Zarathustra".

ABSTRACT

Multiple-Input-Multiple-Output (MIMO) wireless communication systems have attracted an enormous interest in both academy and industry due to the potential to provide remarkable spectral efficiency by taking advantage of multipath fading instead of combating it. Analysis of classic channel models under basic assumptions has demonstrated possibility to scale up linearly the information rate by deploying multiple transmitting and receiving antennas within the same frequency bandwidth. Recent works show that the achievable performance of practical MIMO systems depends heavily on the underlying fading distribution and system configuration. The spectral efficiency may severely degrade due to the high correlation between multipath components, channel rank deficiency or power imbalance.

The objective of this thesis is to study the capacity of correlated, rank-deficient and full-rank MIMO channels. While in many cases the exact capacity expressions are complicated and do not allow for significant insight, an asymptotic approximation for a large number of antennas is used to obtain simpler and well tractable results for a broad class of MIMO channels. Starting from the single keyhole channel as a basic and simple model of a rank-one MIMO channel, the analysis is extended to a family of higher-rank channels (including also the canonical full-rank Rayleigh-fading one) via a transition model which includes a number of statistically independent keyholes (multi-keyhole channels). It is shown that under certain mild conditions on correlation, the outage capacity distribution of the single keyhole and multi-keyhole channels is asymptotically Gaussian. The general conditions and propagation-based implications of the convergence are studied. In some cases, the asymptotic outage capacity distribution follows closely the exact one for a reasonably small number of transmit and receive antennas.

A number of applications of the asymptotic theory are discussed. (i) A new scalar measure of correlation and power imbalance is introduced to quantify the impact of correlation on the capacity and evaluate effective degrees of freedom in MIMO channels. The measure is simple, well tractable and full-ordering (any two channels can be compared). (ii) Finite SNR size-asymptotic diversity-multiplexing trade-off (DMT) is analyzed for the multi-keyhole channels. Unlike the SNR-asymptotic DMT of Zheng and Tse, the size-asymptotic one accurately represents the effect of correlation and power imbalance on

the capacity. (iii) Telatar's conjecture is proven for multi-keyhole channels with a large number of antennas. (iv) The best multipath angular density, which maximizes the asymptotic capacity of a broad class of MIMO channels with linear uniform antenna arrays, is derived. The density is non-uniform, which implies that the popular Clarke's (Jakes) model does not represent the best case scenario.

Using the rigorous methods of hypothesis testing, it is demonstrated that the outage capacity distribution of some measured 5.2GHz indoor MIMO channels is statistically Gaussian with a reasonable significance level already for two antennas at each end. The latter can serve as an empirical validation of the obtained theoretical results and implies that the asymptotic analysis with respect to the number of antennas not only offers a significant insight and simplification, but also can be applied to realistic systems of a moderate size.

ACKNOWLEDGEMENTS

I wish to express my deepest gratitude for the guidance, support and constructive criticism to my thesis supervisor Dr. Sergey Loyka, whose elegant way of approaching problems has considerably influenced my thinking. I am indebted to Dr. Peter Galko from the University of Ottawa for many helpful suggestions, Dr. Vidmantas Bentkus from the Vilnius University for valuable comments on Central Limit Theorems, Dr. Ernst Bonek and his team at the Vienna University of Technology for kindly allowing me to use their measurements of MIMO channels.

I thank my parents, parents in law, my sister and friends for their support and encouragement during the course of this thesis. Finally, I thank my adorable children Polina and Michael and my dear wife Tania, who stood by me during frustrating and hard times, and without whom this work would not have been completed.

CONTENTS

LIST OF ACRONYMS

AOA: Angle of Arrival

AWGN: Additive White Gaussian Noise

BER: Bit Error Rate

BLER: Block Error Rate

BS: Base Station

CDF: Cumulative Distribution Function

CF: Characteristic Function

CSI: Channel State Information

FRMK: Full Rank Multi-Keyhole

IND: Independent

LHS: Left Hand Side

LOS: Line of Sight

MC: Monte-Carlo

MIMO: Multiple Input Multiple Output

MISO: Multiple Input Single Output

MRC: Maximum Ratio Combining

MU: Mobile User

PDF: Probability Density Function

PSK: Phase Shift Keying

QAM: Quadrature Amplitude Modulation

RDMK: Rank Deficient Multi-Keyhole

RHS: Right Hand Side

Rx: Receiver

SER: Symbol Error Rate

SIMO: Single Input Multiple Output

SISO: Single Input Single Output

SNR: Signal to Noise Ratio

STBC: Space Time Block Coding

Tx: Transmitter

UIU: Unitary Independent Unitary

ULA: Uniform Linear Array

LIST OF SYMBOLS

Latin:

$\mathbf{A}$:	Diagonal matrix of keyhole complex gains
A_k:	Coefficients of partial fraction decomposition
a_k:	Complex gain of k^{th} keyhole
b:	Number of bits per feedback channel use
$\mathbf{C}$:	Covariance matrix
C:	Instantaneous capacity
C_1:	Instantaneous capacity per Rx antenna
$\tilde{C}$:	Normalized instantaneous capacity
$\overline{C}$:	Mean (ergodic) capacity
$C_{\max}$:	Maximal capacity per Rx antenna
D	Distance between a pair of antennas
d:	Antenna spacing in ULA (Chapter VII)
$d(r)$:	Diversity gain vs. multiplexing gain
$d'_\gamma(r)$:	Differential diversity gain vs. multiplexing gain
$F_X(x)$:	Cumulative density function of a random variable X
$f_X(x)$:	Probability density function of a random variable X
$f(\mathbf{k})$	Multipath wave-number density
$f_\theta(\theta)$:	Multipath angular density
$f_{\theta\phi}(\theta,\phi)$:	Joint multipath angular density
$f_\psi(\psi)$:	Density of phase difference between two adjacent antennas
$\mathbf{g}$ (either $\mathbf{g}_t$ or $\mathbf{g}_r$):	Zero-mean complex vector with independent entries
g:	Scheduling gain
$\mathbf{H}$:	MIMO channel matrix

$\mathbf{H}_w$:	i.i.d. circular symmetric Gaussian matrix
$\tilde{\mathbf{H}}$:	Random matrix with independent entries
$\mathbf{H}_r$:	Matrix of complex channel gains from Tx end to keyholes
$\mathbf{H}_t$:	Matrix of complex channel gains from keyholes to Rx end
H_0:	Null hypothesis
H_1:	Alternative hypothesis
$\mathbf{h}$ (either $\mathbf{h}_t$ or $\mathbf{h}_r$):	Vector of channel complex gains from Tx (Rx) end to a keyhole
$\mathbf{h}_k$ (either $\mathbf{h}_{tk}$ or $\mathbf{h}_{rk}$):	Vector of channel complex gains from Tx (Rx) end to kth keyhole
$\mathbf{I}$:	Identity matrix
$\mathbf{K}$:	Correlation matrix without power imbalance component
K:	Number of network users
$\mathbf{k}$	Wave-vector
M:	Number of keyholes
n (either n_t or n_r):	Number of antennas (at either Tx or Rx end)
n_{eff}:	Number of efficient degrees of freedom
$\mathbf{P}$:	Power imbalance matrix
P_{out}:	Outage probability
$P_e(M)$:	Symbol error rate vs. modulation level M
P_T:	Total transmitted power
P_R:	Total received power
$\mathbf{Q}$:	Input covariance matrix
$\mathbf{R}$ (either $\mathbf{R}_t$ or $\mathbf{R}_r$):	Correlation matrix (at either Tx or Rx end)
$\mathbf{R}_k$ (either $\mathbf{R}_{tk}$ or $\mathbf{R}_{rk}$):	Correlation matrix (at either Tx or Rx end) associated with kth keyhole
R:	Transmission rate
$R_z(\delta)$, $R_\Delta(\delta)$:	Convergence rate given δ
R_z, R_Δ:	Convergence rate
$\underline{R}$:	Vector representing the measure of correlation and power imbalance

$R(x)$:	Correlation function
r (either r_t or r_r):	Correlation parameter (at either Tx or Rx end), also multiplexing gain (Chapter VIII, Section 8.1)
T_n:	Test statistics
$\mathbf{U}$ (either $\mathbf{U}_t$, $\mathbf{U}_r$, $\mathbf{U}_T$ or $\mathbf{U}_R$):	Eigenbasis matrix (at either Tx or Rx end)
$\mathbf{u}$ (either $\mathbf{u}_t$, $\mathbf{u}_r$):	Eigenvectors
$Z_n(\delta)$:	Lyapounov ratio

Greek:

α:	Equivalent scalar keyhole channel power gain, also miss probability
β (either β_t or β_r):	Equivalent scalar channel power gain (at either Tx or Rx end), also false alarm probability
$\mathbf{\Gamma}$ (either $\mathbf{\Gamma}_t$ or $\mathbf{\Gamma}_r$):	MIMO channel correlation matrix
γ_0:	Average SNR (either per Rx antenna or total at Rx end)
γ_{eff}:	Effective average SNR
θ:	Elevation angle
λ (either λ^t or λ^r):	Vector of eigenvalues of correlation matrix (at either Tx or Rx end)
λ_k (either λ_k^t or λ_k^r):	*k*th eigenvalues of correlation matrix (at either Tx or Rx end)
$\lambda(u)$:	Spectrum of Toeplitz matrix
μ:	Asymptotic mean of instantaneous capacity
ν:	Efficiency of using antennas, also granularity
σ^2:	Asymptotic variance of instantaneous capacity
$\Upsilon(n_t, n_r)$:	Total measure of correlation and power imbalance at Tx and Rx ends
$\Phi_X(\omega)$:	Characteristic function of a random variable X
ϕ:	Azimuth angle
$\Psi(k)$:	Measure of correlation and power imbalance at Tx end

CHAPTER I: INTRODUCTION

1.1. Multi-Antenna Wireless Communications

The future generations of wireless communication systems are designated to offer high data-rates under tight power, spectrum and complexity limits. To meet these objectives, fundamental changes in system configuration and signal processing techniques are required to enable new and effective ways of signal transmission and reception. The Multiple-Input-Multiple-Output (MIMO) architecture satisfies many of these demands. Analysis of classic fading MIMO channels under the assumption of independent and rich scattering has demonstrated that wireless systems are able to achieve remarkable spectral efficiency by deploying a number of antennas transmitting and receiving within the same frequency bandwidth [103], [25]. The techniques, which use multiple antennas for spatial diversity combining, are not new and have been used for many years to combat multipath fading [34]. The idea behind the modern MIMO systems is to take advantage of multipath fading instead of combating it. It is possible, in this case, to scale up the spectral efficiency linearly with the number of antennas, in contrast to the classic combining techniques, where the information rate per unit bandwidth can be increased only logarithmically [18]. The exceptional increase in spectral efficiency of MIMO systems has ignited research activity in many different directions including capacity analysis, space-time coding, modulation techniques, modeling of propagation environments suitable for multi-antenna systems, etc. It is now widely recognized that the performance of practical MIMO systems depends heavily on the channel conditions such as the underlying multipath distribution, spatial correlation, power imbalance and antenna configuration.

Due to the enormous interest in this area, a number of journal special issues are dedicated solely to MIMO systems [3], [95], [96], [31]. The MIMO architecture has been already incorporated in a set of standards such as IEEE 802.11 (Wireless Local Area Network), IEEE 802.15 (Wireless Personal Area Network) and IEEE 802.16 (Wireless Metropolitan Area Network). In addition to these on-going standardization efforts, industrial support has been granted for this research. For instance, a number of

industrial alliances and consortiums such as WiMax [113], WiFi [112], Bluetooth [104] and WINNER [114], which include world leading communication companies, promote the compatibility and interoperability of broadband wireless products based upon the MIMO architecture.

Although there has been much recent progress in the area, many problems still remain open. In particular, the achievable performance and corresponding configuration of MIMO systems have not been sufficiently investigated in many realistic propagation environments. Understanding these issues is a key to the successful implementation of the MIMO architecture in the future.

1.2. Motivation and Prior Work

One of the major performance characteristics of a MIMO channel is its capacity, which gives the ultimate upper limit on the error-free information rate. Capacity represents an important information-theoretic bound which establishes a benchmark for performance of practical systems and often provides analytical tools to maximize the data rate under different channel conditions [18], [26]. For time-variant, fading channels there are multiple capacity definitions including mean (ergodic), outage and delay-limited capacity. An excellent tutorial on the fading channel capacity with single transmit (Tx) and receive (Rx) antennas is given in [9]. This thesis focuses on the mean and outage capacities as the two most general characteristics of MIMO fading channels. The mean capacity is defined as the maximum mutual information between the channel inputs and outputs averaged over all possible channel realizations. This measure upperbounds the error-free information rate supported by ergodic channels, i.e. the channels that vary randomly during transmission time and the variations are ergodic [106]. The outage capacity, in turn, is a more relevant performance measure of non-ergodic channels, and it gives the upper limit on the error-free information rate with a given probability of outage [103], [25], [106]. The mean and outage capacities are usually considered for three broad cases: (i) when the channel state information (CSI) is known at both transmit and receive ends, for example [103], [100], [69], (ii) when CSI is available at the Rx end only, for example [25], [27], [32], (iii) when CSI is not known at both Tx and Rx ends [116]. Apparently, the channel capacity in case (i) is the highest, however in many practical situations it does not

provide an adequate performance measure since a system with an "informed" transmitter is not always feasible as it requires an additional feedback channel, which is not always available, for example due to the bandwidth limitations, or the available feedback channel is not capable to track channel variations and/or to update the transmitter fast enough [25], [116]. A thorough review on capacity achieving transmission and receiving strategies in MIMO channels when the SCI is available at both Tx and Rx ends, Rx end only, or not available at all can be found in [29].

The mean and outage capacities of various MIMO channels have been extensively studied during the last decade. Many analytical and empirical results have been obtained. The Rayleigh, Rice and Nakagami distributed MIMO channels have been well investigated and closed-form expressions for their capacity are now available. For example, the mean and outage capacity of Rayleigh-fading channels were studied in [40], [12]. Several results on the mean capacity of Rayleigh and Rice MIMO channels in low-power (wideband) regime can be found in [67]. The exact expressions for the mean capacity and the outage capacity distribution of semi and double correlated Rayleigh-fading channels are derived in [13], [99]. The capacity analysis along with several capacity bounds for Rice and Nakagami MIMO channels are given in [41], [35], [38].

Much research has been done to evaluate the impact of spatial correlation on the capacity of Rayleigh and Rice MIMO channels. The impact of correlation on the mean and outage capacity of Rayleigh-fading channels has been studied in [100], [10], [33], [62]. Capacity bounds on the mean capacity of correlated Rice MIMO channels have been obtained in [71]. The impact of correlation on the outage capacity of generalized full-rank MIMO channels with unitary-independent-unitary (UIU) structure has been analyzed in [109]. A number of effective channel correlation models have been introduced. The Kronecker correlation model, which significantly simplifies the analysis and modeling of MIMO channels by splitting the effect of correlation between the transmit and receive ends, is proposed and experimentally validated in [37]. Due to its simplicity and tractability, the model has been used in many theoretical analyses [13], [99], [69]. In some cases, however, the Kronecker model underestimates the channel capacity [81]. A more accurate but also more complex correlation model, which takes in account the joint correlation of both ends has been proposed in [111].

In general, the impact of correlation on both mean and outage capacities cannot be characterized in a simple way. While in some cases the correlation is beneficiary [10], [77], [82], in some others it may significantly reduce the capacity of Rayleigh-fading channels [100], [10], [62]. SNR and the correlation structure of the MIMO channel are the key factors in determining the effect of correlation in each particular scenario [10], [77]. To evaluate the impact of correlation and to take in account the correlation structure of a MIMO channel, a number of correlation measures have been proposed. A simple and well tractable measure of correlation has been proposed in [33] as a value reciprocal to the measure of spatial diversity available in Rayleigh-fading channels. It remains unclear, however, whether this measure reflects the impact of correlation on the capacity of the corresponding channels. Another measure of correlation, which is based on the majorization theory, is proposed for the Rayleigh channels with a single Tx or Rx antenna in [10]. The advantage of this measure is that it clearly characterizes the impact of correlation on the mean and outage capacities. However, only a subset of all possible channel correlation structures is measurable in this case, i.e. the measure does not posses a full ordering property [10].

While the exact capacity expressions for Rayleigh and Rice MIMO channels are complicated and usually do not allow for significant insight, a number of theoretical analyses propose simple asymptotic approximations of the mean and outage capacities for a large number of antennas. For example, the asymptotic expressions for the mean and outage capacity distribution of uncorrelated Rayleigh-fading channels are derived in [32]. The capacity of correlated narrow and wide-band Rayleigh channels has been considered in [75], [74], [69]. The asymptotic capacity approximations for Ricean MIMO channels have been analyzed in [35]. The asymptotic outage capacity distributions of generic full-rank uncorrelated and unitary-independent-unitary (UIU) MIMO channels have been obtained in [108], [90], [109]. The common conclusion in all these works is that the outage capacity distribution of a broad class of MIMO channels is asymptotically Gaussian. This indicates that the normal distribution has a high degree of universality for the analysis of MIMO capacity in general. In some cases the discrepancy between the exact capacity distribution and its Gaussian approximation has been found practically indistinguishable already for a moderate number of antennas [101]. An excellent survey of different approaches in asymptotic analysis of MIMO capacity can be found in [109].

While the limiting distribution of the outage capacity is known in many cases, much less attention has been paid to the rigorous analytical evaluation of the accuracy of the asymptotic (Gaussian) approximation when the number of antennas is finite. Some initial results which demonstrate the convergence rate of the outage capacity distribution of generalized full-rank uncorrelated MIMO channels to the Gaussian one are presented in [108]. The convergence rate of the corresponding mean capacity to its asymptotic value is bounded from above in [90]. The convergence rate and appropriate bounds for other types of channels, especially correlated ones, are still to be found.

Another important direction in the current research is the effects of antenna design and multipath angular density on the MIMO capacity. The study of these effects may help to find the optimal configuration of antenna arrays in a particular propagation environment, ways to reduce spatial correlation, and more generally, it may reveal the relationship between the information and electromagnetic theories (for more details about this relationship see [56]). Certain progress in this area has been made in [11], [73], [94], [64], [27]. An asymptotic approach has been used in [87], where by letting the number of antennas at Tx end to go to infinity, the capacity saturation effects in circular antenna arrays were studied for Rayleigh channels correlated at either Tx or Rx end. However, one of the problems that has not been addressed yet, is finding the best multipath angular density that maximizes the capacity of a MIMO channel with a given antenna configuration.

Much interest has been recently paid to the diversity-multiplexing trade-off (DMT) in MIMO channels [117], [107]. A simple, well tractable expression, which has provided a deep insight into the trade-off between the spectral efficiency (spatial multiplexing gain) and the error rate (diversity order) has been derived in [117] for Rayleigh-fading channels at high SNR regime ($SNR \to \infty$). It is now widely recognized that the SNR-asymptotic DMT overestimates the channel performance for finite SNR, especially when the diversity gain is high (low error rate), and/or the number of antennas is large [76], [58], [59]. A more accurate expression for the DMT in Rayleigh-fading channels with finite SNR has been obtained in [76]. This expression is based on the lower bound on the corresponding outage capacity distribution. Unlike the SNR-asymptotic DMT of Zheng and Tse [117], the trade-off in [76] is not a closed-form and has a high degree of complexity without much insight. For example, the impact of

correlation on the DMT is difficult for immediate evaluation. Recently, the DMT has been generalized for a broad class of MIMO channels (not necessarily Rayleigh-fading) using asymptotic approximation of outage capacity distribution when the number of antennas is large [58], [59]. The size-asymptotic DMT is compact, well tractable and approximates with reasonable accuracy the "true" DMT for low to moderate SNR. In contrast to Zheng and Tse DMT, the accuracy of the size-asymptotic one increases with the number of antennas. Due to the simplicity, the size-asymptotic DMT allows for significant insight. In particular, it clearly demonstrates that spatial correlation decreases the diversity gain of a channel at any given transmission rate. While the latter supports the intuition, this fact does not follow from the DMT in [117] due to the SNR-asymptotic approximation.

The theoretical results mentioned above have been validated in a number of measurement campaigns such as, for example, the measurements of 5.2GHz indoor and outdoor MIMO channels [79], [80], [72], the measurements undertaken in Manhattan at 2.6GHz [16], experimental investigation of MIMO channel properties in indoor picocell environments [37], and some others. However, most of the empirical results on MIMO capacity and other channel parameters were not a subject to a rigorous statistical analysis. Rather visual comparison of the measured data plots to the corresponding theoretical models was done with no strictly defined criteria. Such an approach can neither account for the statistical error due to the limited amount of data available (this is especially pronounced for measured channels, where the number of data points measured at single frequency in a particular environment is typically limited to 100–200 at most [79]), nor for the confidence probability of the conclusions. As a result, different conclusions were reported by different authors. For example, the validity of the Gaussian approximation of the outage capacity of MIMO channels with a finite number of antennas has not been a subject to the rigorous statistical analysis.

Unlike other channels, the keyhole MIMO channel has not been studied in sufficient depth yet. This channel was theoretically predicted in [15], [14] as a multipath environment, where certain propagation mechanisms reduce the channel rank. It can be represented as a concatenation of two multipath sub-channels separated by a keyhole whose dimensions are much smaller than the wavelength. The presence of the keyhole degenerates the channel, i.e. its rank is one regardless of the number of Tx and Rx antennas

[15]. Consequently, the capacity of such channels deteriorates significantly compared to the full rank Rayleigh channels with the same number of Tx and Rx antennas. There is a significant interest in keyhole channels in recent literature as they may appear in some practically important propagation scenarios. [14] suggests a keyhole scenario, where the link between Tx and Rx ends is due to the 1-D diffraction only. An example of the keyhole realization is given in [27]. It shows that when the scattering around Tx and Rx ends causes local fading, the channel rank may be low if the scattering rings are too small comparing to the separation between the transmitter and the receiver,. A number of experimental works supports the theoretical predictions above. For instance, measurements of the channel capacity along a hallway, reported in [89] shows the decrease in capacity with distance, which is explained by the keyhole effect in the hallways. The experimental verification of the theoretical capacity reported in [115] reveals the keyhole effect in a controlled free space environment when the separation between the Tx and Rx antennas is large. Another convincing experimental evidence of a keyhole channel is presented in [5], [4], where it is shown, in particular, that the keyhole model describes well wireless channels when the wave propagates via waveguides.

The keyhole channel can also be useful to model amplify-and-forward relay networks [39], where the keyhole represents a relay node rather than a propagation effect. However, this apparent similarity between the network structure and the keyhole propagation environment has not been elaborated in the literature yet. The significance of a keyhole MIMO channel is also due to its unique position as a channel with only one non-zero eigenmode, which describes the worst-case MIMO propagation scenario. Hence, in addition to the practical importance, the study of keyhole channels is necessary, as it reveals how well a system performs in channels other than the Rayleigh ones and how much the results established for the classic Rayleigh-fading channels apply elsewhere.

Despite the interest in keyhole channels, the literature dealing with their information-theoretic analysis is rather limited. Closed-form expressions for the mean capacity of a spatially uncorrelated keyhole channel are presented in [97]. A tight lower bound and approximations of the mean capacity of a spatially correlated keyhole channel are proposed in [20] and [62] respectively. Performance analysis of space-time block codes (STBC) over an uncorrelated keyhole channel is given in [98], [91], where, in

particular, the moment generating function of the instantaneous SNR at the decoder output is derived, and SER for various codes is evaluated. Tight lower and upper Bonferroni-type bounds on this SER and the corresponding BER are obtained in [105]. The diversity order of uncorrelated keyhole channels has been investigated in [92].

Many theoretical and practical questions pertaining to keyhole channels still remain open. For example, keyholes channels with subchannels other than classic Nakagami-*m* and Rayleigh-fading have not been considered. Outage capacity distribution, impact of correlation, and diversity-multiplexing trade-off in keyhole channels have not been investigated. Additional study is required to reveal the optimal transmission and receiving strategies in keyhole channels, and whether the corresponding strategies developed for the canonic Rayleigh-fading channels are robust in the keyhole environment. Thorough comparison analysis between the capacity and BER in keyhole and Rayleigh-fading channels has not been conducted. Even though the existence of a transition model between the rank-one and full-rank MIMO channels has been suggested in [27], there is no a unifying theory that establishes a theoretical link between the rank-one keyhole and classic full-rank Rayleigh-fading MIMO channels.

1.3. Thesis Organization and Contribution

Below we summarize the original contribution contained in Chapters III-IX.

- *Chapter III: Capacity of Keyhole MIMO Channels*

Closed-form expression for the outage capacity distributions of correlated keyhole MIMO channels is derived. A particular but common case where the correlation matrices at the Tx and Rx ends are non-singular and have distinct eigenvalues is considered. It is shown that the keyhole channel distribution is different from that of traditional diversity channels, which also have rank one. However, when the number of either Tx or Rx antennas is large, the keyhole channel capacity achieves asymptotically that of the Rayleigh diversity channel with a single Tx or Rx antenna respectively. The capacity distribution of the keyhole channel is upper-bounded by those of the equivalent Rayleigh diversity channel. For a small number of antennas, spatial correlation results in the loss of SNR and consequently in smaller outage

capacity.

For a large number of antennas, a compact and well tractable asymptotic approximation of the outage capacity distribution of keyhole MIMO channels is derived. It is shown that under certain mild conditions on correlation and despite the degenerate nature of the keyhole channels, the capacity is asymptotically Gaussian; the mean is affected by average SNR and is independent of correlation, while the correlation has a dominant effect on the variance. High correlation increases the variance which results in smaller capacity at low outage probabilities. Simulations show that the asymptotic outage capacity distribution follows closely the exact one for a reasonably small number of Tx and Rx antennas.

- *Chapter IV: Capacity of Multi-Keyhole Channels*

A mathematical model of a multi-keyhole channel, which includes a number of statistically independent keyholes, is proposed to generalize and expand the application range of the single keyhole channel. The multi-keyhole channels are classified and studied in detail. In particular, it is shown that the proposed model is complementary to that in [27], as it describes a sparse double-scattering environment, where the scatterers (keyholes) are located far apart from each other. The different statistical behavior of rank-deficient and full-rank multi-keyhole channels is stressed out. The multi-keyhole channel is shown to be a transition model that links the rank-one keyhole and full-rank Rayleigh-fading channels.

When a number of either Tx or Rx antennas are large, there is an equivalent Rayleigh fading channel, such that the outage capacity of both the multi-keyhole channel and the Rayleigh one are asymptotically equal. When a number of both Tx and Rx antennas is large, the outage capacity distribution of both rank-deficient and full-rank multi-keyhole channels is asymptotically Gaussian. This fact implies that Gaussian distribution of outage capacity is a common asymptotic property of a broad class of MIMO channels.

- *Chapter V: Measure of Correlation and Power Imbalance*

A new scalar measure of channel correlation and power imbalance is introduced based on the asymptotic analysis of multi-keyhole channel capacity. The measure accounts for the total correlation and

power imbalance between multiple antennas and simultaneously affects the asymptotic outage capacity distribution of the MIMO channel; the higher the measure, the lower the capacity at low outage probabilities. It is shown that the proposed measure is compatible with other measures of correlation proposed for Rayleigh-fading channels [10], [33], and therefore, describes the impact of correlation and power imbalance on the capacity of a broad class of MIMO channels. The advantages of the proposed measure are simplicity (no eigenvalue decomposition is required), full ordering property (any two channels can be compared without exceptions) and tractability (it separates the effect of correlation and power imbalance). Analysis of this measure indicates that the effects of channel correlation and power imbalance are independent, and their total negative impact on the outage capacity is characterized by the sum of the two corresponding measures. In this sense, the impact of the power imbalance can be as bad as that of the correlation. Simulations show that the proposed measure of correlation and power imbalance provides an adequate characterization of the impact of correlation and power imbalance on the capacity of the rank-deficient and full rank multi-keyhole channels with a moderate number of antennas.

- *Chapter VI: Asymptotic Normality of Rayleigh Channel Capacity*

General Lyapounov-type condition for the asymptotic normality of Rayleigh fading channel capacity is discussed in detail, and some physical implications of this condition are highlighted. In particular, the convergence rate to the Gaussian distribution is evaluated. In many cases this rate is bounded from below by $1/2$, i.e. the convergence is not slower than $1/\sqrt{n_t}$, where n_t is the number of transmit antennas.

The presented analysis provides theoretical tools to evaluate the accuracy of the Gaussian approximation when the number of antennas is finite. It is shown that for the channels with Toeplitz correlation structure, the Lyapounov-type condition is always satisfied, if the correlation decays faster than $1/\sqrt{D}$, where D is the distance between the antennas. A number of popular correlation models is considered to verify this result.

- *Chapter VII: What is the Best Angular Density in MIMO Channels?*

The framework proposed in [109] is generalized and it is shown that when the number of antennas is large, the asymptotic outage capacity of a broad class of MIMO channels (not necessarily Rayleigh-fading) with an arbitrary correlation structure (not necessarily UIU [109]) does not depend on a particular channel distribution, but only on the correlation between antennas. Special cases include classic i.i.d. Rayleigh-fading channel [103], [25], Rayleigh-fading channel with separable (Kronecker) correlation structure [37], and i.i.d. zero-mean (not necessarily Rayleigh-fading) channel with finite fourth-order statistics considered in [[108], Theorem 2.76].

Using Szego Theorem [30], the multipath angular density that eliminates the correlation between antennas and thus maximizes the asymptotic capacity of this class of MIMO channels is derived, when the receive uniform linear array (ULA) of isotropic antennas and the multipath are located on a plane (2-D). The capacity-maximizing density is non-uniform. Since the asymptotic capacity approximates reasonably well the exact one when the number of antennas is moderate, it is concluded that the popular Clarke's (Jakes) model [34] does not represent the best case propagation scenario. For the optimal multipath angular density, a simple expression that links the measure of correlation and power imbalance (introduced in Chapter V) to the distance between antennas, is obtained. The expression explains the oscillatory behavior of the capacity as a function of antenna spacing.

The study is extended to the multipath distributed in the 3-D space (volume). It is shown that the capacity-maximizing angular density in this case is also non-uniform. The latter provides guidelines for an optimal location of a ULA antenna in a 3-D multipath environment

- *Chapter VIII: Applications of Asymptotic Analysis of Outage Capacity Distribution*

Section 8.1: Finite SNR size-asymptotic diversity multiplexing trade-off (DMT) is obtained for the multi-keyhole channels. It is shown that the DMT adequately characterizes the impact of correlation on the capacity.

Section 8.2: A simple yet reasonably-accurate estimate of symbol error rate (SER) in a fading keyhole channel for a variety of modulation formats is obtained. The estimate becomes especially

accurate when the number of antennas is large, and/or the modulation order is high.

Section 8.3: Telatar's Conjecture [103] is proven for the multi-keyhole channels with a large number of antennas.

Section 8.4: A motivation for the Kronecker correlation model [37] is provided by considering a Rayleigh-fading channel as a multi-keyhole one with a large number of keyholes. It is demonstrated that the Kronecker structure of the correlation is justified, when, for example, there is a physical separation (such a screen) of the correlation-forming mechanism into transmitter (Tx) and receiver (Rx) parts.

Section 8.5: Scheduling gain and the required feedback rate in wireless networks is evaluated assuming that the propagation environment is described by the multi-keyhole channel with a sufficient number of antennas so that the asymptotic Gaussian approximation of channel outage capacity applies. It is shown that both the scheduling gain and the feedback rate increase with the measure of correlation and power imbalance at Tx end and decrease with SNR.

- *Chapter IX: Statistical Analysis of Measured MIMO Channels*

A rigorous mathematical framework for analyzing the statistical characteristics of measured MIMO channels in general and their outage capacity distribution in particular is proposed. The accuracy of a number of statistical tests and their suitability for the statistical analysis is assessed. The tests are first applied to the correlated Rayleigh-fading channels obtained by the Monte-Carlo simulation, and then to the measured 5.2GHz indoor MIMO channels [79], [80]. The rigorous statistical analysis shows that the measured channels is frequency selective Rayleigh-fading with significant correlation (>0.7) at the Rx end. The outage capacity distribution of some measured channel is statistically Gaussian with a reasonable significance level already for two antennas at each end. Even though this section does not aim to verify the validity of the multi-keyhole channel model proposed in Chapter IV, the fact that the outage capacity distribution is statistically Gaussian for a reasonably small number of antennas implies that the asymptotic analysis with respect to a number of antennas not only offers a significant insight, but also can be applied to realistic systems of a moderate size.

1.4. Publications

- *Journal Papers*:

[1] G. Levin, S. Loyka, "On the Outage Capacity Distribution of Correlated Keyhole MIMO Channels", *IEEE Trans. on Inform. Theory*, vol.54, no.7, pp. 3232-3245, July 2008.

[2] G. Levin, S. Loyka, "Comments on Asymptotic Eigenvalue Distributions and Capacity for MIMO Channels under Correlated Fading", *IEEE Transactions on Wireless Communications*, vol.7, no.2, pp. 475-479, February 2008.

[3] S. Loyka, G. Levin, "On Physically-Based Normalization of MIMO Channel Matrices", *submitted to IEEE Trans. on Inform. Theory*, 2007, (13 double space pages, under second review).

[4] G. Levin, S. Loyka, "From Multi-Keyholes to Measure of Correlation and Power Imbalance in MIMO Channels", *submitted to IEEE Trans. on Inform. Theory*, 2007, (36 double space pages, under first review).

- *Conference Papers*:

[5] G. Levin, S. Loyka, "What is the Best Angular Density of Multipath in MIMO Channels?", *submitted to IEEE International Symposium on Information Theory (ISIT2008).*

[6] S. Loyka, G. Levin, "On Finite-SNR Diversity-Multiplexing Tradeoff", *in Proc. 2007 IEEE Global Communications Conference (Globecom2007)*, Washington, DC, Nov. 2007.

[7] G. Levin, S. Loyka, "On Asymptotic Outage Capacity Distribution of Correlated MIMO Channels", *in Proc. the International Symposium on Signals, Systems and Electronics 2007 (ISSSE 2007)*, Montreal, QC, July-Aug., 2007.

[8] S. Loyka, G. Levin, "Diversity-Multiplexing Tradeoff via Asymptotic Analysis of Large MIMO Systems", *in Proc. 2007 IEEE International Symposium on Information Theory (ISIT2007)*, Nice, France, June 2007.

[9] G. Levin, S. Loyka, "Multi-Keyhole MIMO Channels: Asymptotic Analysis of Outage Capacity", *in Proc. IEEE 2006 ISIT, 2006 IEEE International Symposium on Information Theory*, Seattle, WA, July 2006.

[10] G. Levin, S. Loyka, "Multi-Keyholes and Measure of Correlation in MIMO Channels", *in Proc. QBSC'06, 23rd Biennial Symposium on Communications,* Kingston, ON, May-June 2006.

[11] G. Levin, S. Loyka, "On Correlated Keyhole MIMO Channels: SNR and Outage Capacity Distributions", *in Proc. IEEE CCECE'06, IEEE Canadian Conference on Electrical and Computer Engineering 2006*, Ottawa, ON, May 2006.

[12] G. Levin, S. Loyka, "On the Outage Capacity Distribution of Correlated Keyhole MIMO Channels", *in Proc. IEEE WCNC'06, IEEE Wireless Communications and Networking Conference 2006,* Las Vegas, NV, April 2006.

[13] G. Levin, S. Loyka, "Capacity Distribution of a Correlated Keyhole Channel", *in Proc. CWIT'05, Canadian Workshop on Information Theory*, Montréal, QC, June 2005.

[14] G. Levin, S. Loyka, "Statistical Approach to MIMO Capacity Analysis in a Fading Channel", *in Proc. IEEE VTC'04-Fall, IEEE Vehicular Technology Conference,* , Los Angeles, CA, Sep. 2004.

[15] G. Levin, S. Loyka, "Statistical Analysis of a Measured MIMO Channel", *in Proc. IEEE CCECE'04, IEEE Canadian Conference on Electrical and Computer Engineering 2004*, Niagara Falls, ON, May 2004.

CHAPTER II: LITERATURE REVIEW

This chapter conducts a review of the recent research on MIMO capacity. A number of capacity definitions, which provide an adequate channel measure in different propagation environments, are considered. A literature survey of exact (finite number of antennas) and asymptotic (arbitrary large number of antennas) capacities of uncorrelated, correlated Rayleigh-fading and generic MIMO channels is presented under the assumption that the channel state information (CSI) is available at the receive but not the transmit end. A number of correlation models, which have been proven to characterize sufficiently well the structure of MIMO channels, are reviewed. Finally, the mathematical model of the keyhole channel is introduced, and the theoretical background essential for the analysis in the following chapters is given.

2.1. MIMO Channel Capacity

Consider a MIMO channel with n_t Tx and n_r Rx antennas (see Fig. 2.1). Let $\mathbf{H}$ be the channel transfer matrix with elements H_{km}, $k=1...n_r$; $m=1...n_t$, representing a complex channel gain from the m^{th} transmit to the k^{th} receive antenna. There are three general types of $\mathbf{H}$ [103]:

(i) $\mathbf{H}$ is a deterministic matrix. In this case, the capacity per unit bandwidth of a frequency flat MIMO channel with additive spatially white Gaussian noise and CSI available at the Rx end only is given in natural units (*nats*) by

$$C = \ln\left(\det[\mathbf{I} + \gamma_0 \mathbf{H}\mathbf{H}^H / n_t]\right), \tag{2.1}$$

where $(\ )^H$ denotes the Hermitian transpose, $\det[\ ]$ is the determinant, $\mathbf{I}$ is $[n_r \times n_r]$ identity matrix and γ_0 is the average SNR per Rx antenna.

(ii) $\mathbf{H}$ is an ergodic random matrix. From [103]

$$C = E\left\{\ln\left(\det[\mathbf{I} + \gamma_0 \mathbf{H}\mathbf{H}^H / n_t]\right)\right\}, \tag{2.2}$$

where $E\{\cdot\}$ denotes expectation.

(iii) $\mathbf{H}$ is a non-ergodic matrix chosen randomly at the beginning and held constant all the time. In the classical Shannon sense, the channel capacity in this case is generally zero, since there is always non-zero probability (outage probability) that $\mathbf{H}$ may have such values that for any given γ_0 no code would be able to provide arbitrary small probability of error for any rate $R>0$. To define channel capacity for a non-ergodic $\mathbf{H}$, the concept of outage capacity is used in [103], [25] as the maximal achievable information rate R with the given outage probability $F_C(R)$, such that:

$$F_C(R)=\Pr\{C\le R\}, \tag{2.3}$$

where $\Pr\{\cdot\}$ denotes probability, and

$$C=\ln\left(\det[\mathbf{I}+\gamma_0\mathbf{H}\mathbf{H}^H/n_t]\right) \tag{2.4}$$

is the instantaneous capacity, i.e. the capacity of a given realization of $\mathbf{H}$. In this definition C is a random variable, and $F_C(R)$ is the corresponding cumulative density function (CDF). The mean of C coincides with (2.2), but unlike the case where $\mathbf{H}$ is ergodic, $E\{C\}$, in this case, does not have operational meaning, because sending information with the rates close to $E\{C\}$ is usually associated with high probability of outage [103]. To distinguish between C in (2.4) and C in (2.2), the latter is termed the mean (ergodic) capacity of the channel and will be further denoted by $\overline{C}$.

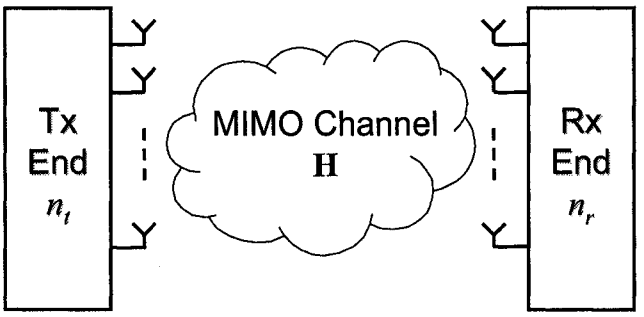

Fig. 2.1 MIMO Channel

This thesis focuses on the capacity defined for random $\mathbf{H}$, as many practical wireless channels are random and often quasi-static during the transmission time (see, for example, IEEE 801.11, IEEE 801.15

and IEEE 801.16). For the quasi-static channels, the outage capacity is a more relevant performance measure from a practical perspective (i.e. for a given quality of service) as compared to the mean capacity.

From (2.2) and (2.3), both $F_C(R)$ and $\overline{C}$ depend on the distribution of $\mathbf{H}$. In particular, the correlation between the elements of $\mathbf{H}$ has a crucial impact on the MIMO capacity [100], [109]. In the following section we introduce a number of popular correlation models that are used in Chapters III-IX to represent the correlation structure of $\mathbf{H}$.

2.2. Correlation Structure of MIMO Channels

The following definitions represent common concepts widely used in the literature and are necessary for the further discussion.

Definition 2.1: A random MIMO channel represented by matrix $\mathbf{H}$ is called Rayleigh-fading, if the elements of $\mathbf{H}$ are jointly distributed zero–mean circular symmetric Gaussian. If the mean is not zero, the channel is called Rician.

The Rician and Rayleigh-fading channels are appropriate models for rich multipath propagation environments with or with no line of sight (LOS), respectively.

Definition 2.2: If

$$\Pr\left\{rank\left(\mathbf{H}\mathbf{H}^{H}\right)=\min\left(n_t,n_r\right)\right\}=1, \tag{2.5}$$

the random channel $\mathbf{H}$ is called full-rank, otherwise it is rank deficient.

Condition (2.5) is satisfied for a broad class of channels such as uncorrelated, correlated Rayleigh, Rice and generic full-rank MIMO channels.

Definition 2.3: Let

$$\mathbf{\Gamma}=E\left\{vec\left(\mathbf{H}\right)\cdot vec\left(\mathbf{H}\right)^{H}\right\}, \tag{2.6}$$

where $vec\left(\mathbf{H}\right)$ represents the operator which creates a column vector by stacking the elements of $\mathbf{H}$ columnwise. If $\mathbf{\Gamma}=c\mathbf{I}$, where $\mathbf{I}$ is identity matrix, and c is a normalization constant, the channel is

uncorrelated, otherwise it is said to be correlated.

$\boldsymbol{\Gamma}$ represents the most general and full description of correlation of channel $\mathbf{H}$. However, the analysis of MIMO channels with arbitrary $\boldsymbol{\Gamma}$ is usually complicated. Hence, a number of more analytically friendly correlation structures of $\boldsymbol{\Gamma}$ has been proposed. A separable (Kronecker) model, which significantly simplifies the analysis and simulation of correlated channels by allowing independent modeling at the Tx and Rx ends has been introduced for Rayleigh-fading channels and experimentally verified in [37]. Following this model,

$$\boldsymbol{\Gamma} = \mathbf{R}_t^T \otimes \mathbf{R}_r, \tag{2.7}$$

where superscript T denotes matrix transposition, and $\otimes$ is the Kronecker product [119] of the transmitter $\mathbf{R}_t$ and receiver $\mathbf{R}_r$ correlation matrices defined by

$$\mathbf{R}_t = n_r^{-1} E\left\{\mathbf{H}^H \mathbf{H}\right\};\ \mathbf{R}_r = n_t^{-1} E\left\{\mathbf{H}\mathbf{H}^H\right\}, \tag{2.8}$$

where it is assumed, without loss of generality, that the channel is normalized so that $n_t^{-1} tr(\mathbf{R}_t) = n_r^{-1} tr(\mathbf{R}_r) = 1$, where $tr(.)$ stands for trace. Eq. (2.7) implies that the correlation between two signals collected by a pair of Rx antennas is restricted to the same value irrespectively of the transmitting antenna the signals origin from. The correlation between a pair of Tx antennas has the same property via duality of the problem. When (2.7) holds true, $\mathbf{H}$ can be represented as [37]

$$\mathbf{H} \propto \mathbf{R}_r^{1/2} \mathbf{H}_w (\mathbf{R}_t^{1/2})^H, \tag{2.9}$$

where $\propto$ means identically distributed, and $\mathbf{H}_w$ is a random matrix of size $\mathbf{H}$ composed of circular symmetric Gaussian i.i.d. entries with unit variance. Kronecker model has become a cornerstone of a large number of analyses [13], [99], [69]. In Chapter VIII we provide a motivation for the Kronecker model and show explicitly that the Kronecker structure of correlation is due to separability property of the correlation-forming effects into transmitter and receiver parts.

The following definition is possible due to the separability property of the Kronecker model.

Definition 2.4 [13], [99]: A MIMO channel is called semicorrelated at either Tx or Rx end, if either $\mathbf{R}_t = \mathbf{I}$ or $\mathbf{R}_r = \mathbf{I}$. If both $\mathbf{R}_t \neq \mathbf{I}$ and $\mathbf{R}_r \neq \mathbf{I}$, the channel is called double correlated.

The semicorrelated channels describe well practical systems where the antennas are separated far enough from each other at one end (for example at a base station (BS)), so the correlation between the antennas is negligible, but the antenna spacing at the other end (for example at a mobile unit (MU)) is small, which results in a high level of correlation at that end. In addition to the practical value, the analysis of semicorrelated channels is often more analytically friendly comparing to the double correlated channels. For this reason, the first analytical results on capacity of correlated MIMO channels, which appeared in the literature, were obtained for the semicorrelated ones [13], [102].

There are cases, however, when the correlation structure of a MIMO channel is not separable. The use of the Kronecker model may then underestimate the channel capacity [81]. A more accurate correlation model, which takes in account the joint correlation of both Tx and Rx ends has been proposed in [111]:

$$\mathbf{H} \propto \mathbf{U}_r(\mathbf{\Omega} \circ \mathbf{H}_w)\mathbf{U}_t^H, \tag{2.10}$$

where operator $\circ$ denotes elementwise matrix multiplication, $\mathbf{U}_t$ and $\mathbf{U}_r$ are eigenbases of $\mathbf{R}_t$ and $\mathbf{R}_r$ respectively, and the elements of $\mathbf{\Omega}$ are given as

$$\mathbf{\Omega}_{m,n} = E\{\left|\mathbf{u}_{r,m}^H \mathbf{H} \mathbf{u}_{t,n}\right|^2\}, \tag{2.11}$$

where $\mathbf{u}_{t,n}$ and $\mathbf{u}_{r,m}$ are n^{th} and m^{th} eigenvectors of $\mathbf{U}_t$ and $\mathbf{U}_r$ respectively. $\mathbf{\Omega}$ is called a coupling matrix since its elements specify the mean amount of energy that is coupled from the mth $\mathbf{U}_t$ eigenvector of Tx end to the nth eigenvector of the Rx end or vice versa. The necessary and sufficient condition for this model to hold is that the eigenbasis at the Rx end is independent of the transmitted signal, and the eigenbasis at the Tx end is independent of the received signal. Comparing to the Kronecker model, the one in (2.10) predicts more accurately the channel capacity, but at the expense of a larger number of parameters to be evaluated. As $\mathbf{U}_t$ and $\mathbf{U}_r$ have to be found for both models, the number of elements in the coupling matrix is $n_t \times n_r$, as compared to $n_t + n_r$ Tx and Rx eigenvalues in the Kronecker model. For MIMO channels, whose correlation structure is separable between Tx and Rx ends, the model in (2.10) reduces to the Kronecker one [111].

While the correlation models above are specifically tailored for Rayleigh-fading MIMO channels, [109] proposes a generic correlation structure given by

$$\mathbf{H} \propto \mathbf{U}_R \tilde{\mathbf{H}} \mathbf{U}_T^H, \tag{2.12}$$

where $\mathbf{U}_T$ and $\mathbf{U}_R$ are deterministic unitary matrices, and $\tilde{\mathbf{H}}$ is a random matrix with independent zero-mean arbitrary but not necessarily identically distributed elements. Due to the unitary-independent-unitary structure in (2.12), this model is referred as UIU and encompasses a broad class of zero–mean MIMO channels as shown below.

(i) If $\tilde{\mathbf{H}} = \mathbf{H}_w$, i.e. it has i.i.d. circular symmetric Gaussian entries, $\mathbf{H}$ represent a canonical uncorrelated Rayleigh-fading channel discussed, for example, in [103], [25].

(ii) If the entries of $\tilde{\mathbf{H}}$ are circular symmetric Gaussian with the separable correlation structure, the UIU model reverts to the Kronecker one, and can be equivalently represented by (2.9), where $\mathbf{U}_T = \mathbf{U}_t$ and $\mathbf{U}_R = \mathbf{U}_r$ [109].

(iii) If $\mathbf{U}_T = \mathbf{I}$ and $\mathbf{U}_R = \mathbf{I}$, the model in (2.12) reduces to an independent (IND) not necessarily identically distributed MIMO channel. This channel can describe, for example, the use of polarization diversity, where despite small antenna spacing, the level of correlation is low [109].

(iv) If $\tilde{\mathbf{H}}$ is IND circular symmetric Gaussian, and $\mathbf{U}_T$ and $\mathbf{U}_R$ are Fourier matrices, i.e. the elements of either $\mathbf{U}_T$ or $\mathbf{U}_R$ are $U_{k,m} = e^{j2\pi km/n}$, $k,m = 1...n$, where n is either n_t or n_r, the UIU model renders the virtual channel representation introduced in [93] for uniform linear antenna arrays (ULA), where the columns of $\mathbf{U}_T$ and $\mathbf{U}_R$ are interpreted as steering vectors transmitting and receiving energy at specific spatial directions.

(v) If $\mathbf{U}_T$ and $\mathbf{U}_R$ are arbitrary unitary matrices, while $\tilde{\mathbf{H}}$ is IND circular symmetric Gaussian, the model in (2.12) is equivalent to that in (2.10).

There are also channels that cannot be represented by the UIU model:

(i) The channels with diagonal correlation discussed in [77]. These channels are considered explicitly for $n_t = n_r = 2$ and have a certain fixed correlation pattern, which can not be described by the UIU model.

(ii) The keyhole channels [14], [15], where $\mathbf{H}$ is the outer product of two random vectors. There the entries of $\mathbf{H}$ can be uncorrelated but not independent.

While the keyhole channels fall outside the UIU model, they are one of the main subjects of this thesis. Section 2.5 in the current chapter provides a mathematical model and physical motivation of a keyhole channel. The outage capacity distribution and effect of correlation in keyhole channels are studied in Chapters III and V.

To evaluate the effect of correlation in an explicit form, the following popular parametric correlation models for $\mathbf{R}_t$ and $\mathbf{R}_r$ are used throughout this thesis.

- *Uniform Correlation Model*:

This model represents a simple case when the correlation between any pair of antennas at Tx or Rx end is equal and real, i.e. the elements of $\mathbf{R}$, either $\mathbf{R}_t$ or $\mathbf{R}_r$, are given by [55]

$$\mathbf{R}_{km} = \begin{cases} 1; & m = k \\ r; & m \neq k \end{cases}, \; -1/(n-1) \leq r \leq 1 \; [1], \tag{2.13}$$

where r is a correlation coefficient between two antennas, n is either n_t or n_r. The uniform model is somewhat artificial since it presumes the same correlation between any pair of antennas regardless of any specifics, while in practice the correlation decreases with antenna spacing. In this sense, the uniform model represents the worst case correlation structure and, in some cases, provides some insight into the operation of MIMO architecture [55].

- *Exponential Correlation Model*:

In this model the elements of $\mathbf{R}$ are represented through a single complex correlation parameter r, which is the correlation between adjacent antennas [86]:

$$\mathbf{R}_{km} = \begin{cases} r^{m-k}; & m \geq k \\ \overline{r}^{k-m}; & m < k \end{cases}, \; |r| < 1 \; , \tag{2.14}$$

[1] In this model r is real and restricted from below to ensure that $\mathbf{R}$ is a correlation matrix, i.e. positive semi-definite [55].

where $\overline{r}$ is the complex conjugate of r. This model allows for significant insight and has been successfully used for many communications problems. Despite its simplicity, it is a physically-reasonable model in the sense that the correlation decreases as distance $|m-k|$ between antennas increases.

- *Quadratic Exponential (QE) Model*:

This is a physically-motivated single-parameter correlation matrix model, where the elements of $\mathbf{R}$ are given by [1], [17]:

$$\mathbf{R}_{km} = \begin{cases} r^{(m-k)^2}; & m \geq k \\ \overline{r}^{(k-m)^2}; & m < k \end{cases}, \quad |r| < 1 \tag{2.15}$$

QE model is incorporated in the IEEE 802.11n Wireless LANs standard [22], and represents the scenario with a Gaussian profile of multipath angle-of-arrival [1], [17]. Comparing to the exponential correlation model, here the correlation between different antennas decays significantly faster with distance $|m-k|$.

- *Tri-diagonal Model*:

When the correlation is significant only among adjacent antennas, the elements of $\mathbf{R}$ can be modeled as [86],

$$\mathbf{R}_{k,m} = \begin{cases} 1, & k = m \\ r, & k = m-1 \\ \overline{r}, & k = m+1 \\ 0, & otherwise \end{cases}, \quad |r| < \frac{1}{2}\left(\cos\frac{\pi}{n+1}\right)^{-1} \tag{2.16}$$

This model offers a significant convenience for mathematical analysis in particular because it has a simple eigenvalue decomposition [86]. However, following (2.16), the model is restricted by the certain values of $|r|$. When this restriction is not satisfied, $\mathbf{R}$ becomes non positive semi-definite and, therefore cannot represent a correlation matrix. Note that for a large number of antennas $n >> 1$, such that $\cos[\pi/(n+1)] \approx 1$, the valid values of $|r| < 1/2$, i.e. $\mathbf{R}$ in (2.16) is defined for low correlations only.

Often, when the number of antennas $n > 2$, a meaningful scalar measure is required to evaluate the amount of correlation represented by a correlation matrix. A simple and well tractable measure of

correlation has been proposed in [33]:

$$\Omega(\mathbf{R}) = \sqrt{\frac{1 - n\|\mathbf{R}\|^2 / tr\{\mathbf{R}\}}{1-n}}, \tag{2.17}$$

where $\|\mathbf{R}\|$ is the L_2 norm of $\mathbf{R}$ [119]. $\Omega(\mathbf{R})$ represents a value reciprocal to the measure of spatial diversity available in Rayleigh-fading channels. For example, if $\mathbf{R}$ is given by the uniform correlation model (2.13), $\Omega(\mathbf{R}) = r$ [33]. However, this measure not only represents the correlation coefficient between adjacent antennas, but also takes into account the structure of $\mathbf{R}$, e.g. the rate of correlation decay with distance. It remains unclear, however, whether $\Omega(\mathbf{R})$ represents adequately the impact of correlation on the channel capacity.

Another measure of correlation is proposed for the Rayleigh channels with a single Tx or Rx antenna in [10]. This measure is based on the majorization theory [68], where a correlation matrix $\mathbf{R}_1$ is said to majorize (more correlated than) $\mathbf{R}_2$ (denoted as $\mathbf{R}_1 \succ \mathbf{R}_2$), if $\sum_{k=1}^{m} \lambda_k^{(1)} \geq \sum_{k=1}^{m} \lambda_k^{(2)}$ for all $m = 1...n$, where $\lambda_k^{(1)}$ and $\lambda_k^{(2)}$ are the eigenvalues of $\mathbf{R}_1$ and $\mathbf{R}_2$ respectively sorted in a descending order [10]. It is shown, in particular, that in multiple input single output (MISO) Rayleigh-fading channels with perfect CSI available at the receiver only, an increase in correlation (higher measure of correlation) results in lower outage capacity, if the average SNR $\gamma_0 \geq e^R - 1$, where the data rate R is given in *nats*. In opposite, when $\gamma_0 \leq (e^R - 1)/2$, the impact of correlation on the outage capacity is beneficial. Apparently, the advantage of the correlation measure in [10] is that it clearly characterizes the impact of correlation on the channel capacity. However, only a subset of all possible channel correlation structures is measurable in this case, i.e. the majorization-theory-based measure is not full ordering [10]. In Chapter V, we introduce a new full-ordering scalar measure of correlation that applies for MIMO channels of arbitrary size and clearly characterizes the impact of correlation on the capacity.

2.3. Capacity of Rayleigh-Fading MIMO Channels

This section summarizes the main results available in the literature for uncorrelated, semicorrelated and double-correlated Rayleigh-fading channels. The purpose of this summary is to draw later a

comparison between canonic Rayleigh-fading and the keyhole channels considered in Section 2.5.

2.3.1. *Uncorrelated Rayleigh-Fading Channels*

The uncorrelated Rayleigh-fading channel model represents practical propagation scenarios, where the antennas at both ends are spaced sufficiently far apart from each other [34]. Based on the eigenvalue distribution of Wishart matrices [70], the characteristic function (CF) of the instantaneous capacity is found in [13] in a compact form

$$\Phi_C(\omega) = K_1 \det\left[\mathbf{U}(\omega)\right], \tag{2.18}$$

where $K_1 = \dfrac{\pi^{n(n-1)}}{\tilde{\Gamma}_n(m)\cdot\tilde{\Gamma}_n(n)}$, $\tilde{\Gamma}_n(p) = \pi^{n(n-1)/2}\prod_{i=1}^{n}(p-i)!$, $n = \min\{n_t, n_r\}$, $m = \max\{n_t, n_r\}$ and $\mathbf{U}(\omega)$ is $n\times n$ Hankel matrix with ij^{th} elements

$$U_{ij}(\omega) = \int_0^\infty x^{m-n+j+i-2} e^{-x}\varphi(x,\omega)dx, \tag{2.19}$$

where $\varphi(x,\omega) = \left(1+\gamma_0 x/n_t\right)^{j\omega}$ and $j = \sqrt{-1}$. A general integral expression for the mean capacity of such a channel is obtained in [103]

$$\bar{C} = \int_0^\infty \ln\left(1+\gamma_0\lambda/n_t\right) f(\lambda)d\lambda, \tag{2.20}$$

where $f(\lambda) = \sum_{i=0}^{n-1}\dfrac{i!}{(i+m-n)!}[L_i^{m-n}(\lambda)]^2\lambda^{m-n}e^{-\lambda}d\lambda$, and $L_i^j(\lambda)$ are Laguerre polynomials of order i [119].

Uncorrelated Rayleigh-fading channel has become the classic model for the full-rank MIMO channels. Some of the results pertaining uncorrelated MIMO channels are discussed later in Chapter VII.

2.3.2. *Semicorrelated Rayleigh-Fading Channels*

The CF of the instantaneous capacity of a semicorrelated Rayleigh-fading channel is derived in [13]. It is assumed that the channel has Kronecker correlation structure (2.9) and is correlated at the Rx end only, i.e. $\mathbf{R}_t = \mathbf{I}$. For $n_r \le n_t$, and non-singular $\mathbf{R}_r$ with distinct eigenvalues λ_k, $k = 1...n_r$, the CF is given by [13]

$$\Phi_C(\omega) = K_2 \det[\mathbf{G}(\omega)], \tag{2.21}$$

where

$$K_2 = K_1 \cdot \prod_{i=1}^{n_r} (i-1)! \frac{\det^{-m}[\mathbf{R}_r]}{\det[\mathbf{V}(\lambda)]} \tag{2.22}$$

$\mathbf{V}(\lambda)$ is the Vandermonde matrix defined as

$$\mathbf{V}(\lambda) = \begin{bmatrix} 1 & 1 & \cdots & 1 \\ -\lambda_1^{-1} & -\lambda_2^{-1} & \cdots & -\lambda_n^{-1} \\ \vdots & \vdots & \ddots & \vdots \\ (-\lambda_1)^{1-n_r} & (-\lambda_2)^{1-n_r} & \cdots & (-\lambda_n)^{1-n_r} \end{bmatrix}, \tag{2.23}$$

and $\mathbf{G}(\omega)$ is an $n_r \times n_r$ matrix with ij^{th} elements

$$G_{ij}(\omega) = \int_0^\infty x^{m-n+j+i-2} e^{-x/\lambda_i} \varphi(x,\omega) dx \tag{2.24}$$

The mean capacity of such a channel is [13]

$$\overline{C} = K_2 \sum_{k=1}^{n_r} \det[\mathbf{W}(k)], \tag{2.25}$$

where $\mathbf{W}(k)$ is an $n_r \times n_r$ matrix with ij^{th} elements

$$W_{i,j}(k) = \int_0^\infty x^{m-m+j-1} e^{-x/\lambda_i} Y_{ij} \ln(1+\gamma_0 x / n_t) dx, \tag{2.26}$$

where $Y_{ij} = \begin{cases} x, & i = j \\ 1, & i \neq j \end{cases}$.

From the duality of the problem, the mean capacity and the CF of the instantaneous capacity of a semicorrelated Rayleigh-fading channel with the correlation at the Tx end can be obtained in the same way by substitution of $\mathbf{R}_t$ in place of $\mathbf{R}_r$ and the corresponding eigenvalues in (2.21) and (2.25).

It turns out that under some general assumptions, the capacities of semicorrelated Rayleigh-fading channels and multi-keyhole channels (will be introduced in Chapter IV), are asymptotically equivalent, when the number of antennas at either Tx or Rx end is large.

2.3.3. *Double Correlated Rayleigh-Fading Channels*

This is the most general channel model considered so far in the literature for which an exact closed-form capacity expression has been derived. The CF of the instantaneous capacity of a double-correlated Rayleigh-fading channels with Kronecker correlation structure (2.9) is given by [99].

$$\Phi_C(\omega) = \mathbf{Y}_n(\omega)\det\left[\mathbf{\Lambda}(\omega)\right]/K_{cor}, \tag{2.27}$$

where

$$\mathbf{Y}_n(\omega) = \prod_{l=1}^{n-1}(j\omega + l)^{-l} \tag{2.28}$$

$$K_{cor} = \left(\frac{\gamma_0}{n_t}\right)^{n(n-1)/2} \prod_{i<j}^{n}(\lambda_{s,j} - \lambda_{s,i}) \prod_{i<j}^{m}(\lambda_{l,j} - \lambda_{l,i}), \tag{2.29}$$

and the elements of $m \times m$ matrix $\mathbf{\Lambda}(\omega)$ are

$$[\mathbf{\Lambda}(\omega)]_{i,j} = \begin{cases} \lambda_{l,j}^{i-1}, & i = 1,2,...,m-n;\ j = 1,2,...,m \\ \lambda_{l,j}^{m-n-1} \int_0^{\infty} (1+\gamma_0\lambda_{s,i-m+n} z/n_t)^{\omega+n-1} e^{-z/\lambda_{l,j}} dz, & i = m-n+1,...m;\ j = 1,2,...,m \end{cases} \tag{2.30}$$

$\lambda_{s,k}\ \ k = 1...n$, $\lambda_{l,q}\ \ q = 1...m$ are the eigenvalues of $\mathbf{R}_s$ and $\mathbf{R}_l$ respectively, where

$$(\mathbf{R}_s, \mathbf{R}_l) = \begin{cases} (\mathbf{R}_t, \mathbf{R}_r), & n_t \le n_r \\ (\mathbf{R}_r, \mathbf{R}_t), & n_r < n_t \end{cases}, \tag{2.31}$$

Based on (2.27), it can be shown that the mean capacity of the double correlated channels is [99]

$$\overline{C} = tr\{\mathbf{\Lambda}^{-1}(0)\mathbf{\Lambda}^{(1)}(0)\} - n + 1, \tag{2.32}$$

where the elements of $m \times m$ matrix $\mathbf{\Lambda}^{(n)}(\omega)$ are

$$[\mathbf{\Lambda}^{(n)}(\omega)]_{i,j} = \begin{cases} 0, & i = 1,2,...,m-n;\ j = 1,2,...,m \\ \lambda_{l,j}^{m-n-1} \int_0^{\infty} (1+\gamma_0\lambda_{s,i-m+n} z/n_t)^{\omega+n-1} \times \\ \times \ln^n(1+\gamma_0\lambda_{s,i-m+n} z/n_t) e^{-z/\lambda_{l,j}} dz, & i = m-n+1,...m;\ j = 1,2,...,m \end{cases} \tag{2.33}$$

The probability density function (PDF) $f_C(R)$ and CDF $F_C(R)$ of the instantaneous capacity can be obtained, in this case, from (2.18), (2.21) or (2.27) by numerical evaluation of the following integrals

$$f_C(R) = (2\pi)^{-1} \int_{-\infty}^{\infty} \Phi_C(\omega) \exp(-j\omega R) d\omega, \tag{2.34}$$

$$F_C(R) = (2\pi)^{-1} \int_{-\infty}^{\infty} \Phi_C(\omega) \frac{1-\exp(-j\omega R)}{j\omega} d\omega, \tag{2.35}$$

where (2.35) is obtained using the fact that C can not be negative.

The expressions presented above have a significant theoretical value as they evaluate the outage capacity distribution and the mean capacity of Rayleigh-fading MIMO channels for an arbitrary number of antennas, SNR and a broad class of correlation matrices $\mathbf{R}_t$ and $\mathbf{R}_r$. However, due to the mathematical complexity, these expressions do not allow for significant insight. In particular, the impact of correlation is not immediately evident. A simple compound upper bound on the mean capacity of the Rayleigh-fading channels, which overcomes this complexity, is proposed in [61] using Jensen inequality [18] and the concavity of the *log det* function

$$\bar{C} \le \min\{\bar{C}_t, \bar{C}_r\}, \tag{2.36}$$

where $\bar{C}_t \le \ln\left(\det\left[\mathbf{I} + \gamma_0 n_r \mathbf{R}_t / n_t\right]\right)$ and $\bar{C}_r \le \ln\left(\det\left[\mathbf{I} + \gamma_0 \mathbf{R}_r\right]\right)$. When the channel is uncorrelated, i.e. $\mathbf{R}_t = \mathbf{I}$, $\mathbf{R}_r = \mathbf{I}$, the compound bound reverts to

$$\bar{C} \le \min\{n_t \ln(1 + \gamma_0 n_r / n_t), n_r \ln(1 + \gamma_0)\} \tag{2.37}$$

Based on results obtained in [32], [69], the bounds (2.36), (2.37) are asymptotically tight when the number of antennas is large. The analysis of the compound bound instead of the exact expressions is much simpler. In particularly, based on bound (2.36) and using the exponential parametric model (2.14) for $\mathbf{R}_t$ and $\mathbf{R}_r$, it has been shown that an increase in correlation is equivalent to a decrease in SNR, which, in turn, results in lower mean capacity [65].

It is significantly more difficult, however, to see the impact of various parameters such as SNR and correlation on the outage capacity distribution, especially when the number of antennas is large. In the next section we review a number of asymptotic approximations of the outage capacity distribution obtained for uncorrelated, correlated Rayleigh-fading and generic MIMO channels with a large number of antennas. Similar approach is used later in Chapters III and IV to obtain asymptotic expressions for the

capacity of keyhole and multi-keyhole channels.

2.4. Asymptotic Capacity Distribution of MIMO Channels

Asymptotic capacity analysis of MIMO channels with an arbitrary large number of antennas is widely used to overcome mathematical complexity and often allows for a significant insight. For example, the impact of correlation, number of Tx, Rx antennas and SNR becomes more evident. In many cases, the asymptotic results describe reasonably accurate the practical channels with a moderate number of antennas, and therefore not only have a theoretical value but also can be used in practice. There is a number of asymptotic theorems indicating that as n_t and/or $n_r \to \infty$ the instantaneous capacity C of a variety of MIMO channels (not necessarily Rayleigh-fading)) obeys

$$\tilde{C} = \frac{C - \mu}{\sigma} \xrightarrow{d} N(0,1), \tag{2.38}$$

where $\tilde{C}$ is normalized instantaneous capacity, $\xrightarrow{d}$ denotes convergence in distribution, and $N(0,1)$ stands for the Gaussian distribution with zero mean and unit variance. μ and σ^2 are called asymptotic mean and asymptotic variance respectively and depend on a particular channel as shown below.

2.4.1. Outage Capacity Distribution of Uncorrelated Rayleigh-Fading MIMO Channels

Theorem 2.1 [32] (large n_r, fixed n_t): As $n_r \to \infty$, the normalized instantaneous capacity of an uncorrelated Rayleigh-fading channel is asymptotically Gaussian in distribution with μ and σ^2 given below

$$\mu = n_t \ln\left(1 + \gamma_0 n_r / n_t\right);\ \sigma^2 = n_t / n_r \tag{2.39}$$

Theorem 2.2 [32] (large n_t, fixed n_r): As $n_t \to \infty$, the normalized instantaneous capacity of an uncorrelated Rayleigh-fading channel is asymptotically Gaussian in distribution with the following μ and σ^2:

$$\mu = n_r \ln(1+\gamma_0);\ \sigma^2 = \frac{n_r \gamma_0^2}{n_t (1+\gamma_0)^2} \tag{2.40}$$

Theorem 2.3 [32] (large n_t and n_r): (i) As both $n_t, n_r \to \infty$, and $\gamma_0 \to 0$, the normalized instantaneous capacity of an uncorrelated Rayleigh channel is asymptotically Gaussian in distribution with the following μ and σ^2:

$$\mu = n_r \gamma_0;\ \sigma^2 = n_r \gamma_0^2 / n_t \tag{2.41}$$

(ii) As both $n_t, n_r \to \infty$, and $\gamma_0 \to \infty$, the normalized instantaneous capacity of an uncorrelated Rayleigh channel is asymptotically Gaussian in distribution with the following μ and σ^2:

$$\begin{aligned} \mu &= n \ln(\gamma_0 / n_t) + \sum_{i=1}^{m-n} n i^{-1} - \gamma_e n + \sum_{i=1}^{n-1} i (m-i)^{-1} \\ \sigma^2 &= \sum_{i=1}^{n-1} \frac{i}{(m-n+i)^2} + n\left[\frac{\pi^2}{6} - \sum_{i=1}^{m-1} \frac{1}{i^2}\right] \end{aligned}, \tag{2.42}$$

where $n = \min\{n_t, n_r\}$, $m = \max\{n_t, n_r\}$

Note that the expressions for the asymptotic mean capacity μ in (2.39) and (2.40) (Theorems 2.1 and 2.2) are equivalent to those in the compound upper bound (2.37), i.e. the bound is asymptotically tight. It also follows that under the conditions of Theorems 2.2, 2.3(i) and 2.3(ii) ($n_t < n_r$), μ increases linearly with n_r. This fact stresses out the advantage of using MIMO systems with multiple antennas. Moreover, under the conditions of Theorems 2.1, 2.2 and 2.3(i), the variance of the outage capacity distribution $\sigma^2 \to 0$. Such asymptotic behavior is called "channel hardening" [32], and implies that in terms of capacity, the i.i.d. Rayleigh-fading channel converges asymptotically to the additive white Gaussian one with no fading. In such a case, if the number of antennas is sufficiently large so that $\sigma^2 << 1$, the mean capacity approximates well the instantaneous one, i.e. $C \approx \overline{C}$. This result is extended further to a broad class, so called Rayleigh-like MIMO channels (not necessarily Rayleigh-fading) with arbitrary correlation structure (not necessarily i.i.d.) in Chapter VII.

Simulations done in [101] demonstrate that the approximation of the outage capacity by Gaussian distribution is sufficiently accurate already for 2x2 MIMO channels for low SNR ($\gamma_0 \le 5dB$) and it is

"practically indistinguishable" from the true distribution when there are five or more antennas at each end.

Analytical analysis conducted in [90] shows that the mean capacity of uncorrelated Rayleigh-fading channels converges to its asymptotic value not slower than $1/\sqrt{n_r}$, where it is assumed that $n_r / n_t < 1$. In Chapter IV we extend this result to correlated Rayleigh-fading channels, whose asymptotic capacity is reviewed below.

2.4.2. Outage Capacity Distribution of Correlated Rayleigh-Fading MIMO Channels

The following theorem is stipulated for MIMO channels, where the channel state information is available at both Tx and Rx ends.

Theorem 2.4 [69]: (i) If n_r is fixed and

$$\lim_{n_t \to \infty} \|\lambda\|_3 / \|\lambda\|_2 = 0, \tag{2.43}$$

where $\|\lambda\|_m = \left(\sum_{i=1}^{n} (\lambda_i)^m\right)^{1/m}$ is the L_m norm of the eigenvalues of $\mathbf{R}_t^{1/2}\mathbf{Q}\mathbf{R}_t^{1/2}$, $\mathbf{Q}$ is the input covariance matrix, $\mathbf{R}_t^{1/2}$ is the Hermitian square root of $\mathbf{R}_t$, the normalized instantaneous capacity of a Rayleigh-fading channel with Kronecker correlation structure is asymptotically Gaussian in distribution as $n_t \to \infty$ with the following μ and σ^2

$$\mu = \ln(\det[\mathbf{I} + tr\{\mathbf{Q}\mathbf{R}_t\}\mathbf{R}_r]) \tag{2.44}$$

$$\sigma^2 = \|\mathbf{Q}\mathbf{R}_t\|^2 \cdot \sum_{k=1}^{n_r} \left(\frac{\lambda_k^r}{1 + \gamma_0 \bar{\lambda}_k}\right)^2, \tag{2.45}$$

where λ_k^r, $k = 1...n_r$ are the eigenvalues of $\mathbf{R}_r$, and $\bar{\lambda}_k = tr\{\mathbf{Q}\mathbf{R}_t\}\lambda_k^r$.

(ii) Due to the symmetry of (2.4), similar expressions can be obtained for fixed n_t and $n_r \to \infty$, if Tx and Rx ends are exchanged [69].

Similarly to the results obtained in Theorems 2.1, the asymptotic mean capacity (2.44) is equivalent to that in the compound bound (2.36), if $\mathbf{Q} = \mathbf{I}P_T / n_t$ (P_T is the total transmit power), i.e. under the

conditions of Theorem 2.4 the bound is asymptotically tight. Moreover, when the channel is uncorrelated (all $\lambda_k^r = 1$), condition (2.43) is satisfied, and the mean (2.44) and variance (2.45) reduce to the corresponding moments in (2.40). In contrast, when the channel is fully-correlated ($\mathbf{R}_t$ has a single non-zero eigenvalue), condition (2.43) is not satisfied, and, consequently, the outage capacity distribution, in this case, is not asymptotically Gaussian. Simulations done in [69] show that the Gaussian approximation is accurate for a moderate number of antennas ($n_t = 5$, $n_r = 2$), when the parametric exponential model (2.14) is used to represent $\mathbf{R}_t$ and $\mathbf{R}_r$. The lower the correlation parameter $|r|$, the better the approximation [69]. Theorem 2.4 has been recently generalized in [74] for Rayleigh-fading channels whose correlation structure cannot be represented by the Kronecker model (2.9).

A number of open questions arise from Theorem 2.4. For example, when, if at all, is condition (2.43) satisfied in real propagation environments? Are there other conditions equivalent to (2.43), which do not require eigenvalue decomposition of an asymptotically large correlation matrix? Is it possible to evaluate analytically the convergence rate of the outage capacity distribution to its limiting value in this case? Whether the results obtained in [69] using simulations hold true in general? These questions are addressed in Chapter VI.

Another important issue, which has not been fully covered in the literature yet, is the effect of correlation on the asymptotic capacity. When is the correlation beneficial, and when does it decrease the outage capacity? What is the relationship between the correlation and the probability of outage? These and some other issues are studied in Chapter V.

2.4.3. Outage Capacity Distribution of Generic MIMO Channels

Currently much attention is being paid to a generic type of MIMO channels, which are not necessarily Rayleigh or Rician. The capacity analysis of such channels is based primarily on the asymptotic approximation with respect to the number of antennas as indicated by the following theorem.

Theorem 2.5 [[108], Theorem 2.76]: Let $\mathbf{H}$ be an $n_r \times n_t$ channel matrix whose entries are i.i.d. zero mean random variables (not necessarily Gaussian) with unit variance such that $E[|H_{ij}|^4] = 2$. As both

$n_t, n_r \to \infty$ and $\beta = n_t / n_r$ is a constant, the instantaneous capacity in (2.4) is asymptotically (in n_t, n_r) Gaussian in distribution, with the following mean $\overline{C}$ and variance σ^2:

$$\frac{\overline{C}}{n_r} = \beta \ln\left(1+\frac{\gamma}{\beta}-\frac{1}{4}F\left(\frac{\gamma}{\beta},\beta\right)\right)+\ln\left(1+\gamma-\frac{1}{4}F(\frac{\gamma}{\beta},\beta)\right)-\frac{\beta}{4\gamma_0}F\left(\frac{\gamma}{\beta},\beta\right), \qquad (2.46)$$

$$\sigma^2 = -\ln\left(1-\beta\left[\frac{1}{4\gamma}F\left(\frac{\gamma}{\beta},\beta\right)\right]^2\right), \qquad (2.47)$$

where $F(x,z) = (\sqrt{x(1+\sqrt{z})^2+1}-\sqrt{x(1-\sqrt{z})^2+1})^2$.

The proof is based on the classic Marcenko-Pasture law that governs the asymptotic behavior of matrices with i.i.d. entries [108]. Theorem 2.5 is extended in [90], where it is shown that the normalized instantaneous capacity (2.38) is asymptotically Gaussian when the entries of $\mathbf{H}$ are independent but not necessarily identically distributed. Since the distribution of C in (2.4) is invariant under a unitary transformation of $\mathbf{H}$, the latter result applies automatically to a broad class of MIMO channels with UIU structure (2.12). As stated above, the UIU framework, however, does not include keyhole MIMO channels, which are the subject of the next section.

2.5. Keyhole MIMO Channels

The keyhole (pinhole) channel was theoretically predicted in [14], [15] to describe a rich scattering environment with a single propagation eigenmode that establishes the link between transmitter and receiver. In this case, the channel can be represented as a concatenation of two Rayleigh-fading subchannels separated by a screen that prevents propagation from the transmitter to the receiver except through a little hole (the keyhole) whose diameter is much less than the wavelength (see Fig. 2.2). The keyhole channel matrix is given in [15] as the following vector product

$$\mathbf{H} = \mathbf{h}_r \mathbf{h}_t^H, \qquad (2.48)$$

where $\mathbf{h}_t\,[n_t \times 1]$ and $\mathbf{h}_r\,[n_r \times 1]$ are the vectors representing the complex gains from the transmit antennas to the keyhole and from the keyhole to the receive antennas respectively. It is usually assumed

that $\mathbf{h}_t$ and $\mathbf{h}_r$ are mutually independent, complex circular symmetric correlated Gaussian vectors with correlation matrices $\mathbf{R}_t = E\{\mathbf{h}_t\mathbf{h}_t^H\}$ and $\mathbf{R}_r = E\{\mathbf{h}_r\mathbf{h}_r^H\}$ respectively.

Due to (2.48), the rank of a keyhole channel is always one regardless of the number of Tx and Rx antennas. As the result, the capacity of such a channel is significantly less than that of the Rayleigh-fading channel of the same size. A comprehensive comparison between the capacities of keyhole and Rayleigh-fading channels are given in Chapters III, IV and V.

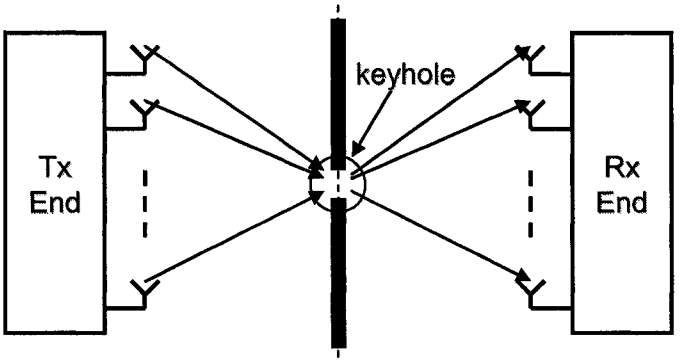

Fig. 2.2 The Keyhole MIMO channel. The sub-channels on each end (Tx or Rx) is Rayleigh fading.

Substituting (2.48) in (2.4) and using the fact that for any proper matrices $\mathbf{A}$ and $\mathbf{B}$, $\det[\mathbf{I}+\mathbf{AB}] = \det[\mathbf{I}+\mathbf{BA}]$, it is shown that the instantaneous capacity of the keyhole channel is [84]

$$C = \ln\left(1+\frac{\gamma_0}{n_t}\alpha\right), \tag{2.49}$$

where $\alpha = \|\mathbf{h}_t\|^2\|\mathbf{h}_r\|^2$ is the equivalent scalar channel power gain. Up to a constant factor, α determines the instantaneous SNR ($=\alpha\cdot\gamma_0/n_t$) in the equivalent scalar channel. The Alamouti scheme [2] is an example of a space-time code which achieves the capacity in (2.49) with no CSI at the transmitter for $n_t = 2$ [2]. When $n_t > 2$, the outage capacity of a keyhole channel can be achieved in this case using universal coding strategy [[106], Appendix B8].

---

[2] This is in contrast to the Rayleigh-fading channels, where the Alamouti space time code achieves full diversity gain, but does not achieve the capacity for $n_t = 2$, $n_r > 1$. In keyhole channels, the Alamouti scheme is the optimal transmitting strategy for $n_t = 2$, as it simultaneously achieves both the capacity and the maximal diversity.

Unlike Rayleigh and Rice fading channels, the literature dealing with information theoretical analysis of the keyhole channels is rather limited. Some of the results are reviewed below. The CF of α for the uncorrelated keyhole channel ($\mathbf{R}_t = \mathbf{I}$ and $\mathbf{R}_r = \mathbf{I}$) has been obtained in [98]

$$\Phi_\alpha(\omega) = {}_2F_0(n_t, n_r;;-\omega\gamma_0/n_t), \tag{2.50}$$

where ${}_pF_q(\cdot)$ is the generalized hypergeometric function [119]. The mean capacity of the uncorrelated keyhole channel is given in [97]

$$\bar{C} = \ln(\gamma_0/n_t) + (\psi(n_t) + \psi(n_r)) + \frac{1}{\Gamma(n_t)\Gamma(n_r)} G_{2,4}^{3,2}\left(\frac{n_t}{\gamma_0}\middle| \begin{matrix} 1, & 1 \\ n_r, n_t, 1, 0 \end{matrix}\right), \tag{2.51}$$

where $G_{p,q}^{m,n}(\cdot)$ is the Meijer's G-function [119], $\Gamma(n)$ is the Gamma function, and $\psi(n) = \frac{d\Gamma(n)/dn}{\Gamma(n)}$ is the digamma function, which can also be calculated for integer n as $\psi(n) = -\gamma_e + \sum_{i=1}^{n-1} i^{-1}$ [97]. As $\gamma_0 \to \infty$, the last term in (2.51) vanishes and the mean capacity becomes [97]

$$\bar{C} = \ln(\gamma_0/n_t) + (\psi(n_t) + \psi(n_r)) \tag{2.52}$$

Using the same approach as in [61], it has been shown that an upper bound on the mean capacity is [97]

$$\bar{C} \le \ln(1 + \gamma_0 n_r), \tag{2.53}$$

A tight lower bound on the mean capacity of a spatially correlated keyhole channel has been proposed in [20]

$$\bar{C} \ge \ln(1 + \gamma_0 \exp[\Theta(\mathbf{R}_t) + \Theta(\mathbf{R}_r)]/n_t), \tag{2.54}$$

where, from Eq. 15 in [20], if $\mathbf{R}$, either $\mathbf{R}_t$ or $\mathbf{R}_r$, is non-singular with distinct eigenvalues λ_k^t or λ_k^r respectively, $\Theta(\mathbf{R}) = -\gamma_e + \sum_{k=1}^{n} A_k \ln(\lambda_k)$, and A_k are the coefficients of the partial fraction decomposition [70] of CF of either $\|\mathbf{h}_t\|^2$ or $\|\mathbf{h}_r\|^2$.

Approximations of the mean capacity of 2x2 correlated keyhole channel have been proposed in [62]

$$\begin{aligned} \bar{C} &\approx \ln\left(1 + \gamma_0 + \frac{\gamma_0}{2}\left[1 - E^2\{|r_{12}|\}\right]\right) \\ \bar{C} &\approx \ln\left(1 + \gamma_0 + \frac{\gamma_0}{2}\left[1 - E\{|r_{12}|^2\}\right]\right) \end{aligned}, \tag{2.55}$$

where r_{ij}, $i,j=1..2$ are the elements of matrix $\mathbf{HH}^H$. It has been shown that the approximations are tight, when r_{12} has the following exponential PDF [62]

$$f_{r_{12}}(x)=c\cdot\exp\left[\frac{|x|}{\alpha}\right];\ |x|\le 1, \tag{2.56}$$

where α determines the standard deviation of r_{12}, and c is a normalization constant. Eq. (2.55) shows that the correlation between separate Rx antennas (r_{12}) has a dominant impact on the mean capacity as compared to the received power at the Rx end (r_{11} and r_{22}).

Diversity order of a keyhole channel has been addressed in [92]. It was shown that for $n_t \neq n_r$, the order is $\min\{n_t,n_r\}$. This supports well the intuition as the keyhole channel is the concatenation of a multiple-input-single-output (MISO) and single-input-multiple-output (SIMO) channels, with diversity gains n_t and n_r respectively. Since the subchannel with the smaller diversity is a bottleneck for the data transmission, the diversity order of the whole channel cannot exceed $\min\{n_t,n_r\}$. It follows from this analysis that the diversity order of the keyhole channel is significantly lower comparing to that of a full-rank Rayleigh-fading channel where it is $n_t \times n_r$.

Another interesting results was also obtained in [92] for $n_t = n_r$. It follows that in this case the diversity order cannot be characterized by an integer number and attains a value in between $n_t - 1$ and n_t.

The above results, however, do not consider the outage capacity distribution of the keyhole channels in general and the correlated keyhole channels in particular. In the next chapters we derive exact and asymptotic expressions for instantaneous SNR and capacity CDF ($F_\alpha(x)$ and $F_C(x)$) of correlated keyhole MIMO channels, study the effect of correlation and discuss the relationship between the Rayleigh and keyhole channels.

CHAPTER III: CAPACITY OF KEYHOLE MIMO CHANNELS

In this chapter the exact and asymptotic outage capacity distributions of spatially correlated keyhole MIMO channels are derived. The impact of SNR and spatial correlation on the mean and outage capacities and also the relationship between the keyhole and classic Rayleigh-fading channels are investigated. It is shown that the recently proposed upper and lower bounds on the mean capacity of the keyhole channels are asymptotically tight.

3.1. Exact Outage Capacity Distribution

Consider a spatially correlated keyhole MIMO channel (see Fig. 2.2) with the channel matrix given by (2.48). Assume that $\mathbf{h}_t$ and $\mathbf{h}_r$ are mutually independent complex circular symmetric correlated Gaussian random vectors with zero means and correlation matrices $\mathbf{R}_t = E\{\mathbf{h}_t\mathbf{h}_t^H\}$ and $\mathbf{R}_r = E\{\mathbf{h}_r\mathbf{h}_r^H\}$ respectively. Without loss of generalization $\mathbf{H}$ is normalized so that $E\{\|\mathbf{H}\|^2\} = n_t n_r$, where $\|\ \|$ is the L_2 norm, and $n_t^{-1}E\{\|\mathbf{h}_t\|^2\} = n_r^{-1}E\{\|\mathbf{h}_r\|^2\} = 1$, which also implies $n_t^{-1}tr\{\mathbf{R}_t\} = n_r^{-1}tr\{\mathbf{R}_r\} = 1$.

When the channel state information (CSI) is available at the Rx end but not the Tx end, the instantaneous capacity (i.e. the capacity of a given channel realization) of a frequency flat quasi-static keyhole MIMO channel in natural units $[nat]$ is given by (see Section 2.5):

$$C = \ln\left(1 + \frac{\gamma_0}{n_t n_r}\alpha\right), \tag{3.1}$$

where $\alpha = \|\mathbf{h}_t\|^2 \|\mathbf{h}_r\|^2$ is the power gain of the equivalent scalar channel, and γ_0 is the total average SNR at the Rx end[3]. Since the instantaneous capacity is a continuous, monotonically increasing function of α, the CDF of C, which is also the outage capacity distribution $F_C(x)$, is given by:

$$F_C(x) = F_\alpha\left(n_t n_r (e^x - 1)/\gamma_0\right), \tag{3.2}$$

[3] See more on physical interpretation of MIMO channel normalization in [60].

where $F_\alpha(x)$ is the CDF of α. The exact expression for $F_\alpha(x)$ is given by the following theorem.

Theorem 3.1: Let $\alpha = \beta_t \cdot \beta_r$, where $\beta_t = \|\mathbf{h}_t\|^2$, $\beta_r = \|\mathbf{h}_r\|^2$ and $\mathbf{h}_t$, $\mathbf{h}_r$ are mutually independent complex circular symmetric correlated Gaussian random vectors. When both $\mathbf{R}_t$ and $\mathbf{R}_r$ are non-singular and have distinct eigenvalues λ_k^t, $k = 1...n_t$, and λ_m^r, $m = 1...n_r$ respectively, the PDF $f_\alpha(z)$ and the CDF $F_\alpha(z)$ of α are as follows:

$$f_\alpha(x) = 2\sum_{k=1}^{n_t}\sum_{m=1}^{n_r} \frac{A_k^t A_m^r}{\lambda_k^t \lambda_m^r} K_0\left(\sqrt{\frac{4x}{\lambda_k^t \lambda_m^r}}\right), \; x \geq 0 \tag{3.3}$$

$$F_\alpha(x) = 1 - \sum_{k=1}^{n_t}\sum_{m=1}^{n_r} A_k^t A_m^r \sqrt{\frac{4x}{\lambda_k^t \lambda_m^r}} K_1\left(\sqrt{\frac{4x}{\lambda_k^t \lambda_m^r}}\right), \; x \geq 0, \tag{3.4}$$

where $K_n(x)$ is the n-order modified Bessel function of the second kind [119], A_k^t and A_m^r are the coefficients of a partial fraction decomposition given by

$$A_k = \prod_{\substack{m=1 \\ m \neq k}}^{n} \left(1 - \lambda_m / \lambda_k\right)^{-1}, \tag{3.5}$$

and A_k is either A_k^t or A_k^r, λ_k is either λ_k^t or λ_k^r, and n is either n_t or n_r.

Proof: See Appendix A.

To obtain an insight consider a number of cases where Theorem 3.1 does not apply or applies with some straightforward modifications. (i) The channel at the Tx, Rx or both ends is uncorrelated, i.e. $\lambda_k = 1$ for $k = 1...n$ (the eigenvalues are not distinct). While Theorem 3.1 does not apply in this case, $f_\alpha(x)$ and $F_\alpha(x)$ can be evaluated based on the characteristic function (CF) $\Phi_\alpha(\omega)$ given in (2.50) for uncorrelated keyhole channels. (ii) There is a number of fully correlated antennas, i.e. $\mathbf{R}_t$, $\mathbf{R}_r$ or both have some zero eigenvalues. In this case the PDF and CDF of α are also given by (3.3) and (3.4) respectively, but the summation is taken over the non-zero eigenvalues only, i.e. zero eigenvalues and corresponding eigenvectors are excluded as they do not contribute to the SNR. This follows directly from the proof of Theorem 3.1 (see Appendix A). In particular, when the channel is fully correlated at both the Tx and Rx ends, it is equivalent to a keyhole channel with a single antenna at each end and the gains equal to n_t and n_r respectively. In this case, $A_1^t = A_1^r = 1$, $\lambda_1^t = n_t$ and $\lambda_1^r = n_r$, so that (3.3) and (3.4) reduce to

$$f_{\alpha}(x)=\frac{2}{n_t n_r}K_0\left(\sqrt{\frac{4x}{n_t n_r}}\right),\ x\geq 0 \tag{3.6}$$

$$F_{\alpha}(x)=1-\sqrt{\frac{4x}{n_t n_r}}K_1\left(\sqrt{\frac{4x}{n_t n_r}}\right);\ x\geq 0 \tag{3.7}$$

In all these cases, the exact expression for the outage capacity distribution is obtained from (3.2) using the instantaneous SNR CDF's.

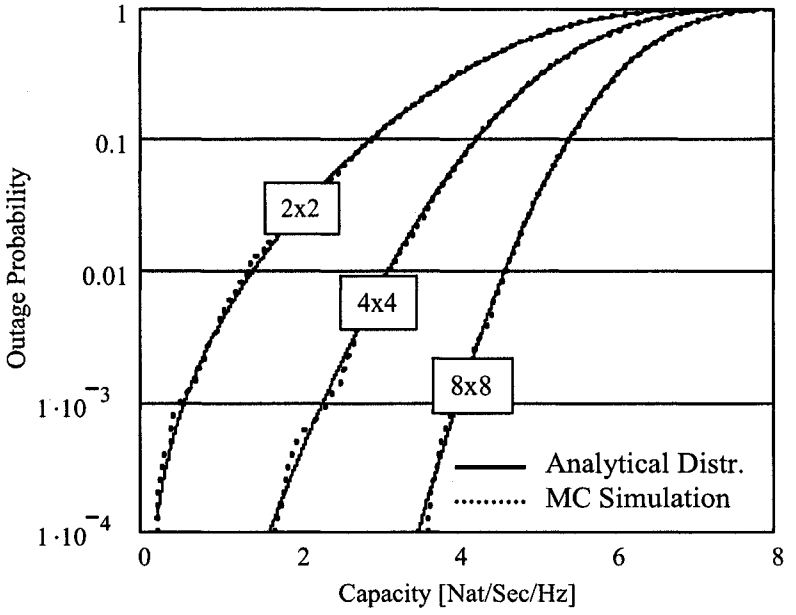

Fig. 3.1 Outage capacity of a keyhole channel: Analytical distribution (3.2) and Monte-Carlo (MC) simulation.

The SNR and the outage capacity distribution expressions have been validated by Monte-Carlo (MC) simulations for various n_t, n_r, γ_0, $\mathbf{R}_t$ and $\mathbf{R}_r$. As an example, Fig. 3.1 shows the outage capacity distribution (3.2) and the corresponding MC simulated one using 10,000 trials for $\gamma_0 = 20dB$ and $n_t \times n_r = 2\text{x}2$, 4x4 and 8x8. $\mathbf{R}_t$ and $\mathbf{R}_r$ were modeled using exponential correlation matrix (2.14) with correlation parameters $r_t = 0.5$ and $r_r = 0.8$ at the Tx and Rx ends respectively. The maximum deviation of the simulated distribution is within the $\pm\sigma$ error range, where σ is a standard deviation of the simulated distribution due to the finite statistics (10,000 trials) (see [21] and Chapter IX for more details

on the statistical analysis of MIMO channels). The $\pm\sigma$ boundaries are not shown for the figure clarity.

To get some insight into (3.2), consider a 2x2 keyhole MIMO channel with equal correlation matrices:

$$\mathbf{R}_t = \mathbf{R}_r = \begin{bmatrix} 1 & r \\ \bar{r} & 1 \end{bmatrix}, \ |r| < 1, \tag{3.8}$$

where $\bar{r}$ is a complex conjugate of r. Using the Maclaurin series of $x \cdot K_1(x)$ and $\exp(x)$, it is straightforward to show that for small x

$$F_C(x) \geq c \cdot \left[\frac{x}{\gamma_0 (1 - |r|^2)} \right]^2, \tag{3.9}$$

where $c = 5 - 4(\gamma_e - \ln(2))$ and $\gamma_e \approx 0.577$ is the Euler constant [119]. Using numerical simulations, we found that the lower bound in (3.9) gives a good approximation for the capacity distribution at outage probabilities $F_C(x) > 10^{-7}$. Moreover, (3.9) allows defining an effective average SNR γ_{eff}, as the SNR of an uncorrelated keyhole channel with the same probability of outage:

$$\gamma_{eff} = \gamma_0 (1 - |r|^2) \tag{3.10}$$

Apparently, an increase in correlation decreases the effective average SNR and results in lower capacity. For example, $|r| = 0.7$ corresponds to a $\approx 3dB$ decrease in γ_{eff}. Interestingly, (3.10) is identical to the effective SNR in the correlated Rayleigh channels with maximum ratio combining (MRC) [34]. Numerical simulations show that the impact of correlation on the outage capacity is accurately characterized by the effective average SNR not only for 2x2 keyhole channels, but also for channels with up to four antennas at each end. To demonstrate this, Fig. 3.2 compares the outage capacity distribution of 2x2, 3x3 and 4x4 correlated keyhole channels to that of the equivalent (with respect to effective average SNR) uncorrelated keyhole channels. For the correlated channels, $\mathbf{R}_t$ and $\mathbf{R}_r$ are simulated using exponential correlation model (2.14) with the same correlation parameter $|r| = 0.7$ at both Tx and Rx ends. The average SNR at the uncorrelated channels is set to γ_{eff} given by (3.10). It can be seen that the discrepancy between the capacity distributions of correlated and corresponding uncorrelated channels

increases with the number of antennas. Similar observations have been made for the channels where $\mathbf{R}_t$ and $\mathbf{R}_r$ were modeled by quadratic exponential correlation matrices (2.15). For more than 4x4 systems, the effective SNR alone is not enough to represent the effect of correlation. In this case (3.2) has a complicated form, which makes it difficult to obtain insight and to evaluate the effect of various parameters on the capacity. In particular, the effect of correlation is difficult to see. Moreover, when n_t or n_r are large and the correlation at the Tx or Rx ends is low, the partial fraction decomposition coefficients A_k in (3.5) become too large, so that numerical evaluation of (3.2) suffers from the loss of precision. To overcome these problems, we derive below the asymptotic outage capacity distributions when n_t, n_r or both are asymptotically large.

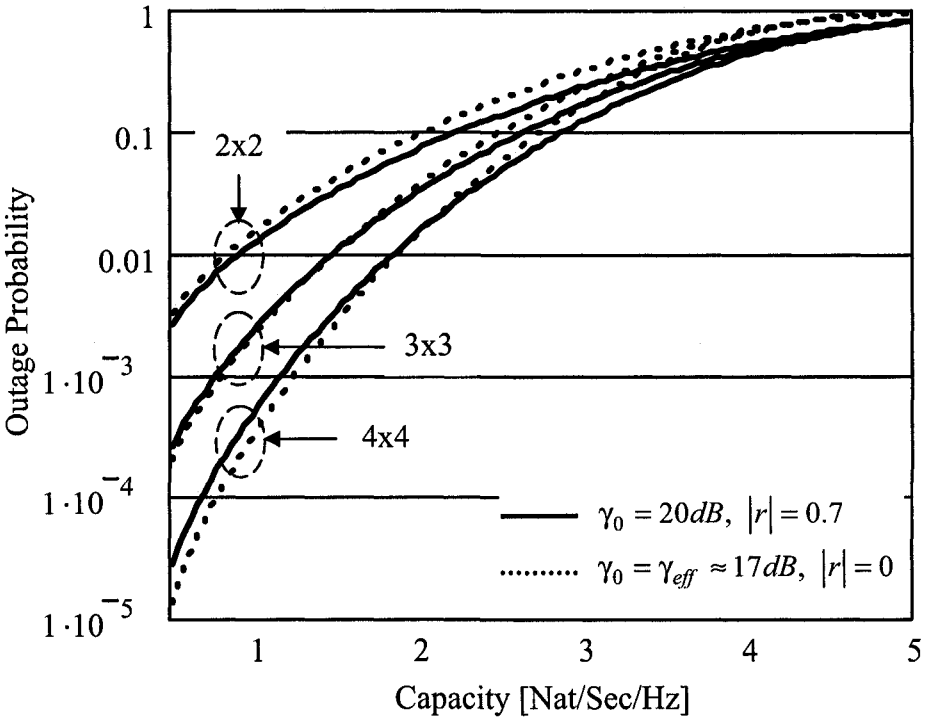

Fig. 3.2 Outage capacity distribution: Correlated keyhole channel (bold line), uncorrelated keyhole channel with effective average SNR (dotted line).

3.2. Asymptotic Outage Capacity Distributions

We begin with the following theorem.

Theorem 3.2: Consider an $n_t \times n_r$ keyhole channel, where $\mathbf{h}_t$ and $\mathbf{h}_r$ are mutually independent complex circular symmetric correlated Gaussian random vectors with zero mean and correlation matrices $\mathbf{R}_t$ and $\mathbf{R}_r$. (i) If $\lim_{n_t \to \infty} n_t^{-1} tr\{\mathbf{R}_t\} < \infty$ and $\lim_{n_t \to \infty} n_t^{-1} \|\mathbf{R}_t\| = 0$, then there is an asymptotically equivalent $1 \times n_r$ Rayleigh fading channel, so that the instantaneous capacities of both the keyhole and Rayleigh channels are identical in distribution as $n_t \to \infty$, i.e.

$$C \xrightarrow{d} \ln\left(1 + \gamma_0 \beta_r / n_r\right) \text{ as } n_t \to \infty \tag{3.11}$$

(ii) Due to the symmetry in (3.1) and under the same conditions, (3.11) holds true as $n_r \to \infty$, if Tx and Rx ends are exchanged.

Proof: see Appendix A.

The asymptotic behavior of the keyhole channel indicated by Theorem 3.2 is well explained by the fact that when $n_t (n_r) \to \infty$, the Rayleigh sub-channel (see Fig. 2.2) at the Tx (Rx) end is asymptotically a non-fading AWGN one with a single equivalent Tx (Rx) antenna, and the whole keyhole channel is equivalent to the Rx (Tx) diversity Rayleigh channel. This observation has already been made in [98] for uncorrelated keyhole channels. Theorem 3.2 shows that the same is true for the correlated keyhole channels under the aforementioned conditions.

Corollary 3.2: (i) If $\mathbf{R}_r$ is non-singular and has distinct eigenvalues, the asymptotic outage capacity distribution of the keyhole channel is given by

$$F_C(x) \to F_{\beta_r}\left(n_r (e^x - 1)/\gamma_0\right) \text{ as } n_t \to \infty, \tag{3.12}$$

where

$$F_{\beta_r}(x) = 1 - \sum_{k=1}^{n} A_k^r \exp\{-x/\lambda_k\}, x \geq 0 \tag{3.13}$$

(ii) Due to the symmetry in (2.49) and under the same conditions, (3.12) holds true as $n_r \to \infty$, if Tx and Rx ends are exchanged.

Proof: see Appendix A.

Consider the outage capacity distribution of a keyhole channel when the number of antennas increases. Assume that new antennas do not change the electromagnetic environment and thereby the channel for already existing ones. In such a case, an increase in the number of Tx antennas has two opposite effects: (i) under a total Tx power constraint, it decreases the average transmitted power per Tx antenna, and (ii) increases the diversity order of the channel. At low outage probabilities the effect of the increasing diversity order is dominant, which causes $F_C(x)$ to decrease. At high outage probabilities, the effect of decreasing Tx power prevails over the increasing diversity order so that $F_C(x)$ increases. Thus, the CDF curves of two keyhole channels with n and m $(m>n)$ Tx antennas and a fixed (same) number of Rx antennas should cross each other, so that at low outage probabilities the channel with m antennas has higher outage capacity and, correspondently, the channel with n antennas has higher outage capacity at high outage probabilities. Since the equivalent Rayleigh diversity channel is an asymptotic case of the keyhole channel as $n_t \to \infty$ the following inequality holds at low outage probabilities,

$$F_C^R(x) \le F_C^K(x), \tag{3.14}$$

where $F_C^K(x)$ and $F_C^R(x)$ are the capacity distributions of the keyhole and equivalent Rayleigh diversity channels respectively (i.e. at low outage probabilities, the outage capacity of the equivalent Rayleigh channel upper-bounds that of the keyhole one). To validate (3.14), the capacity distributions of correlated $n_t \times 3$ keyhole and equivalent 1x3 Rayleigh diversity channels are plotted in Fig. 3.3. The exponential correlation model (2.14) with the correlation parameter $|r| = 0.7$ was used to simulate both $\mathbf{R}_t$ and $\mathbf{R}_r$. Clearly, the outage capacity of the Rayleigh channel is higher than that of the keyhole one, the latter approached the former as n_t increases.

Even though Theorem 3.2 shows the relationship between the keyhole channel and the equivalent Rayleigh diversity channels, the asymptotic distribution in (3.12) is still complicated and does not contribute much to the understanding of the impact of various parameters in general and correlation in particular on the outage capacity. To gain such understanding, we proceed with the following theorem:

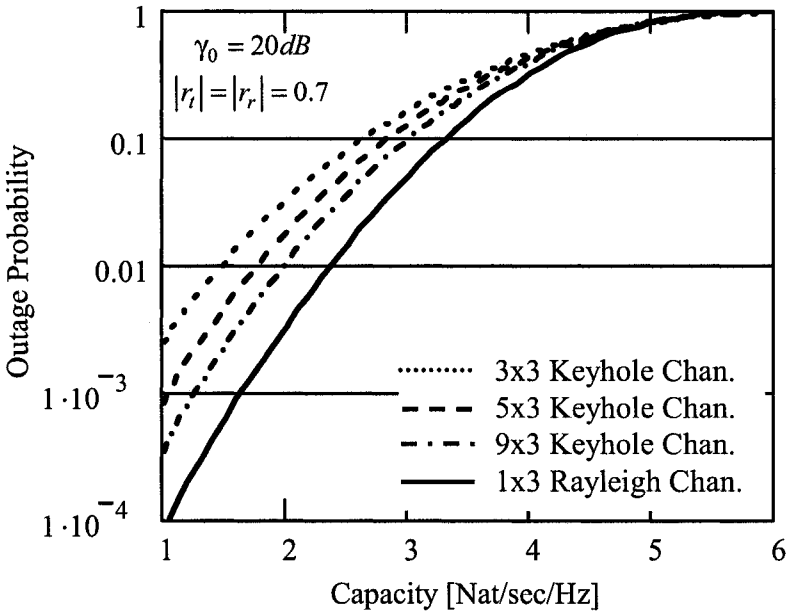

Fig. 3.3 Outage capacity distributions: n_tx3 keyhole and 1x3 Rayleigh correlated channels.

Theorem 3.3: Let C be the instantaneous capacity of the correlated keyhole channel defined in (3.1). When both n_t and n_r tend to infinity, the distribution of C is asymptotically Gaussian, if $\lim_{n_t\to\infty} n_t^{-1} tr\{\mathbf{R}_t\} < \infty$, $\lim_{n_r\to\infty} n_r^{-1} tr\{\mathbf{R}_r\} < \infty$ and $\lim_{n_t\to\infty} n_t^{-2} \|\mathbf{R}_t\|^2 = 0$, $\lim_{n_r\to\infty} n_r^{-2} \|\mathbf{R}_r\|^2 = 0$. Moreover, if $\mathbf{h}_t$ and $\mathbf{h}_r$ are normalized so that $\lim_{n_t\to\infty} n_t^{-1} tr\{\mathbf{R}_t\} = \lim_{n_r\to\infty} n_r^{-1} tr\{\mathbf{R}_r\} = 1$, the mean μ and the variance σ^2 of C are as follows:

$$\mu = \ln(1+\gamma_0);\ \sigma^2 = \left(\frac{\gamma_0}{1+\gamma_0}\right)^2 \left(\frac{1}{n_t^2}\|\mathbf{R}_t\|^2 + \frac{1}{n_r^2}\|\mathbf{R}_r\|^2\right) \tag{3.15}$$

Proof: see Appendix A.

Note that the conditions of Theorem 3.3 do not require distinct eigenvalues of the correlation matrices $\mathbf{R}_t$ and $\mathbf{R}_r$. Hence, the outage capacity distribution of the uncorrelated keyhole MIMO channel with $\mathbf{R}_t = \mathbf{R}_r = \mathbf{I}$ is asymptotically Gaussian, with $\mu = \ln(1+\gamma_0)$ and $\sigma^2 = [\gamma_0/(1+\gamma_0)]^2[n_t^{-1} + n_r^{-1}]$. It does not follow from (3.15) that an increase in the number of antennas always decreases the variance and thereby the outage probability, but only if σ^2 is monotonically decreasing with n_t and n_r, i.e. if $\|\mathbf{R}_t\|$ and $\|\mathbf{R}_r\|$ increase not faster than $n_t^{1-\varepsilon_1}$ and $n_r^{1-\varepsilon_2}$ respectively, for some $\varepsilon_1, \varepsilon_2 > 0$. Even though the

conditions of Theorem 3.3 do not require such monotonicity, we show below that exponential (2.14) and quadratic exponential correlation models (2.15) possess this property.

Since μ is a function of γ_0 only, the effect of correlation on the mean capacity vanishes asymptotically. In contrast, the variance σ^2 is affected by the correlation, but does not depend on the average SNR from moderate to high γ_0, since $\gamma_0/(1+\gamma_0) \approx 1$ in (3.15). This explains why for large n_t and n_r the effect of correlation is not adequately represented by the effective average SNR in (3.10). Note that the asymptotic mean capacity in (3.15) is identical to the upper bound on the mean capacity of the finite order uncorrelated keyhole channel given in [98], i.e. Theorem 3.3 shows that the bound also holds for the correlated channels and it is asymptotically tight.

To analyze σ^2 in (3.15), consider $\mathbf{R} \in \Re$, where $\Re$ is a set of all $n \times n$ correlation matrices such that $tr(\mathbf{R}) = n$. It is straightforward to show (see Chapter V) that

$$n^{-1} \le n^{-2} \|\mathbf{R}\|^2 \le 1, \tag{3.16}$$

where the lower bound is achieved if $\lambda_k = \lambda_m$ for all $k,m = 1...n$ ($\mathbf{R} = \mathbf{I}$), where λ_k are eigenvalues of $\mathbf{R}$, i.e. $n^{-2}\|\mathbf{R}\|^2$ achieves minimum when the channel at the Tx(Rx) end is uncorrelated with the same power at each Tx (Rx) antenna. The upper bound is achieved if $\lambda_k = n$ for some k, and $\lambda_m = 0 \ \forall m \ne k$, i.e. $n^{-2}\|\mathbf{R}\|^2$ achieves maximum when the channel at the Tx (Rx) end is fully correlated. For more detailed discussion on the metric $n^{-2}\|\mathbf{R}\|^2$ see Chapter V.

Corollary 3.3: Consider two keyhole channels with the same n_t, n_r, γ_0 and with different $\mathbf{R}_t$, $\mathbf{R}_r$, so that $\sigma_1^2 > \sigma_2^2$. Under the conditions of Theorem 3.3, $F_C^1(x) > F_C^2(x)$ for $x < \mu$, and $F_C^1(x) < F_C^2(x)$ for $x > \mu$, i.e. the channel with higher σ^2 has smaller outage capacity (higher outage probability) at the small outage region ($F_C(x) < 1/2$), and larger one at the high outage region ($F_C(x) > 1/2$); (this range, however, has limited importance from practical perspective).

Proof: Under the conditions of Theorem 3.3, the outage capacity of both channels is asymptotically Gaussian with equal means $\mu_1 = \mu_2 = \mu$. Compare two equal-mean Gaussian CDF's $F_C^1(x)$ (with variance σ_1^2) and $F_C^2(x)$ (with variance σ_2^2). It follows that they cross each other at the single point $x = \mu$ such that $F_C^1(\mu) = F_C^2(\mu) = 1/2$, and that $F_C^1(x) > F_C^2(x)$ for $x < \mu$, and $F_C^1(x) < F_C^2(x)$ for $x > \mu$. **Q.E.D.**

To validate the general discussion above and to show explicitly the impact of correlation on the asymptotic outage capacity distribution, consider two single-parameter correlation matrix models for $\mathbf{R}_t$ and $\mathbf{R}_r$.

Exponential Correlation Model: $\mathbf{R}$ given by the exponential model (2.14) satisfies the conditions of Theorem 3.3, i.e. $n^{-1}tr\{\mathbf{R}\}=1$ and $\lim_{n_t\to\infty} n_t^{-2}\|\mathbf{R}_t\|^2=0$, since

$$\lim_{n\to\infty} n^{-1}\|\mathbf{R}\|^2=\frac{1+|r|^2}{1-|r|^2}<\infty,\ |r|<1 \tag{3.17}$$

(see Appendix A for a proof). Thus, when both $\mathbf{R}_t$ and $\mathbf{R}_r$ are given by the exponential model, the outage capacity distribution of such a keyhole channel is asymptotically Gaussian with the mean given in (3.15) and the variance well approximated for large n_t and n_r by

$$\sigma^2\approx\left(\frac{\gamma_0}{1+\gamma_0}\right)^2\left(\frac{1}{n_t}\cdot\frac{1+|r_t|^2}{1-|r_t|^2}+\frac{1}{n_r}\cdot\frac{1+|r_r|^2}{1-|r_r|^2}\right), \tag{3.18}$$

where r_t and r_r are the correlation parameters in $\mathbf{R}_t$ and $\mathbf{R}_r$ respectively. Note that the asymptotic approximation of σ^2 is monotonically decreasing with n_t and n_r (monotonicity property). To get some insight, assume that $n=n_t=n_r$ and $r=r_t=r_r$; then, for the same γ_0 in both channels, the capacity distributions of uncorrelated $r=0$ and correlated $r\neq 0$ channels have the same mean $\mu=\ln(1+\gamma_0)$, but different variances σ_u^2 and σ_c^2, so that for large n_t and n_r

$$\eta=\frac{\sigma_c^2}{\sigma_u^2}\approx\frac{1+|r|^2}{1-|r|^2}\geq 1,\ |r|<1 \tag{3.19}$$

From (3.19), η is a monotonically increasing function of $|r|$, i.e. the larger $|r|$ results in larger σ_c^2 comparing to σ_u^2. Thus, following the general discussion above, the outage capacity of the uncorrelated asymptotic channel is larger than that of the correlated one at outage probabilities less than 0.5. Note that if $|r|$ is very small, the capacity gap between correlated and uncorrelated channels can still be significant at low outage probabilities. As an example, Fig. 3.4 shows the asymptotic outage capacity distributions of the 3x3 keyhole channels with exponential correlation at both ends for $|r|=|r_t|=|r_r|$. Clearly, the outage

capacity decreases at outage probabilities less than 0.5 as $|r|$ increases. For $|r| \le 0.2$, correlation has no significant impact on the asymptotic capacity except at extremely low outage probabilities.

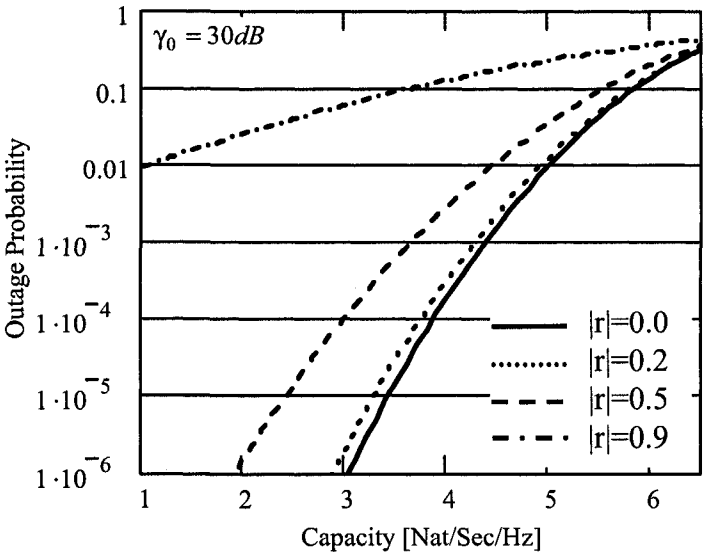

Fig. 3.4 Asymptotic outage capacity distributions of 3x3 keyhole channels with exponential correlation.

Quadratic Exponential (QE) Model: $\mathbf{R}$ given by the QE model (2.15) satisfies the conditions of Theorem 3.3, i.e. $\lim_{n\to\infty} n^{-1} tr\{\mathbf{R}\} = 1 < \infty$ and

$$\left[1 + \sqrt{\frac{\pi}{-2\ln|r|}} \cdot erfc\{\sqrt{-2\ln|r|}\}\right] \le \lim_{n\to\infty} n^{-1} \|\mathbf{R}\|^2 \le \left[1 + \sqrt{\frac{\pi}{-2\ln|r|}}\right], \quad |r| < 1, \tag{3.20}$$

where $erfc(x)$ is the complementary error function [119] (see Appendix A for a proof). Since both the upper and lower bounds on $\lim_{n\to\infty} n^{-1} \|\mathbf{R}\|^2$ are finite, $\lim_{n\to\infty} n^{-2} \|\mathbf{R}\|^2 = 0$. Thereby, from Theorem 3.3, the outage capacity distribution of the keyhole channel with QE correlation at both the Tx and Rx ends is asymptotically Gaussian with the mean $\mu = \ln(1+\gamma_0)$ and the variance bounded asymptotically by

$$\begin{aligned} \sigma^2 &\le \left(\frac{\gamma_0}{1+\gamma_0}\right)^2 \left(\frac{1}{n_t} \cdot \left[1 + \sqrt{\frac{\pi}{-2\ln|r_t|}}\right] + \frac{1}{n_r} \cdot \left[1 + \sqrt{\frac{\pi}{-2\ln|r_r|}}\right]\right) \\ \sigma^2 &\ge \left(\frac{\gamma_0}{1+\gamma_0}\right)^2 \left(\frac{1}{n_t} \cdot \left[1 + \sqrt{\frac{\pi}{-2\ln|r_t|}} \cdot erfc\{\sqrt{-2\ln|r_t|}\}\right] + \frac{1}{n_r} \cdot \left[1 + \sqrt{\frac{\pi}{-2\ln|r_r|}} \cdot erfc\{\sqrt{-2\ln|r_r|}\}\right]\right), \end{aligned} \tag{3.21}$$

where the bounds are obtained for large n_t and n_r. Numerical simulations show that σ^2, as well as its upper and lower bounds, decreases monotonically with n_t and n_r (monotonicity property), and increases with $|r_t|$ and/or $|r_r|$. As the result, similarly to the exponential model, the outage capacity decreases with correlation at outage probabilities less than 0.5.

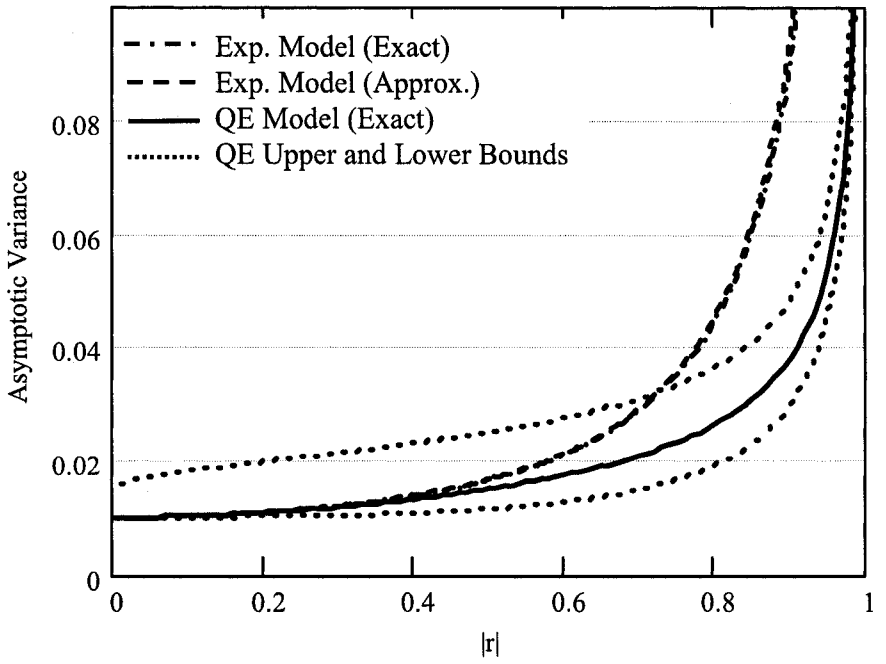

Fig. 3.5 $n^{-2}\|\mathbf{R}\|^2$ in exponential and QE models vs. correlation parameter. The variance of outage capacity distribution follows the same tendency (see (3.15)).

To demonstrate the effect of rate of correlation decay with distance $|m-k|$ on the outage capacity, Fig. 3.5 shows $n^{-2}\|\mathbf{R}\|^2$ vs. $|r|$ for $n=100$ when $\mathbf{R}$ is given by the exponential and QE models. $n^{-2}\|\mathbf{R}\|^2$ is numerically evaluated for both models and is shown together with the approximation in (3.17) (for the exponential model) and the bounds in (3.20) (for the QE model). For low correlations, $|r|<0.4$, $n^{-2}\|\mathbf{R}\|^2$ in both models are very close. For $|r|\geq 0.4$, $n^{-2}\|\mathbf{R}\|^2$ in the exponential model increases more rapidly with $|r|$ as compared to the QE model. Apparently, the more rapidly the correlation decays with distance, as in the QE model, the higher r can be tolerated without significant loss in capacity. Thus, the effect of correlation on outage capacity is characterized not just by the correlation between adjacent antennas, but

also by its rate of decay with distance $|m-k|$.

We have also considered the uniform correlation model (2.13). Unlike the exponential and QE, this model does not satisfy the conditions of Theorem 3.3 ($\lim_{n\to\infty} n^{-2}\|\mathbf{R}\|^2 \neq 0$), so it impossible to say based on Theorem 3.3 whether the outage capacity of a keyhole channel with uniform correlation is asymptotically Gaussian as $n_t, n_r \to \infty$.

- *Convergence rate and numerical results*:

From the practical point of view, the asymptotic analysis above is important as an approximation to real channels with a finite number of antennas. From the proof of Theorem 3.3 (see Appendix A), the outage capacity converges to the Gaussian distribution with the same rate as $n_t^{-1}\|\mathbf{R}_t\|$ and $n_r^{-1}\|\mathbf{R}_r\|$ go to zero, which is $1/\sqrt{n}$ (n is either n_t or n_r) for the exponential and QE correlation models as follows from (3.17) and (3.20). Extensive numerical simulations were used to assess the accuracy of the asymptotic approximation. Some of the results are shown in Fig. 3.6, where the exact capacity distributions of 2x2, 3x3 and 5x5 keyhole channels with exponential correlation at both Tx and Rx ends are compared to the corresponding Gaussian approximations. The difference between the Gaussian approximation and the exact distribution is negligible for most practical purposes. In general, for finite n_t and n_r, the asymptotic distribution overestimates the exact one. When the approximation (3.17) or the upper bound in (3.20) are used in place of the true σ^2, the exact distribution, in some cases, follows closely the asymptotic one already for 2 antennas at each end. However, we were not able to find a compact general rule indicating the accuracy of the approximation for arbitrary parameters.

The asymptotic normality of the outage capacity is not a unique property of the keyhole channels with Rayleigh fading sub-channels but can be generalized for a wider class of keyhole channels as follows from the following theorem.

Theorem 3.4: Let C be the instantaneous capacity of the correlated keyhole channel, where $\mathbf{h}_t \propto \mathbf{R}_t^{1/2}\mathbf{g}_t$ and $\mathbf{h}_r \propto \mathbf{R}_r^{1/2}\mathbf{g}_r$, $\propto$ denotes identical distribution, $\mathbf{g}_t$ and $\mathbf{g}_r$ are zero mean complex random vectors with independent entries (not necessarily identically distributed or complex Gaussian). Let the distribution of $\mathbf{g}_t$ and $\mathbf{g}_r$ be invariant under unitary transformation. When both n_t and n_r tend to

infinity, the distribution of C is asymptotically normal if: (i) $m_{2+\delta}(k)<\infty$ and $m_2(k)>0$ for all k and some $\delta>0$, where $m_\delta(k)=E\{(|g_k|^2-E\{|g_k|^2\}^\delta\}$ is the central moment of $|g_k|^2$ of order δ, and g_k is the k^{th} entry of either $\mathbf{g}_t$ or $\mathbf{g}_r$. (ii) Both $\mathbf{R}_t$ and $\mathbf{R}_r$ satisfy a Lyapounov-type condition

$$\lim_{n_t\to\infty}\|\lambda\|_{2+\delta}/\|\lambda\|_2=0, \tag{3.22}$$

where $\|\lambda\|_m=\left(\sum_{i=1}^{n}(\lambda_i)^m\right)^{1/m}$ is the L_m norm of the eigenvalues.

Proof: see Appendix A.

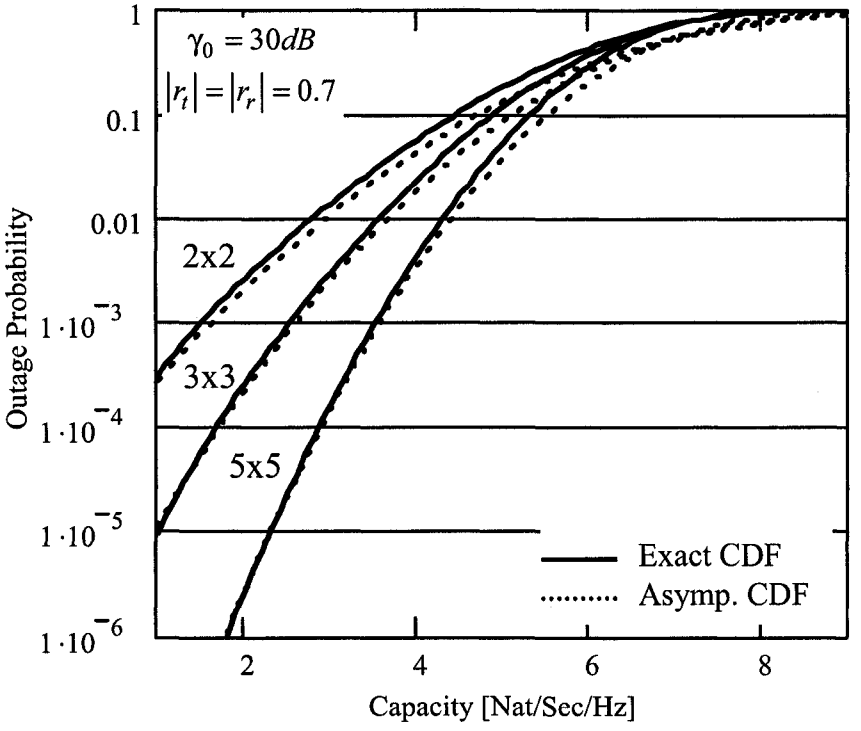

Fig. 3.6 Keyhole channel exact outage capacity and its asymptotic approximation.

The Lyapounov-type condition (3.22) is also important for asymptotic analysis of Rayleigh-fading channels [69]. Its detailed theoretical analysis and some physical interpretations are presented in Chapter VI. Even though condition (3.22) has a closed form, its usefulness for practical computations is rather limited due to two reasons: (i) The eigenvalues are known in a closed form only for some simple matrices. Consequently, the above condition can be evaluated analytically only in such cases. (ii)

Numerical evaluation of this condition is also difficult, since the numerical complexity (number of operations, inaccuracy, etc.) of the eigenvalue problem increases rapidly with n, so that for $n \to \infty$ it is problematic if possible at all. The following corollary gives a condition that is easier to evaluate.

Corollary 3.4: If both $\mathbf{R}_t$ and $\mathbf{R}_r$ have Toeplitz structure, i.e. the k-m^{th} element of $\mathbf{R}$ (either $\mathbf{R}_t$ or $\mathbf{R}_r$) is $R_{km} = R_{k-m}$, then (3.22) is equivalent to

$$\lim_{n\to\infty} n^{-1} \|\mathbf{R}\|^2 < \infty \tag{3.23}$$

for both $\mathbf{R}_t$ and $\mathbf{R}_r$.

Proof: see Appendix A.

Note that if $\lim_{n\to\infty} n^{-1} \|\mathbf{R}\|^2 < \infty$, then $\lim_{n\to\infty} n^{-2} \|\mathbf{R}\|^2 = 0$, i.e. there is an analogy between the conditions of Theorem 3.3 and Corollary 3.4, as both require $n^{-1}\|\mathbf{R}\|$ to vanish asymptotically. Theorem 3.3, however, does not require Toeplitz structure of $\mathbf{R}_t$ and $\mathbf{R}_r$ but is restricted to complex Gaussian $\mathbf{h}_t$ and $\mathbf{h}_r$. Since Corollary 3.4 applies to a wider class of $\mathbf{h}_t$ and $\mathbf{h}_r$, it indicates that the measure $n^{-1}\|\mathbf{R}\|$ has a higher degree of universality than just for MIMO channels defined through complex Gaussian random vectors.

3.3. Bounds on Mean Capacity

Even though the outage capacity is the relevant performance measure for non-ergodic fading channels, the mean capacity is also important as it gives an upper limit on error-free information rate supported by ergodic channels. The exact expression for the mean capacity $\overline{C}$ of a correlated keyhole channel is rather complicated and involves Meijer G-functions (see (2.51)). However, under the adopted normalization and using (3.1) and Jensen inequality [119], it is straightforward to show that the upper bound on $\overline{C}$ of correlated keyhole channels is

$$\overline{C} \le \ln(1+\gamma_0) \tag{3.24}$$

This bound does not depend on correlation and identical to that proposed by in [97] for the uncorrelated channels. [20] has proposed a tight lower bound

$$\bar{C} \geq \ln(1+\gamma_0 \exp[\Theta(\mathbf{R}_t)+\Theta(\mathbf{R}_r)]/[n_t n_r]), \tag{3.25}$$

where, based on Eq. 15 in [20], if $\mathbf{R}$, either $\mathbf{R}_t$ or $\mathbf{R}_r$, is non-singular and have distinct eigenvalues,

$$\Theta(\mathbf{R}) = -\gamma_e + \sum_{k=1}^{n} A_k \ln(\lambda_k) \tag{3.26}$$

(for a proof see Appendix A). From Theorem 3.3, the upper bound (3.24) is asymptotically tight with respect to the number of antennas at both the Tx and Rx ends. In addition, in Appendix A, we show that: (i) the lower bound (3.25) is easily obtained using the instantaneous SNR distribution given by Theorem 3.1 (this indirectly validates (3.3), (3.4)). (ii) While the upper bound (3.24) is tight as $\gamma_0 \to 0$, the lower bound (3.25) is tight as $\gamma_0 \to \infty$ (the last statement has been demonstrated in [20] for non-correlated channels; we extend this results for correlated channels as well). To illustrate (i) and (ii), Fig. 3.7 shows the mean capacity and its bounds of 2x2 and 12x12 keyhole channels vs. γ_0. $\bar{C}$ was numerically evaluated using the instantaneous SNR PDF in (3.3). The exponential correlation model with the same correlation parameter $|r_t| = |r_r| = 0.5$ was used at both the Tx and Rx ends. Clearly, the lower bound is tight (for 12x12 channel, it is practically indistinguishable from the true mean capacity), the upper bound becomes tight for both 2x2 and 12x12 at low SNR.

- *Impact of correlation*:

Unlike the outage capacity, which reduces significantly with correlation, the mean capacity of keyhole channels is almost independent of correlation (even very high one), see Fig. 3.8. An intuitive explanation of this is that very high correlation reduces the effective rank of a full-rank channel; for instance, the rank of a fully correlated channel ($|r| = 1$) is one regardless of the number of antennas. As the result, the mean capacity of a full-rank channels reduces dramatically with correlation when it is high [63], primarily due to loss in the effective rank at high correlation. Unlike full-rank channels, the rank of a keyhole channel is already one, regardless of correlation, and hence no further loss in rank is possible, so that the mean capacity is not affected much.

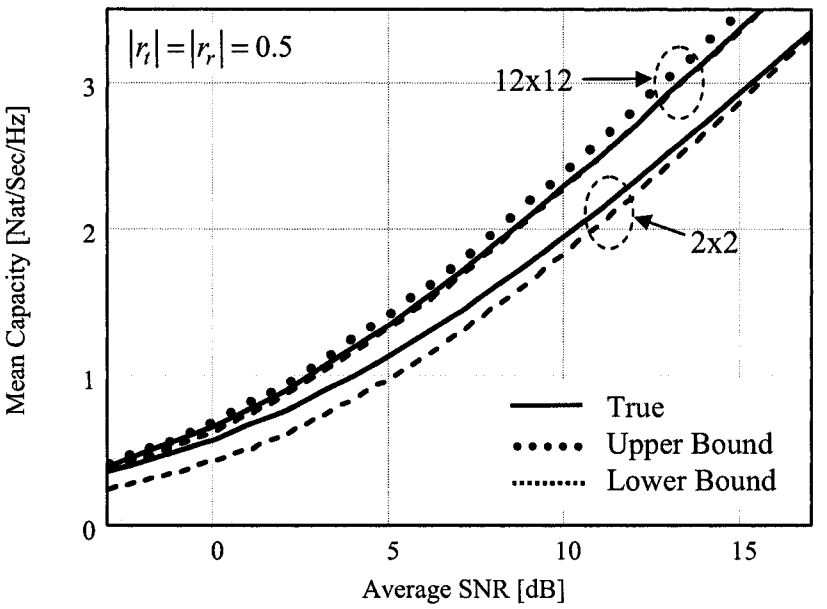

Fig. 3.7 Mean capacity of correlated keyhole channels vs. SNR.

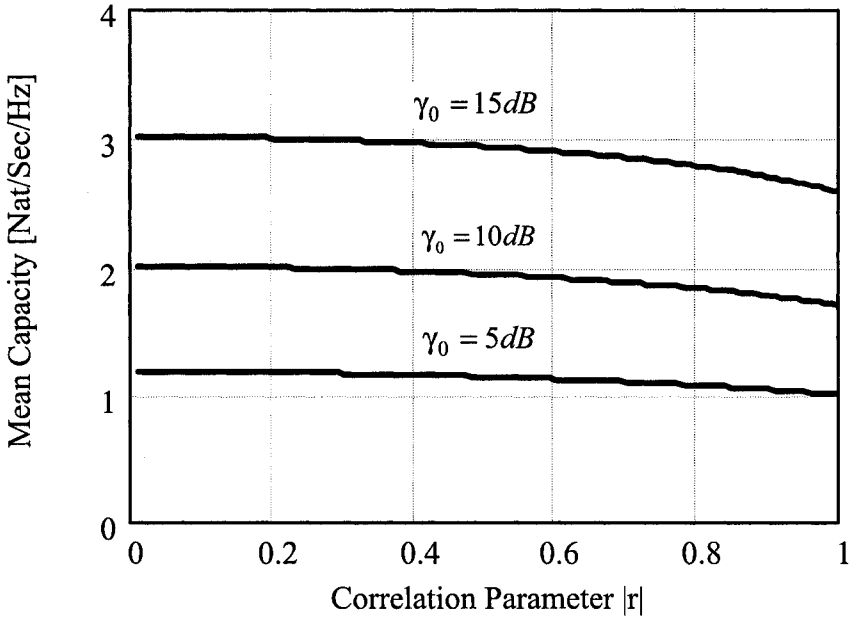

Fig. 3.8 Mean capacity of 2x2 keyhole channel with exponential correlation vs. correlation parameter $|r| = |r_t| = |r_r|$.

It also follows from the comparison between the mean capacity of various keyhole channels and the upper bound in (3.24) that the discrepancy between the two does not exceed 30% in the worst case. Thus, the upper bound can be used as a simple rough approximation for the mean capacity regardless of correlation.

3.4. Summary

A profound reason to study keyhole channels is not only in practical applications (i.e. as a model of physical propagation channels), but also due to the unique position of these channels as a model of the worst case MIMO propagation scenario (i.e. rank-one MIMO channels). The investigation of the keyhole channels can reveal how well a system performs in channels other than the Rayleigh ones (which were extensively studied and are well understood by now), and how much the results established for the Rayleigh channels apply elsewhere (i.e. robustness). The present study shows that the outage capacity of the keyhole channel is upper-bounded by that of the equivalent Rayleigh diversity channel. Despite the degenerated nature of keyhole channels, their outage capacity, similarly to full-rank Rayleigh channels, is asymptotically Gaussian, when the number of antennas is large. Subchannel distribution changes the keyhole channel statistics, but the asymptotic normality is preserved. This conclusion, together with other results on the asymptotic outage capacity of uncorrelated and correlated MIMO channels [69], [75], [108], [32] indicates that the Gaussian distribution has a high degree of universality in the outage capacity analysis of MIMO channels in general.

The results of this chapter are presented in [47] and [51].

CHAPTER IV: CAPACITY OF MULTI-KEYHOLE CHANNELS

The ideal keyhole channel is not often encountered in practice [4], [5], since the assumption of a single non-zero eigenmode is only a rough approximation for most propagation scenarios. In this chapter we introduce a more realistic model for channels with multiple keyholes, the "multi-keyhole channel", which describes the channels where the link between Tx and Rx ends is established, for example, due to multiple edge diffractions, propagation via several waveguides, or a number of relay nodes. It is shown that the proposed multi-keyhole model overlaps the double-scattering model [27]. Unlike the latter, the present model describes a propagation environment where the scatterers are located far apart from each other and, therefore, statistically independent. The outage capacity distribution of the multi-keyhole channels is studied in this chapter under the assumption that the number of antennas at Tx, Rx or both ends is asymptotically large.

4.1. Mathematical Model

Consider a spatially correlated multi-keyhole MIMO channel (see Fig. 4.1). In analogy with the keyhole channel (see Chapter III), the channel matrix $\mathbf{H}$ can be represented by the following linear combination:

$$\mathbf{H} = \sum_{k=1}^{M} a_k \mathbf{h}_{rk} \mathbf{h}_{tk}^H = \mathbf{H}_r \mathbf{A} \mathbf{H}_t^H, \tag{4.1}$$

where M is a number of keyholes, a_k, $k = 1...M$ is a complex gain of the k-th keyhole, $\mathbf{h}_{tk}$ $[n_t \times 1]$ and $\mathbf{h}_{rk}$ $[n_r \times 1]$ are random vectors representing the complex gains from the transmit antennas to the k-th keyhole and from the k-th keyhole to the receive antennas respectively; $\mathbf{H}_t = [\mathbf{h}_{t1}...\mathbf{h}_{tM}]$, $\mathbf{H}_r = [\mathbf{h}_{r1}...\mathbf{h}_{rM}]$ are $[n_t \times M]$ and $[n_r \times M]$ matrices respectively, and $\mathbf{A}$ is a $[M \times M]$ diagonal matrix with elements $\mathbf{A}_{kk} = a_k$.

We assume that (i) for every k, $\mathbf{h}_{tk}$ and $\mathbf{h}_{rk}$ are mutually independent complex circular symmetric Gaussian vectors with corresponding correlation matrices $\mathbf{R}_{tk} = E\{\mathbf{h}_{tk}\mathbf{h}_{tk}^H\}$ and $\mathbf{R}_{rk} = E\{\mathbf{h}_{rk}\mathbf{h}_{rk}^H\}$, (ii) the

keyholes are statistically independent, i.e. $E\{\mathbf{h}_{tk}\mathbf{h}_{tm}^H\} = E\{\mathbf{h}_{rk}\mathbf{h}_{rm}^H\} = \mathbf{0}$ for any $k \neq m$, and (iii) $\mathbf{h}_{tk}$ and $\mathbf{h}_{rk}$ are normalized so that for every k, $n_t^{-1}E\{\|\mathbf{h}_{tk}\|^2\} = 1$ and $n_r^{-1}E\{\|\mathbf{h}_{rk}\|^2\} = 1$, which implies, under $E\{\|\mathbf{H}\|^2\} = n_t n_r$, that

$$\sum_{k=1}^{M} |a_k|^2 = 1, \tag{4.2}$$

Note that the channel model in (4.1) overlaps with the double-scattering model proposed in [27]. In the former case the keyholes represent scatterers located far apart from each other. The main differences between the two models (see (4.1) and [[27], Eq. 13]) are:

(i) Unlike the double-scattering model, where all $\mathbf{R}_{tk}$, $\mathbf{R}_{rk}$ are equal to the common Tx and Rx correlation matrices $\mathbf{R}_t$, $\mathbf{R}_r$ respectively, each keyhole (scatterer) in the multi-keyhole model has a distinct pair $\mathbf{R}_{tk}$, $\mathbf{R}_{rk}$, $k = 1...M$. Apparently, when the distance between keyholes is large, the corresponding Tx and Rx correlation cannot be accurately described by only two Tx, Rx correlation matrices common for all keyholes, due to the wide spread of angle-of-arrival (AOA) (see [93] for more detail).

(ii) While the model in [27] considers, in general, correlated scatterers, the keyholes in the multi-keyhole model are assumed to be uncorrelated due to the large separation. In this sense, the multi-keyhole model is complementary to that in [27], as both models describe a sparse and dense double-scattering propagation environments respectively.

By substituting (4.1) in (3.1), it is straightforward to show that the instantaneous capacity of a frequency flat quasi-static multi-keyhole MIMO channel in natural units $[nat]$ with CSI available at Rx end only is given by:

$$C = \ln\det[\mathbf{I} + \gamma_0 \mathbf{B}_r \mathbf{A} \mathbf{B}_t \mathbf{A}^H], \tag{4.3}$$

where $\mathbf{B}_t = \mathbf{H}_t^H \mathbf{H}_t / n_t$ and $\mathbf{B}_r = \mathbf{H}_r^H \mathbf{H}_r / n_r$. Following (4.3), the multi-keyhole and the Rayleigh fading channels have different outage capacity distribution. However, there is a relationship between the two channels, which is indicated by the following theorem.

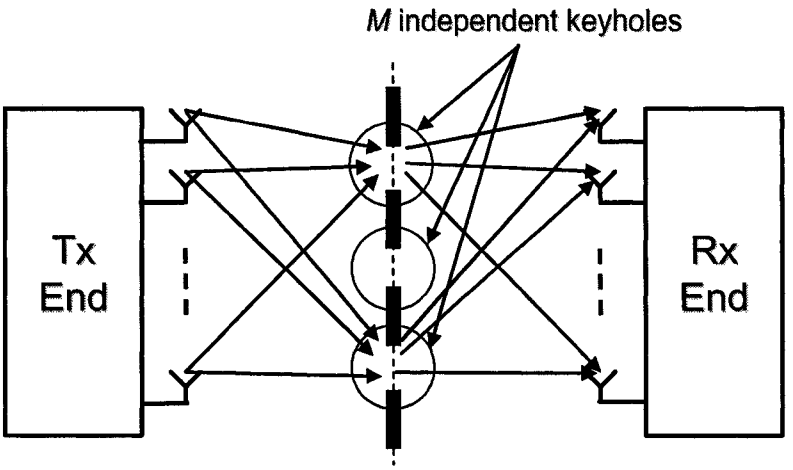

Fig. 4.1 Multi-keyhole MIMO channel. Each end has multipath so that the sub-channels are correlated Rayleigh fading.

Theorem 4.1: (i) If $n_t^{-1}tr\{\mathbf{R}_{tk}\}=c<\infty$ and $n_t^{-2}tr[\mathbf{R}_{tk}\mathbf{R}_{tm}]\to 0$ as $n_t\to\infty$ for $\forall k,\ m=1...M$, then for an $[n_t\times n_r]$ multi-keyhole channel with M independent keyholes, there is an equivalent $[M\times n_r]$ Rayleigh fading channel, so that the instantaneous capacities of both channels are identical in probability as $n_t\to\infty$. If $c=1$, the instantaneous capacity is

$$C\xrightarrow{p}\ln\left(\det[\mathbf{I}+\gamma_0\mathbf{H}_r\mathbf{Q}\mathbf{H}_r^H/n_r]\right)\text{ as }n_t\to\infty, \tag{4.4}$$

where $\xrightarrow{p}$ means convergence in probability, $\mathbf{H}_r$ is a matrix of the equivalent Rayleigh channel, and $\mathbf{Q}=\mathbf{A}\mathbf{A}^H$ is the Tx covariance matrix.

(ii) Due to the symmetry in (4.3), (4.4) also holds true as $n_r\to\infty$, if Tx and Rx ends are exchanged.

Proof: see Appendix B.

The following arguments give an intuitive explanation of Theorem 4.1. For large n_t, the Rayleigh sub-channel at the Tx end (see Fig. 4.1) is asymptotically non-fading AWGN due to the large diversity order, so that the total channel becomes Rayleigh-fading with M equivalent uncorrelated Tx antennas, each with the power gain $|a_k|^2$. The equivalent antennas are uncorrelated as the keyholes are assumed to be independent. Similarly, when n_r is large, the total channel is asymptotically Rayleigh fading with M equivalent uncorrelated Rx antennas, each with the power gains $|a_k|^2$. Theorem 4.1 is a generalization of

Theorem 3.2 obtained for $M=1$. As a numerical example, the outage capacity distributions of $[n_t \times 2]$ multi-keyhole channels with 2 independent keyholes ($|a_1|=|a_2|=1/\sqrt{2}$) and the equivalent 2x2 Rayleigh channel are shown in Fig. 4.2. The Kronecker correlation model (2.9) has been used to simulate the correlation in the Rayleigh channel. All correlation matrices for both the multi-keyhole and Rayleigh channels have been modeled using the exponential correlation model (2.14) with correlation parameter $r=0.5$ at both the Tx and Rx ends[4]. From Fig. 4.2, as the number of Tx antennas increases, the outage capacity (for a given outage probability) increases with the number of Tx antennas and asymptotically approaches the outage capacity of the equivalent 2x2 Rayleigh channel (a bold solid line). The difference between the capacities becomes practically negligible for $n_t=8$.

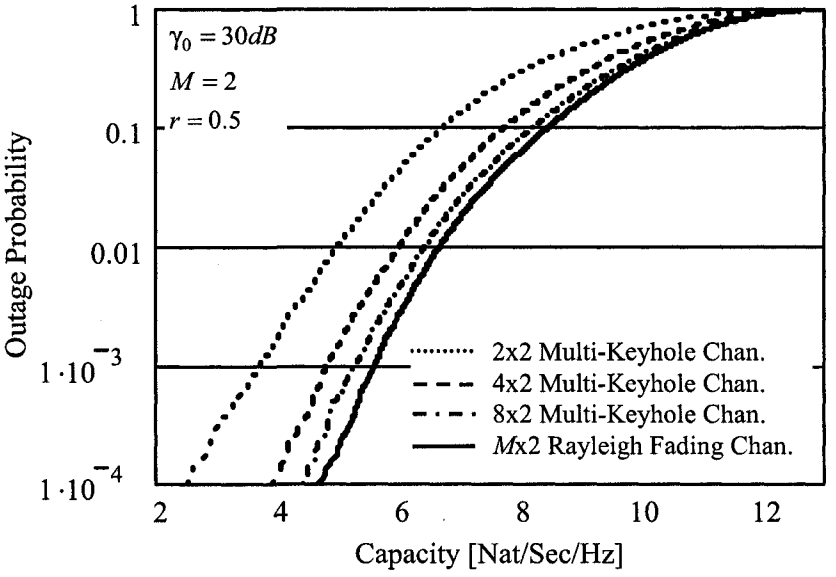

Fig. 4.2 Outage capacity distribution of multi-keyhole channel.

By examing (4.1), one may distinguish between two different types of multi-keyhole MIMO channels: (i) a full-rank multi-keyhole (FRMK) channel, where $M \geq \min\{n_t, n_r\}$, and (ii) rank-deficient multi-keyhole (RDMK) channel, where $M < \min\{n_t, n_r\}$. Note that similarly to a Rayleigh-fading

[4] Unless otherwise is stated, the Kronecker and exponential correlation models are applied across this chapter for numerical examples.

channel, the multiplexing gain of a FRMK one is limited by $\min\{n_t, n_r\}$. In contrast, the multiplexing gain of a RDMK channel is limited by M. These qualities play a major role in different statistical behavior of FRMK and RDMK channels, as shown by the following analysis.

4.2. Full-Rank Multi-Keyhole Channels

Below we show that a FRMK channel becomes a Rayleigh fading one as $M \to \infty$. While this result is intuitively clear[5], it requires some non-trivial conditions as given by the following theorem.

Theorem 4.2: (i) Consider a full-rank multi-keyhole channel with channel matrix $\mathbf{H}$ given by (4.1), where $\mathbf{h}_{tk}$ and $\mathbf{h}_{rk}$ are not necessarily Gaussian but have a circular symmetric distribution with finite fourth-order moments, i.e. $E\{\|\mathbf{h}_{tk}\|^4\} < \infty$ and $E\{\|\mathbf{h}_{rk}\|^4\} < \infty$ for $\forall k$. Let the inverse of matrix $\mathbf{C} = \sum_{k=1}^{M} |a_k|^2 \left(\mathbf{R}_{tk}^T \otimes \mathbf{R}_{rk}\right)$ exist as $M \to \infty$. Then $\mathbf{H}$ is asymptotically circular symmetric complex Gaussian in distribution as $M \to \infty$, if under normalization (4.2)[6]

$$\lim_{M\to\infty} \sum_{k=1}^{M} |a_k|^3 = 0 \tag{4.5}$$

(ii) Assume that $\mathbf{C}$ does not depend on M[7]. Let $\Delta_M(\mathbf{x}) = |F_M(\mathbf{x}) - \Phi(\mathbf{x})|$, where $F_M(\mathbf{x})$ is the CDF of $\mathbf{x} = vec(\mathbf{H})$ for given M, and $\Phi(\mathbf{x})$ is a normal CDF with the same mean and variance as that of $vec(\mathbf{H})$. Then $\Delta_M(\mathbf{x}) \to 0$ as $M \to \infty$ with at least the same rate as $\sum_{k=1}^{M} |a_k|^3$.

Proof: see Appendix B.

Let us consider some special cases when Theorem 4.2 does not apply. These cases can be characterized using the following corollary:

Corollary 4.2.1: Consider $|a_1| \geq |a_2| \geq \ldots \geq |a_M|$ sorted in a non-increasing order. (4.5) does not hold true, if there is a finite set of keyholes which are not dominated by the rest, i.e. there exists such k that

---

[5] The multipath becomes richer with M and so the channel distribution has more pronounced Rayleigh statistics.

[6] It is implied that for every M there is a complete sequence $\{a_k\} = \{a_k^M\}$, such that both (4.2) and (4.5) are satisfied simultaneously. We drop the superscript M to avoid abusive notation.

[7] Note that under the normalization (4.2), $\mathbf{C}$ is the "average correlation matrix", averaged over $k = 1...M$. Thus, the assumption above is equivalent to considering a set of matrices $\mathbf{R}_{tk}^T \otimes \mathbf{R}_{rk}$, where the "average matrix" does not depend on the set size.

$$c = \lim_{M\to\infty} \frac{\sum_{i=k+1}^{M} |a_i|^3}{\sum_{i=1}^{k} |a_i|^3} < \infty, \ \sum_{i=1}^{k} |a_i|^3 \neq 0 \tag{4.6}$$

Proof: see Appendix B.

While condition (4.6) is less general than (4.5), it allows for an insight as follows. Consider two broad cases where Corollary 4.2.1 applies:

(i) The number of non-zero keyholes is finite ($= k < \infty$), then $\sum_{i=k+1}^{M} |a_i|^3 = 0$ and consequently $c = 0$. Thus, a necessary physical condition for Theorem 4.2 to hold is that the number of active ($|a_k| \neq 0$) keyholes must approach infinity as $M \to \infty$.

(ii) The largest keyhole ($|a_1|$) is significantly dominant over the rest, i.e.

$$c = \lim_{M\to\infty} \sum_{i=2}^{M} |a_i|^3 / |a_1|^3 < \infty, \tag{4.7}$$

which holds true, for example, when $|a_2| M^{1/3} / |a_1| < \infty$ as $M \to \infty$.

While necessary conditions for $\mathbf{C}$ to be invertible are rather complicated, the following corollary gives simple sufficient conditions.

Corollary 4.2.2: The inverse of $\mathbf{C} = \sum_{k=1}^{M} |a_k|^2 \left(\mathbf{R}_{tk}^T \otimes \mathbf{R}_{rk}\right)$ exists as $M \to \infty$, if

(i) all $\mathbf{R}_{tk}$, $\mathbf{R}_{rk}$, $k = 1...M$ are non-singular.

(ii) the number of singular matrices $\mathbf{R}_{tk}$, $\mathbf{R}_{rk}$ is finite.

(iii) the number of singular matrices $\mathbf{R}_{tk}$, $\mathbf{R}_{rk}$ is infinite, and $\sum_{k\notin S} |a_k|^2 > 0$, where S is a subset of singular keyholes, i.e. the power contribution of non-singular keyholes is asymptotically not zero.

Proof: see Appendix B.

As an example of when both Corollary 4.2.1 and Corollary 4.2.2 apply, consider a multi-keyhole channel with M identical keyholes, i.e. $|a_k| = M^{-1/2}$, $\mathbf{R}_t = \mathbf{R}_{tk}$ and $\mathbf{R}_r = \mathbf{R}_{rk}$ for all k, and both $\mathbf{R}_t$, $\mathbf{R}_r$ are non singular. Note that in this case (4.2), (4.5) hold true, and the inverse of $\mathbf{C} = \mathbf{R}_t^T \otimes \mathbf{R}_r$ exists since $\mathbf{C}$ is positive definite. Thus from Theorem 4.2(i), such a multi-keyhole channel converges in distribution to a Rayleigh fading channel as $M \to \infty$. Moreover, since $\mathbf{C}$ does not depend on M, from Theorem 4.2(ii), the convergence rate is at least as $M^{-1/2}$.

Since the channel capacity is a continuous function of $\mathbf{H}$ (see (2.4)), the next corollary follows

immediately from Theorem 4.2.

Corollary 4.2.3: Under the conditions of Theorem 4.2, the instantaneous capacity of a FRMK channel converges in distribution to that of an equivalent Rayleigh fading channel.

Proof: by Slutsky Theorem [[23], Theorem 6a].

Fig. 4.3 compares the outage capacity distributions of a 2x2 multi-keyhole channel with $|a_k| = \sqrt{1/M}$ and that of the equivalent Rayleigh fading one. Both channels are exponentially correlated with correlation parameter $r = 0.5$ at both Tx and Rx ends. Clearly, the outage probability of the multi-keyhole channel decreases with M and becomes close to that of the equivalent Rayleigh channel for $M = 10$.

Since a FRMK channel converges to the Rayleigh fading one as $M \to \infty$, Theorem 4.3 [69] below is of particular interest. We state the Theorem for the case when the CSI is available at the Rx end only, while the original proof includes a more general scenario.

Theorem 4.3 [69]: Let C be an instantaneous capacity of a correlated Rayleigh MIMO channel which has the Kronecker correlation structure (2.9) and normalized such that $n_t^{-1} tr\{\mathbf{R}_t\} = 1$ and $n_r^{-1} tr\{\mathbf{R}_r\} = 1$. Then,

(i) if for a fixed n_r

$$\lim_{n_t \to \infty} \|\lambda\|_3 / \|\lambda\|_2 = 0, \tag{4.8}$$

where $\|\lambda\|_m = \left(\sum_{i=1}^{n} (\lambda_i)^m\right)^{1/m}$ is the L_m norm of the eigenvalues $\mathbf{R}_t$, C is asymptotically Gaussian in distribution as $n_t \to \infty$ with the mean μ and variance σ^2 as follows

$$\mu = \ln(\det[\mathbf{I} + \gamma_0 \mathbf{R}_r / n_r]) \tag{4.9}$$

$$\sigma^2 = \left(\frac{\gamma_0}{n_t n_r}\right)^2 \cdot \|\mathbf{R}_t\|^2 \cdot \sum_{k=1}^{n_r} \left(\frac{\lambda_k^r}{1 + \gamma_0 \lambda_k^r / n_r}\right)^2, \tag{4.10}$$

where λ_k^r, $k = 1 \ldots n_r$ are the eigenvalues of $\mathbf{R}_r$.

(ii) Due to the symmetry of (4.3), (4.9) and (4.10) hold true for fixed a n_t and $n_r \to \infty$, if Tx and Rx ends are exchanged.

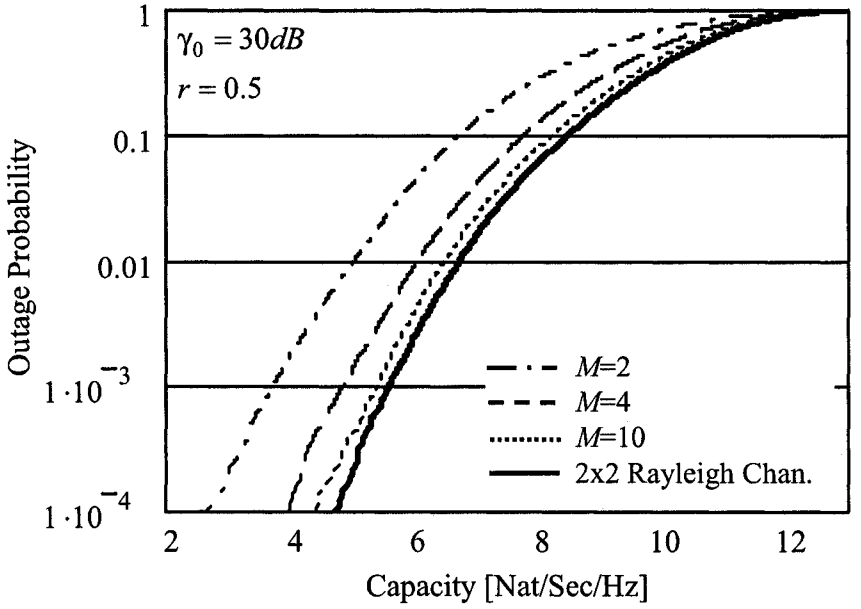

Fig. 4.3 Outage capacity distribution of 2x2 MIMO channels.

From (4.9), μ increases with γ_0 and is affected by the correlation at the end with less antennas (for instance, the Rx end if n_r is fixed and $n_t \to \infty$). In turn, σ^2, which determines the slope of the asymptotic capacity distribution, is affected by both $\mathbf{R}_t$ and $\mathbf{R}_r$. The following corollary shows the impact of correlation on μ as both $n_t, n_r \to \infty$.

Corollary 4.3: Under the conditions of Theorem 4.3(i), let $\lim_{\substack{n_t\to\infty \\ n_r\to\infty}} n_r \|\mathbf{R}_t\|/n_t = 0$, and $\lim_{n_r\to\infty} n_r^{-1}\|\mathbf{R}_r\| = 0$.[8] Then, (i) if $\|\mathbf{C}^{-1/2}\|^3 \cdot \sum_{k=1}^{M}|a_k|^3 \left(E\{\|\mathbf{h}_{tk}\|^4\}\cdot E\{\|\mathbf{h}_{rk}\|^4\}\right)^{3/4} \to 0$ as $n_t, n_r, M \to \infty$[9], the mean capacity of a FRMK channel converges as

$$\mu \to \gamma_0(1-\gamma_0 \cdot n_r^{-2}\|\mathbf{R}_r\|^2/2), \tag{4.11}$$

for $n_r^{-1}\|\mathbf{R}_r\| \le \gamma_0^{-1}$. (ii) Due to the symmetry, (4.11) holds true under the conditions of Theorem 4.3(ii), if

[8] The conditions of Corollary 4.3 do not contradict those of Theorem 4.3, as (2.43) implies $\lim_{n_t\to\infty} n_t^{-1}\|\mathbf{R}_t\| = 0$ or $\lim_{n_r\to\infty} n_r^{-1}\|\mathbf{R}_r\| = 0$ as $n_t \to \infty$ or $n_r \to \infty$ respectively (for more details see Chapter VI).

[9] This condition implies that M must be significantly larger than n_t, n_r. For example, it is straightforward to show that when the channel is uncorrelated ($\mathbf{R}_{tk} = \mathbf{I}$, $\mathbf{R}_{rk} = \mathbf{I}$, $\forall k$), (4.11) holds if $(n_t n_r)^6 / M \to 0$ as $n_t, n_r, M \to \infty$.

Tx and Rx ends are exchanged.

Proof: see Appendix B.

Without loss of generality, let us consider a case where $n_t >> n_r$. From (4.11), for large n_t and n_r, the mean capacity decreases linearly with $n_r^{-1}\|\mathbf{R}_r\|$ and does not depend on correlation at Tx end. This dependence on L_2 norm of the correlation matrix is important as it motivates the measure of correlation and power imbalance to be introduced in Chapter V.

Under the conditions of Corollary 4.3, the asymptotic variance of a FRMK channel follows from (4.10) and can be also expressed through this norm by considering σ^2 in high and low SNR regimes. Assume that $\mathbf{R}_r$ is positive definite ($\lambda_k^r > 0$), then it is straightforward to show using Taylor series expansion that

$$\sigma^2 \to \frac{n_r}{n_t^2}\|\mathbf{R}_t\|^2 + o(\gamma_0^{-1}), \text{ high SNR regime,} \tag{4.12}$$

where $o(x)$ is a value such that $\lim_{x\to 0} o(x)/x = 0$, and

$$\sigma^2 \to (\gamma_0)^2 \cdot n_t^{-2}\|\mathbf{R}_t\|^2 \cdot n_r^{-2}\|\mathbf{R}_r\|^2 + o(\gamma_0), \text{ low SNR regime,} \tag{4.13}$$

From (4.12) and (4.13), when γ_0 is either high or low, the correlation affects the variance mostly via L_2 norm of only $\mathbf{R}_t$ or both $\mathbf{R}_t$ and $\mathbf{R}_r$. In the high SNR regime the variance does not depend on γ_0. In summary, when γ_0 is high, the correlation at the Rx end affects the mean capacity, while the variance is affected by the correlation at the Tx end.

4.3. Rank-Deficient Multi-Keyhole Channels

Theorem 4.4: Let C be the instantaneous capacity of a rank-deficient multi-keyhole channel ($M < \min\{n_t, n_r\}$). If $\lim_{n_t\to\infty} n_t^{-1}\mathbf{R}_{tk} < \infty$, $\lim_{n_r\to\infty} n_r^{-1}\mathbf{R}_{rk} < \infty$, $\lim_{n_t, M\to\infty} n_t^{-2}\sum_{k=1}^{M}\sum_{m=1}^{M} tr[\mathbf{R}_{tk}\mathbf{R}_{tm}] = 0$, $\lim_{n_r, M\to\infty} n_r^{-2}\sum_{k=1}^{M}\sum_{m=1}^{M} tr[\mathbf{R}_{rk}\mathbf{R}_{rm}] = 0$ for every $k, m = 1...M$, then

$$C \xrightarrow{d} \sum_{k=1}^{M} \ln(1 + |a_k|^2 \gamma_0 \|\mathbf{h}_{tk}\|^2 \|\mathbf{h}_{rk}\|^2 / [n_t n_r]) \text{ as both } n_t, n_r \to \infty, \tag{4.14}$$

Proof: see Appendix B.

From Theorem 4.4, the asymptotic instantaneous capacity of a multi-keyhole channel is the sum of the capacities of M single keyhole channels.

Corollary 4.4: Under the conditions of Theorem 4.4, the instantaneous capacity of a rank-deficient multi-keyhole channel is asymptotically Gaussian with the mean μ and variance σ^2 as follows

$$\begin{aligned} \mu &= \sum_{k=1}^{M} \ln\left(1+|a_k|^2 \gamma_0\right); \\ \sigma^2 &= \left(\frac{\gamma_0}{1+\gamma_0}\right)^2 \left(\frac{1}{n_t^2}\sum_{k=1}^{M}\|\mathbf{R}_{tk}\|^2 + \frac{1}{n_r^2}\sum_{k=1}^{M}\|\mathbf{R}_{rk}\|^2\right) \end{aligned} \tag{4.15}$$

Proof: Under the conditions of Theorem 4.4, C in (4.15) is a sum of independent random variables, which, from Theorem 3.3[10], are asymptotically Gaussian. Therefore, C is also asymptotically Gaussian with the mean and variance given by (4.15). **Q.E.D.**

Similarly to the Rayleigh channel in the high SNR regime (see Corollary 4.3), σ^2 does not depend on γ_0 and is affected by the correlation. In contrast, μ is a function of γ_0.

Using Jensen inequality and the normalization (4.2), it is straightforward to show that

$$\mu \le M \ln\left(1+\gamma_0 / M\right) \tag{4.16}$$

with equality if $|a_k| = \sqrt{1/M}$, $k = 1...M$, i.e. if the gains of all the keyholes are same. Since $M\ln\left(1+\gamma_0/M\right)$ increases monotonically with M, the channel with more equal-gain keyholes has higher mean capacity. However, this is not necessarily true for the outage capacity, since an increase in M increases not only μ but also σ^2 (see (4.15)). Thus, the outage capacity for some outage probabilities may increase, while for others it may decrease. To demonstrate this, consider a marginal case where the channel has M equal-gain keyholes and M is large. From (4.16), $\lim_{M\to\infty}\mu = \gamma_0$, i.e. asymptotically does not depend on the number of keyholes. In contrast, σ^2 increases with M. Thus, applying Corollary 3.3 to two Gaussian CDF's with the same mean and different variances, we conclude that an increase in M decreases the outage capacity of such a multi-keyhole channel at outage probabilities less than 0.5 and increases it at outage probabilities greater than 0.5 (we stress that this conclusion holds true under

[10] Note that if the conditions of Theorem 4.4 are fulfilled, then the conditions of Theorem 3.3 are also satisfied.

normalization (4.2) and may change if a different normalization is adopted).

Note that when both $n_t, n_r \to \infty$, any multi-keyhole channel with $M < \infty$ is RDMK since $M < \min\{n_t, n_r\}$. In contrary, if $M \geq \min\{n_t, n_r\}$ while both $n_t, n_r \to \infty$, then necessarily $M \to \infty$. Therefore, Theorem 4.3, Corollary 4.3 and Theorem 4.4 describe the outage capacity distribution of the entire range of multi-keyhole channels where both n_t and n_r go to infinity.

4.4. Summary

The multi-keyhole channel model has been introduced to generalize the single keyhole channel. It follows that the multi-keyhole channels serve as a link between the rank-one keyhole and full-rank Rayleigh fading MIMO channels. The present study shows that the Gaussian approximation of outage capacity has a high degree of universality and applies to a broad class of MIMO channels, far beyond the Rayleigh fading one. The asymptotic approach provides a number of analytical tools, which can be applied not only to multi-keyhole channels, but also to analyze the analogue multi-hope relay networks with cooperative diversity [39], where a keyhole may represent a relaying antenna rather than a propagation effect.

The results of this chapter are presented in [46], [47], [49].

CHAPTER V: MEASURE OF CORRELATION AND POWER IMBALANCE

The analysis conducted in the previous chapters shows that the moments of the asymptotic outage capacity distribution of a broad class of MIMO channels are the functions of $\|\mathbf{R}_t\|$ and $\|\mathbf{R}_r\|$ (see (3.15), (4.11), (4.12), (4.13)). This motivates a simple and well defined measure of correlation and power imbalance, which is introduced in this chapter. Despite the asymptotic assumptions, the measure adequately describes the impact of correlation on the capacity of channels with a moderate number of antennas. The properties of this measure are studied and it is compared to other correlation measures proposed in the literature.

5.1. Basic Properties

Consider an $[n\times n]$ correlation matrix $\mathbf{R}$ at either Tx or Rx end. Let $\mathbf{R}\in\Re$, where $\Re$ is a set of all $n\times n$ correlation matrices such that $tr(\mathbf{R})=n$. Using Cauchy-Schwarz's inequality

$$n^{-2}\|\mathbf{R}\|^2 = n^{-2}\sum_{k=1}^{n}\lambda_k^2 \geq n^{-2}\left(n^{-1/2}\sum_{k=1}^{n}\lambda_k\right)^2 = n^{-1}, \tag{5.1}$$

with the equality if $\lambda_k=\lambda_m$ for all $k,m=1...n$, where λ_k are eigenvalues of $\mathbf{R}$, i.e. if $\mathbf{R}=\mathbf{I}$. Thus, $n^{-2}\|\mathbf{R}\|^2$ achieves its minimum when the channel at the Tx(Rx) end is uncorrelated with the same power at each Tx(Rx) antenna. Furthermore, since every $\mathbf{R}\in\Re$ is positive semi-definite ($\lambda_k\geq 0$, $k=1...n$)

$$n^{-2}\|\mathbf{R}\|^2 = n^{-2}\sum_{k=1}^{n}\lambda_k^2 \leq n^{-2}\left(\sum_{k=1}^{n}\lambda_k\right)^2 = 1, \tag{5.2}$$

with the equality if $\lambda_k=n$ for some k, and $\lambda_m=0\ \ \forall m\neq k$. Thus, $n^{-2}\|\mathbf{R}\|^2$ achieves its maximum when the channel at the Tx (Rx) end is fully correlated. From (5.1), (5.2) and following the properties of the L_2 norm [119], $n^{-2}\|\mathbf{R}\|^2$ is a mapping of $\Re$ onto a closed interval of real numbers $[1/n;\ 1]$ (note that $[1/n;\ 1]$ converges to $(0;\ 1]$ as $n\to\infty$, which has a certain degree of similarity with the scalar correlation coefficient). The corollary below follows from Theorem 3.3, Theorem 4.3, Corollary 4.3, and Theorem 4.4:

Corollary 5.1: Asymptotically, the MIMO channel correlation affects the outage capacity distribution through the L_2 norm of the correlation matrices, i.e. even though two correlation matrices $\mathbf{R}_1$ and $\mathbf{R}_2$ (at either end) are different, they affect the capacity in the same way if

$$\|\mathbf{R}_1\| = \|\mathbf{R}_2\| \tag{5.3}$$

Corollary 5.1 introduces $n^{-1}\|\mathbf{R}\|$ as a measure of correlation for channels with large n. Following (5.1) and (5.2), there are two major effects that can increase $n^{-1}\|\mathbf{R}\|$: (i) non-uniform power distribution across the antennas (also termed power imbalance) and (ii) non-zero correlation. To analyze those effects separately, let us split $\mathbf{R} \in \Re$ into a sum of two matrices as follows:

$$\mathbf{R} = \mathbf{K} + \mathbf{P}, \tag{5.4}$$

where $\mathbf{P} = diag\{\mathbf{R}\} - \mathbf{I}$ and $\mathbf{K} = \mathbf{R} - \mathbf{P}$; $diag\{\mathbf{R}\}$ is the diagonal matrix whose main diagonal is that of $\mathbf{R}$. Clearly, $\mathbf{P}$ and $\mathbf{K}$ account for the power imbalance and the correlation respectively. Since for any $\mathbf{R} \in \Re$, $tr(\mathbf{K}) = n$ and $tr(\mathbf{P}) = 0$, it is straightforward to show that the decomposition (5.4) is norm-orthogonal, i.e.

$$\|\mathbf{R}\|^2 = \|\mathbf{K}\|^2 + \|\mathbf{P}\|^2 \tag{5.5}$$

$n^{-2}\|\mathbf{P}\|^2$ is bounded by

$$0 \le n^{-2}\|\mathbf{P}\|^2 \le 1 - n^{-1}, \tag{5.6}$$

where the lower bound is achieved when all antennas have the same power (no power imbalance), i.e. $diag\{\mathbf{R}\} = \mathbf{I}$, and the upper bound is achieved when there is only one effective Tx or Rx antenna, i.e. there exists k such that $R_{kk} = n$, and $R_{mm} = n \ \ \forall m \neq k$, where R_{km} is the km-th element of $\mathbf{R}$. Since $n^{-2}\|\mathbf{K}\|^2 \le n^{-2}\|\mathbf{R}\|^2$, it follows directly from (5.5) and (5.1), (5.2) that

$$n^{-1} \le n^{-2}\|\mathbf{K}\|^2 \le 1, \tag{5.7}$$

where the lower bound is achieved when $\mathbf{K} = \mathbf{I}$ (the channel at Tx (Rx) end is uncorrelated), and the upper bound is achieved when the channel at the Tx (Rx) end is fully correlated. Below we introduce the following definitions:

Definition 5.1: A MIMO channel with correlation matrix $\mathbf{R}_1 \in \Re$ at either Tx or Rx end is said to be equally or more correlated than a channel with $\mathbf{R}_2 \in \Re$ if

$$\|\mathbf{K}_1\| \geq \|\mathbf{K}_2\|, \tag{5.8}$$

where $\mathbf{K}_1$ and $\mathbf{K}_2$ correspond to $\mathbf{R}_1$ and $\mathbf{R}_2$ respectively through (5.4).

Definition 5.2: A MIMO channel with correlation matrix $\mathbf{R}_1 \in \Re$ at either Tx or Rx end has higher power imbalance than a channel with $\mathbf{R}_2 \in \Re$ if

$$\|\mathbf{P}_1\| \geq \|\mathbf{P}_2\|, \tag{5.9}$$

where $\mathbf{P}_1$ and $\mathbf{P}_2$ correspond to $\mathbf{R}_1$ and $\mathbf{R}_2$ respectively through (5.4). Note that for any $\mathbf{R} \in \Re$, the measure of correlation $n^{-1}\|\mathbf{K}\| \in (0;1]$ and the measure of power imbalance $n^{-1}\|\mathbf{P}\| \in [0;1)$ as $n \to \infty$.

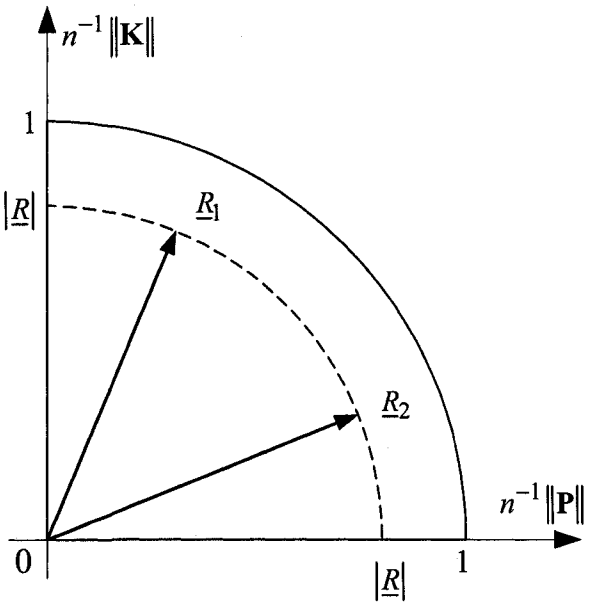

Fig. 5.1 Geometrical interpretation of power imbalance and correlation effects.

To get some insight, consider a simple geometrical interpretation of Definitions 5.1 and 5.2 shown in Fig. 5.1. From (5.5), $n^{-1}\|\mathbf{K}\|$ and $n^{-1}\|\mathbf{P}\|$ create an orthonormal basis in a vector space, and $n^{-1}\|\mathbf{R}\|$ is a mapping of $\Re$ onto a circle sector in that basis. The channel correlation matrix $\mathbf{R}$ is represented by the vector $\underline{R}$ such that

$$\left|\underline{R}\right| = n^{-1}\left\|\mathbf{R}\right\|;\ \ angle\{\underline{R}\} = \tan^{-1}\{\left\|\mathbf{P}\right\|/\left\|\mathbf{K}\right\|\} \tag{5.10}$$

Following (3.15), (4.11), (4.12), (4.13), the asymptotic outage capacity is affected by the length of $\underline{R}$ but not by its angle. Consider two channels with correlation matrices (at either Tx or Rx end) represented by the vectors $\underline{R}_1$ and $\underline{R}_2$ such that $\left|\underline{R}_1\right| = \left|\underline{R}_2\right| = \left|\underline{R}\right|$ (see Fig. 5.1). Following Definitions 5.1 and 5.2, the channel with $\underline{R}_1$ is more correlated that one with $\underline{R}_2$. In contrast, the channel with $\underline{R}_2$ has more power imbalance across antennas. Nonetheless, the impact on asymptotic outage capacity of both channels is the same, i.e. the power imbalance and correlation between antennas have the same impact on the asymptotic capacity distribution of MIMO channels if $\left|\underline{R}_1\right| = \left|\underline{R}_2\right|$.

Consider, as an example, the exponential correlation matrix model (2.14). From (5.4), $\left\|\mathbf{K}\right\| = \left\|\mathbf{R}\right\|$ and $\left\|\mathbf{P}\right\| = 0$, i.e. this model does not capture the effect of power imbalance but the correlation only. It follows from (3.17) that the measure of correlation increases monotonically with $\left|r\right|$. This fact supports Definition 5.1. Moreover, $n^{-1}\left\|\mathbf{K}\right\|$ monotonically decreases with n and eventually converges to zero as $n \to \infty$, i.e. even though the correlation between adjacent antennas may be high, an increase in the number of antennas reduces the measure of correlation due to smaller correlation between distant antennas. Another model with similar asymptotic behavior is quadratic exponential correlation model (2.15). As in the exponential correlation model, the measure of correlation in this case increases monotonically with $\left|r\right|$ (see Fig. 3.5), which supports Definition 5.1, and monotonically converges to zero as $n \to \infty$ (3.20). It is straightforward to show, based on the analysis in Chapter IV, that when both Tx and Rx correlations are either exponential or quadratic exponential, the outage capacity distribution of FRMK and RDMK channels is asymptotically normal.

Note that the distribution of C in (2.4) is invariant under unitary transformation of $\mathbf{H}$ regardless of the distribution of the latter. Let $\mathbf{\Lambda}$ be an eigenvalue matrix of a correlation matrix $\mathbf{R} \in \Re$. Since the eigenvalue decomposition is a particular case of unitary transformations, the impact of correlation on the channel capacity is the same whether the correlation matrix is $\mathbf{R}$ or $\mathbf{\Lambda}$. Thus, the effects of correlation and power imbalance are indistinguishable in the eigenspace of correlation matrices, yet the separation of these two factors is important from a practical point of view.

Note that when n is large, the scalar measure of the channel correlation and power imbalance given by Definitions 5.1 and 5.2 is compatible with the measure proposed in [33], and it is also an alternative to the measure given in [10]. Unlike [10], the proposed measure is not based on the majorization theory [68] and does not require eigenvalue decomposition. Moreover, there is a direct relationship between the two measures indicated by the following theorem.

Theorem 5.1: Let $\Re_M$ be a subset in $\Re$ of all $[n\times n]$ correlation matrices which can be majorized[11]. Then, for any $\mathbf{R}_1$, $\mathbf{R}_2 \in \Re_M$, $\mathbf{R}_1 \succ \mathbf{R}_2$ if and only if $n^{-1}\|\mathbf{R}_1\| \geq n^{-1}\|\mathbf{R}_2\|$.

Proof: see Appendix C.

Thus, the proposed measure of correlation and power imbalance is also compatible with the one based on the majorization theory. In addition, instead of a partial ordering, it provides a complete (full-ordering) correlation characterization of a MIMO channel with no exception, i.e. not only $\mathbf{R}_1$, $\mathbf{R}_2 \in \Re_M$, but any two $\mathbf{R}_1$, $\mathbf{R}_2 \in \Re$ can be compared (see the remark to the Definition 1 in [10]).

Below we characterize the impact of correlation and power imbalance on the outage capacity using the asymptotic results from Chapters III and IV.

5.2. Impact on Asymptotic Outage Capacity Distribution

First consider an RDMK channel with a large number of antennas[12]. From (4.15), the mean capacity of this channel depends on γ_0, and its variance is a sum of measures of correlation and power imbalance over all keyholes at Tx and Rx ends. Following Definitions 5.1 and 5.2, the variance increases with correlation and power imbalance. In contrast, the mean remains unchanged. Thereby, from Corollary 3.3, the outage capacity of a RDMK channel decreases with the correlation and/or power imbalance at outage probabilities $P_{out} < 0.5$ and increases at $P_{out} > 0.5$.

Similar approach clarifies the impact of correlation on the capacity of an FRMK channel with a

---

[11] A correlation matrix $\mathbf{R}_1$ is said to majorize (more correlated than) $\mathbf{R}_2$ and denoted by $\mathbf{R}_1 \succ \mathbf{R}_2$, if $\sum_{k=1}^{m} \lambda_k^{(1)} \geq \sum_{k=1}^{m} \lambda_k^{(2)}$ for all $m = 1...n$, where $\lambda_k^{(1)}$ and $\lambda_k^{(2)}$ are the eigenvalues of $\mathbf{R}_1$ and $\mathbf{R}_2$ respectively sorted in a descending order [10].

[12] Note that the keyhole channel studied in Chapter III is a particular case of the RDMK one.

large number of antennas. From (4.11), the mean capacity of this channel decreases with the measure of correlation and power imbalance at the end with less antennas. From (4.12) and (4.13), its variance increases with either the measure of correlation and power imbalance at the end with more antennas (high SNR regime), or at the both ends (low SNR regime). Since the capacity of a FRMK channel is asymptotically normal, both a decrease in the mean capacity and/or an increase in the variance result in smaller outage capacity at $P_{out} < 0.5$.

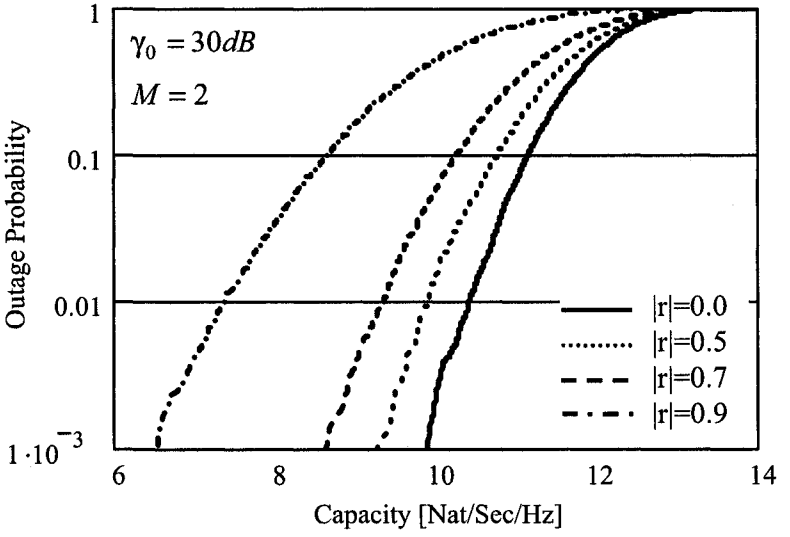

Fig. 5.2 Outage capacity distribution of 10x10 RDMK channel.

While the moments of outage capacity distribution of multi-keyhole channels (either RDMK or FRMK) in Chapter IV are expressed through the measure of correlation and power imbalance only as $n_t, n_r \to \infty$, they describe well the impact of correlation and power imbalance on capacity of realistic channels with moderate n_t, n_r. Fig. 5.2 shows Monte-Carlo simulation of outage capacity distribution of 10x10 RDMK channel with 2 keyholes for various correlation parameters r (same at both Tx and Rx ends). Clearly, an increase in correlation does not affect significantly the mean capacity (≈ 12 [nat/sec/Hz]), but increases the distribution variance, which results in an increasing outage probability. Fig. 5.3 and Fig. 5.4 show Monte-Carlo simulations of outage capacity distribution of 2x10 Rayleigh-fading channel to represent a FRMK channel with a large number of keyholes (see Theorem 4.2).

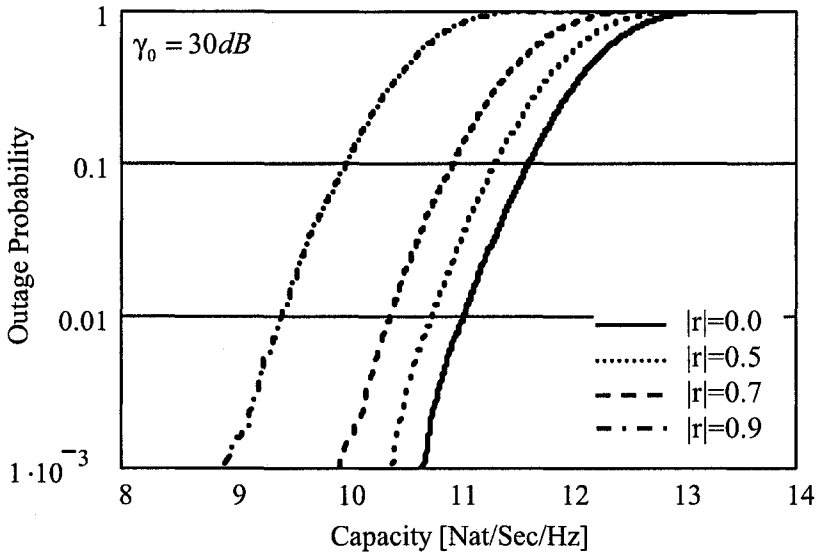

Fig. 5.3 Outage capacity distribution of 2x10 Rayleigh channel correlated at Tx end. $n_t << n_r$, therefore, the correlation at the Tx end affects the capacity mean.

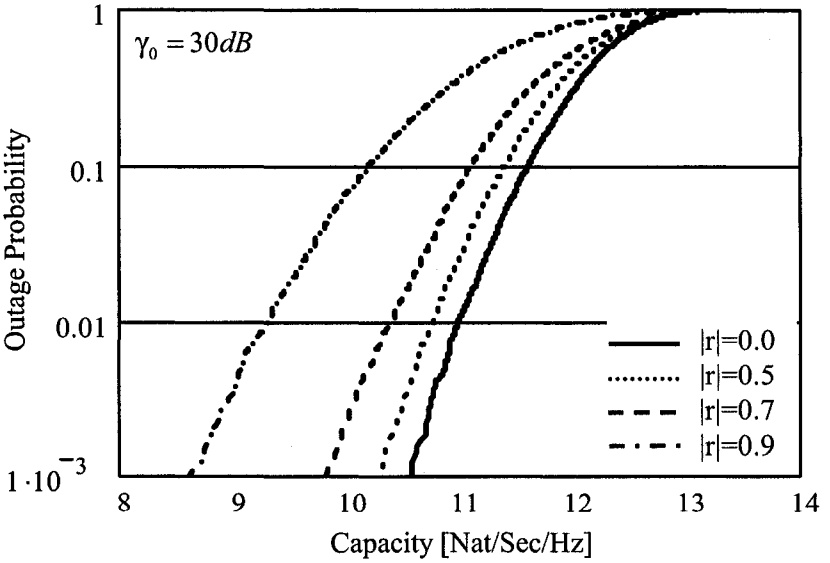

Fig. 5.4 Outage capacity distribution of 2x10 Rayleigh channel correlated at Rx end. $n_t << n_r$, therefore, the correlation at the Rx end affects the capacity variance.

Fig. 5.3 shows the channel capacity for various correlation parameters $|r|$ at Tx end, while the Rx end is uncorrelated. Fig. 5.4 shows the channel capacity for various correlation parameters $|r|$ at Rx end, while the Tx end is uncorrelated. From Fig. 5.3, an increase in correlation at Tx end mostly reduces the distribution mean, while the variance remains unchanged. In contrast, from Fig. 5.4, an increase in correlation at Rx end increases the distribution variance and has almost no impact on the mean. Both effects are predicted by the asymptotic analysis of FRMK channels at high SNR regime (see (4.11) and (4.12)).

5.3. Number of Effective Degrees of Freedom via the Measure of Correlation and Power Imbalance

The measure of correlation and power imbalance can be used to evaluate the effective degrees of freedom available in the channel [100]. Comparing the correlated channel to a non-correlated one with the same outage capacity, the effective degrees of freedom is the number of antennas in the latter, i.e.

$$n_{eff}^{-1} = n^{-2} \|\mathbf{R}\|^2, \tag{5.11}$$

where the right and left sides are the measures of correlation and power imbalance of the uncorrelated and correlated channels with n_{eff} and n antennas respectively. Let $\nu = n_{eff}/n$ be the efficiency of using n antennas in the correlated and power-imbalanced channel. From (5.11)

$$\nu = n \cdot \|\mathbf{R}\|^{-2} \tag{5.12}$$

Clearly, ν decreases with the correlation and power imbalance. From (5.1) and (5.2), $n^{-1} \le \nu \le 1$, where the lower and upper bounds correspond to the fully correlated and uncorrelated channels at Tx (Rx) end respectively. Note that ν does not depend on SNR and quantifies the communication channel regardless of the transmission or reception strategy. As an example, consider the exponential model (2.14). Substituting (3.17) in (5.12), one obtains

$$\nu = \frac{1-|r|^2}{1+|r|^2}; \ |r|<1 \tag{5.13}$$

Clearly, ν decreases monotonically with $|r|$, and, in this case, does not depend on n. It is straightforward to show that the same holds true when $\mathbf{R}$ is given by the quadratic exponential model (2.15).

5.4. Summary

It has been shown that the scalar measure of correlation and power imbalance is a useful analytical tool to quantify the impact of correlation on MIMO capacity. The similarity of the proposed measure with the measure proposed in [33] for Rayleigh-fading channels in the low-power regime, and the measure based on majorization theory [68] implies that the proposed measure has a certain degree of universality and describes the impact of correlation and power imbalance on several characteristics of MIMO channels simultaneously. The advantages of the proposed measure are simplicity (no eigenvalue decomposition is required), full ordering property (any two channels can be compared without exceptions) and tractability (it separates the effect of correlation and power imbalance). It has been demonstrated that the effects of correlation and power imbalance are independent, and their total negative impact on the outage capacity is characterized by the sum of the two corresponding measures. In this sense, the impact of the power imbalance can be as bad as that of the correlation. Using Monte-Carlo simulations we demonstrated that the proposed measure provides an adequate characterization of the impact of correlation and power imbalance on the multi-keyhole channel capacity with a moderate number of antennas.

The results of this chapter are presented in [46], [48], [49].

CHAPTER VI: ASYMPTOTIC NORMALITY OF RAYLEIGH CHANNEL CAPACITY

Following the analysis in Chapters III and IV, the asymptotic normality of the outage capacity of a number of MIMO channels is established through the Lyapounov-type condition (see (3.22) and (4.8)). Some physical aspects of this condition are discussed. Simple alternative conditions, which do not require eigenvalue decomposition, are proposed for the MIMO channels whose correlation matrix has a Toeplitz structure. It is demonstrated that a number of popular correlation matrix models [1], [17], [86] satisfy this condition. In many cases, the convergence to the asymptotic normality is at least as $1/\sqrt{n_t}$, where n_t is the number of Tx antennas.

6.1. Generalized Lyapounov-Type Convergence Condition

Theorem 4.3 gives a condition under which the outage capacity distribution of a Rayleigh-fading channel is asymptotically Gaussian as $n_t \to \infty$. The condition follows from the Lyapounov central limit theorem [69]. The generality of this condition can be further extended without corresponding increase in complexity. Specifically, from a more general formulation of Lyapounov Theorem[13], the generalized condition for Theorem 4.3 is that, for some $\delta > 0$ [14],

$$\lim_{n_t \to \infty} Z_{n_t}(\delta) = \lim_{n_t \to \infty} \frac{\left\|\boldsymbol{\lambda}^t\right\|_{2+\delta}}{\left\|\boldsymbol{\lambda}^t\right\|_2} = 0, \tag{6.1}$$

where the norm $\left\|\boldsymbol{\lambda}^t\right\|_m = \left(\sum_{i=1}^{n_t} (\lambda_i^t)^m\right)^{1/m}$, and $\boldsymbol{\lambda}^t = \{\lambda_i^t,\ i = 1...n_t\}$ is the eigenvalues of the correlation matrix $\mathbf{R}_t$. Furthermore, in this particular case, a stronger result holds as indicated below.

Lemma 6.1: If $\lim_{n_t \to \infty} Z_{n_t}(\delta) = 0$ for some $\delta > 0$, it also converges to zero for all $\delta > 0$.

---

[13] Initially, in 1900, Lyapounov showed that a sum of independent random variables x_n is asymptotically normal if $E(|x_n|^3)$ exists, and $\sqrt[3]{m_3} / \sqrt[2]{m_2} \to 0$ as $n \to \infty$, where $m_k = \sum_{i=1}^{n} E(|x_n|^k)$. Shortly after, in 1901, he found that it is enough to request existence of only some absolute moments $E(|x_n|^{2+\delta})$, $\delta > 0$, and the sum is asymptotically normal if $\sqrt[2+\delta]{m_{2+\delta}} / \sqrt[2]{m_2} \to 0$ as $n \to \infty$ [[28], Ch. 8].

[14] Note that the same condition is stipulated in Theorem 3.4 as a condition for asymptotic normality of keyhole channels.

Proof: Let $\lim_{n_t\to\infty} Z_{n_t}(\delta_0)=0$. From [54], $\left(\left\|\lambda^t\right\|_{2+\delta_2}/\left\|\lambda^t\right\|_2\right)^{1/\delta_2} \le \left(\left\|\lambda^t\right\|_{2+\delta_1}/\left\|\lambda^t\right\|_2\right)^{1/\delta_1}$, where $\delta_1 \ge \delta_2$. Thereby, $Z_{n_t}(\delta)\to 0$ for all $\delta \le \delta_0$. On the other hand, following [[8], Fact 9.7.16], $\left\|\lambda^t\right\|_{2+\delta_1} \le \left\|\lambda^t\right\|_{2+\delta_2}$, therefore, from (6.1), if $Z_{n_t}(\delta_0)\to 0$, then $Z_{n_t}(\delta)\to 0$ for all $\delta \ge \delta_0$. Combining the two inequalities, Lemma 6.1 follows. **Q.E.D.**

Theorem 6.1: Condition (6.1) is satisfied and so Theorem 4.3 holds, if

$$\lim_{n_t\to\infty}\frac{\left\|\lambda^t\right\|_\infty}{\left\|\lambda^t\right\|_2}=\lim_{n_t\to\infty}\frac{\max\{\lambda^t\}}{\left\|\lambda^t\right\|_2}=\lim_{n_t\to\infty}\frac{\left|\mathbf{R}_t\right|}{\left\|\mathbf{R}_t\right\|}=0, \tag{6.2}$$

where $\left|\mathbf{R}_t\right|$ and $\left\|\mathbf{R}_t\right\|$ are strong (spectral) and L_2 (Frobenius) norms respectively [8].

Proof: Follows immediately from Lemma 6.1, by choosing $\delta\to\infty$ in (6.1). **Q.E.D.**

Note that calculation of $\left|\mathbf{R}_t\right|$ requires only one maximal eigenvalue, Frobenius norm $\left\|\mathbf{R}_t\right\|=\left(\sum_{k,m=1}^{n_t}\left|[\mathbf{R}_t]_{k,m}\right|^2\right)^{1/2}$ ($[\mathbf{R}_t]_{k,m}$ are elements of $\mathbf{R}_t$) does not require eigenvalue decomposition at all, so that unlike (6.1), condition (6.2) is easier to verify. Nevertheless, it is important to consider $Z_{n_t}(\delta)$ for a range of δ, rather than for one particular value (such as $\delta=1$ in (2.43), or $\delta\to\infty$), since the best overall convergence rate to asymptotic normality is determined by the supremum over $\delta>0$ as indicated below. Let $Z_{n_t}(\delta)\to 0$ for some $\delta>0$. Due to Lyapounov's Inequality [[28], Theorem on p. 228]:

$$Z_{n_t}(\delta)\ge n_t^{-1/2+1/(2+\delta)} \tag{6.3}$$

Proposition 6.1: Define a convergence rate of $Z_{n_t}(\delta)$ to zero as $n_t\to\infty$ for given δ by

$$R_Z(\delta)=\lim_{n_t\to\infty}-\frac{\ln Z_{n_t}(\delta)}{\ln n_t}\le\frac{1}{2}-\frac{1}{2+\delta}, \tag{6.4}$$

where the inequality is due to (6.3). The best overall convergence rate is determined by the supremum of (6.4) taken over all $\delta>0$,

$$R_Z=\sup_{\delta>0}R_Z(\delta)\le 1/2, \tag{6.5}$$

i.e. in the best possible case $Z_{n_t}(\delta)\to 0$ as $1/\sqrt{n_t}$. This best rate is achieved, for example, by Toeplitz correlation matrices (see Section 6.3). Note that using a specific fixed δ to find R_Z may lead to an

incorrect result[15], i.e. the supremum in (6.5) is essential. It should also be pointed out that the generalized Lyapounov Theorem does not require δ to be a constant [54], [118]: it can be a function of n_t, $\delta(n_t)>0$, which further extends the generality of (6.1). [54], [118] give specific examples, which demonstrate greater generality of this formulation.

While the conditions (6.1) and (6.2) are not easy to deal with, some cases when Theorem 4.3 does not apply can be characterized in a simple way, which provides simple necessary conditions for that theorem.

Corollary 6.1: Let $\lambda_1^t \geq \lambda_2^t \geq ... \geq \lambda_{n_t}^t$ be the eigenvalues of $\mathbf{R}_t$ sorted in decreasing order. (6.1) does not hold true, so that Theorem 4.3 cannot be applied if there is a finite set of eigenvalues, which are not dominated by the rest, i.e. there exists k such that

$$c = \lim_{n_t \to \infty} \frac{\sum_{i=k+1}^{n_t} \left(\lambda_i^t\right)^2}{\sum_{i=1}^{k} \left(\lambda_i^t\right)^2} < \infty, \tag{6.6}$$

which physically means that the multipath is not rich enough as $n_t \to \infty$.

Proof: see Appendix D.

From (6.6), a necessary condition for Theorem 4.3 is that $c=\infty$.While condition (6.6) is less general than (6.1) or (6.2), it allows for an insight and is simple to evaluate since it involves only the second-order moments of λ^t. Consider two broad cases where Corollary 6.1 applies: (i) $\mathbf{R}_t$ has a finite number (k) of non-zero eigenvalues as $n_t \to \infty$, which corresponds to a limited number of multipath in the propagation channel. Then $\sum_{i=k+1}^{n_t} \left(\lambda_i^t\right)^2 = 0$ and consequently $c=0$. Thus, a necessary physical condition for Theorem 4.3 to hold is that the number of multipath components goes to infinity with n_t. (ii) The largest eigenvalue is not dominated by all other eigenvalues,

$$c = \lim_{n_t \to \infty} \sum_{i=2}^{n_t} \left(\lambda_i^t\right)^2 \Big/ \left(\lambda_1^t\right)^2 < \infty, \tag{6.7}$$

which hold true, for example, when $\lambda_2^t \sqrt{n_t} / \lambda_1^t < \infty$ as $n_t \to \infty$. Thus, a necessary condition for Theorem

[15] For example, the results in [69] correspond to $\delta = 1$, which implies $R_Z \leq 1/6$.

4.3 is that $\lim_{n_t\to\infty}\lambda_1'\Big/\left(\lambda_2'\sqrt{n_t}\right)=0$. Consider, as an example, the uniform correlation matrix (2.13), when all the non-diagonal entries of $\mathbf{R}_t$ are equal to r_t. The eigenvalues in this case can be found explicitly in a closed form: $\lambda_1'=1+(n_t-1)\cdot r_t$; $\lambda_2'=\ldots=\lambda_{n_t}'=1-r_t$, where r_t is the parameter indicating the correlation between two adjacent antenna elements. Thus, for $k=1$ and $r_t\neq 0$, $c=0$, i.e. λ_1' is not dominated by all the other eigenvalues. In this case, $\lim_{n_t\to\infty} Z_{n_t}(\delta)=1$ and Theorem 4.3 does not apply.

6.2. Accuracy of Gaussian Approximation

For finite n_t, the Gaussian distribution serves as an approximation of the true one. Its accuracy can be estimated from the following results.

Proposition 6.2: Let $\Delta_{n_t}(\mathbf{x})=\left|F_{n_t}(\mathbf{x})-\Phi(\mathbf{x})\right|$, where $F_{n_t}(\mathbf{x})$ is the CDF of $\boldsymbol{\lambda}$ given n_t, where $\boldsymbol{\lambda}$ are the eigenvalues of the channel matrix $\mathbf{H}$, and $\Phi(\mathbf{x})$ is a normal CDF with the same mean and covariance as that of $\boldsymbol{\lambda}$. From [[7], Theorem 1.1.][16],

$$\Delta_{n_t}=\sup_{\mathbf{x}}\Delta_{n_t}(\mathbf{x})\le c\cdot n_r^{1/4}Z_{n_t}(\delta)^{2+\delta},\ 0<\delta\le 1, \tag{6.8}$$

where $c\le 4$ is an absolute constant. Moreover, since the channel capacity C is a continuous function of $\boldsymbol{\lambda}$, and the upper bound in (6.8) is valid for all $\mathbf{x}$, it also applies to $\Delta_{n_t}(x)=\left|F_{n_t}(x)-\Phi(x)\right|$, where $F_{n_t}(x)$ is the channel outage capacity distribution given n_t, and $\Phi(x)$ is the Gaussian CDF with the same mean and variance as of C.

In analogy with (6.4), the rate of convergence $\Delta_{n_t}\to 0$ is defined as

$$R_\Delta(\delta)=\lim_{n_t\to\infty}-\frac{\ln\Delta_{n_t}}{\ln n_t}\ge(2+\delta)R_Z(\delta),\ 0<\delta\le 1, \tag{6.9}$$

where the inequality is due to (6.4) and (6.8). From (6.4), the best convergence rate of $Z_{n_t}(\delta)\to 0$ for given δ is $R_Z(\delta)=1/2-1/(2+\delta)$. In this best case,

$$R_\Delta=\sup_{\delta}R_\Delta(\delta)\ge 1/2, \tag{6.10}$$

[16] [[7], Theorem 1.1.] is stated for $\delta=1$, but it can also be extended to $0<\delta\le 1$ [6].

i.e. the convergence is at least as $1/\sqrt{n_t}$. It should be noted that: (i) Even though the lower bound in (6.10) corresponds to $\delta=1$, it does not necessarily mean that the upper bound in (6.8) gives the best estimate of Δ_{n_t} for $\delta=1$[17]. (ii) In some cases, the upper bound in (6.8) significantly overestimates Δ_{n_t}, so that the convergence is better than expected from the bound (see also the summary to this chapter).

6.3. Convergence Condition for Channels with Toeplitz Correlation Structure

While the conditions in (6.1) and (6.2) are important theoretical tools, their usefulness for practical computations is rather limited due to two reasons: (i) The eigenvalues are known in a closed form only for some simple matrices. Consequently, these conditions can be evaluated analytically only in such cases. (ii) Numerical evaluation of these conditions is difficult, since the numerical complexity (number of operations, inaccuracy, etc.) of the eigenvalue problem increases rapidly with n_t, so that for $n_t \to \infty$ it is problematic if possible at all. The following theorem gives a condition that is easier to evaluate.

Theorem 6.2: Let $\mathbf{R}_t$ be a Toeplitz correlation matrix with elements $[\mathbf{R}_t]_{k,m} = t_{k-m}$, such that

$$0 < M_t = \lim_{n_t \to \infty} \sum_{k=-n_t+1}^{n_t-1} |t_k|^2 < \infty, \tag{6.11}$$

i.e. $\mathbf{R}_t$ is non-degenerate and square-summable[18]. Then for $\forall \delta > 0$, the following holds:

$$\lim_{n_t \to \infty} Z_{n_t}(\delta) = \left(I_{2+\delta}\right)^{1/(2+\delta)} \left(I_2\right)^{-1/2} \cdot \lim_{n_t \to \infty} n_t^{\frac{\delta}{2(2+\delta)}} = 0, \tag{6.12}$$

where

$$I_p = (2\pi)^{-1} \int_0^{2\pi} f^p(x)dx < \infty, \text{ for } \forall p > 0 \tag{6.13}$$

and a non-negative real function $f(x) = \sum_{k=-\infty}^{\infty} t_k \cdot e^{jkx}$ is the spectrum of $\mathbf{R}_t$ [30].

Proof: see Appendix D.

Not only does Theorem 6.2 give a practical way to evaluate the condition (6.1) for Toeplitz

---

[17] See [85] for detailed discussion of this issue.

[18] If $\mathbf{R}_t$ is non-degenerate and absolutely summable, it also satisfies (6.11), since $\sum_{k=-n_t+1}^{n_t-1} |t_k|^2 \le \left(\sum_{k=-n_t+1}^{n_t-1} |t_k|\right)^2$.

correlation matrices[19] without using eigenvalue decomposition, it also shows that under condition (6.11), the outage capacity is always asymptotically normal.[20] From Corollary 3.4

$$M_t = \lim_{n_t \to \infty} \sum_{k=-n_t+1}^{n_t-1} |t_k|^2 = \lim_{n_t \to \infty} n_t^{-1} \|\mathbf{R}_t\|^2 \tag{6.14}$$

Thus in the case of Toeplitz matrices, a necessary condition for $Z_{n_t}(\delta)$ to converge to zero and hence for Theorem 4.3 to hold is that the measure of correlation and power imbalance $n_t^{-1}\|\mathbf{R}_t\| \to 0$ as $n_t \to \infty$[21].

Furthermore, from (6.12) $R_Z = 1/2$, (the supremum is at $\delta \to \infty$), i.e. under the conditions of Theorem 6.2, the upper bound in (6.5) is achieved and the convergence is as $1/\sqrt{n_t}$. This result is general for a wide class of Toeplitz correlation matrices which satisfy (6.11), regardless of any other details. As a numerical example, Fig. 6.1 shows the upper bound in (6.8) and $\Delta_{n_t}(x_0)$ vs. n_t, where x_0 is outage capacity such that the outage probability $\Phi(x_0) = 0.01$. $Z(\delta)$ is calculated at $\delta = 1$ for $\mathbf{R}_t$ given by the exponential correlation model (2.14) with correlation parameter $r_t = 0.5$, $\Delta_{n_t}(x_0)$ is obtained by Monte-Carlo (MC) simulation using 10^5 trials. As expected, the upper bound (solid line) decreases as $1/\sqrt{n_t}$ (see the dashed line for comparison). $\Delta_{n_t}(x_0)$ lies well below the upper bound, and decreases with n_t at least as $1/\sqrt{n_t}$.

When $\mathbf{R}_t$ is not Toeplitz, Theorem 6.2 does not apply. However, it is shown in Appendix D for correlation matrices with an arbitrary structure, that $Z_{n_t}(1)$ is bounded by the norm of $\mathbf{R}_t$ as follows:

$$\left(n_t^{-1}\|\mathbf{R}_t\|\right)^{1/3} \le Z_{n_t}(1) \le 1 \tag{6.15}$$

Similarly to the Toeplitz correlation structures considered above, a necessary condition for $Z_{n_t}(1)$ to converge to zero and hence for Theorem 4.3 to hold is that the measure of correlation $n_t^{-1}\|\mathbf{R}_t\| \to 0$ as $n_t \to \infty$. Moreover, since $n_t^{-1}\|\mathbf{R}_t\| \to 0$ increases with correlation (see Chapter V), the overall tendency for $Z_{n_t}(1)$ is to increase with correlation, which results in slower convergence for higher correlated

---

[19] Toeplitz correlation matrix physically corresponds to uniform antenna array geometry, when correlation depends on the spacing between elements only, but not on their positions.

[20] Note that the uniform correlation matrix [55] does not satisfy (6.11), unless $r_t = 0$.

[21] In this sense, the Tx antennas are asymptotically uncorrelated.

channels.

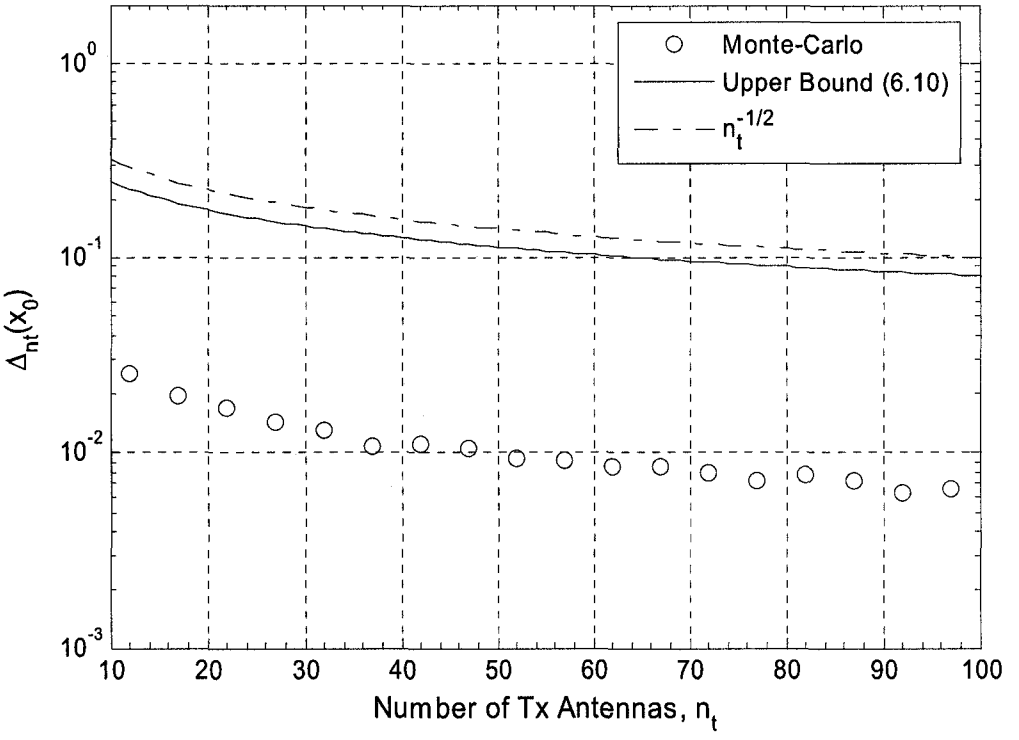

Fig. 6.1 Distance between the outage capacity distribution of Rayleigh-fading channel and the Gaussian approximation; $c=0.4$, $n_r=2$, $\Phi(x_0)=0.01$.

6.4. Convergence for Some Popular Correlation Models

While the exponential correlation matrix (2.14) has been used in the numerical examples above, it was not demonstrated that it satisfies the condition (6.1). In fact, the eigenvalues in this case are given by a transcendental equation [86], which does not allow easy evaluation of (6.1). However, using d'Alambert Ratio Test [119], it can be shown that in this case $M_t<\infty$ for $|r_t|<1$, so that following Theorem 6.2, condition (6.1) is indeed satisfied. Moreover, using (6.12)

$$\lim_{n_t\to\infty} Z_{n_t}(1)=\frac{\left(1+4|r_t|^2+|r_t|^4\right)^{1/3}}{\left(1+|r_t|^2\right)^{1/2}\cdot\left(1-|r_t|^2\right)^{1/6}}\cdot\lim_{n_t\to\infty} n_t^{-1/6}=0\,,\ |r_t|<1 \tag{6.16}$$

From the definition of a limit, for any $\varepsilon > 0$, there is n_0 such that for all $n_t > n_0$ $Z_{n_t}(1) \le \varepsilon$. (6.16) shows that n_0 is an increasing function of $|r_t|$, i.e. larger correlation results in slower convergence. This supports the conclusion in the previous section, and explains the corresponding observation in [69] that was based on numerical results. When the correlation is significant only among adjacent antennas, the elements of $\mathbf{R}_t$ are given by the tri-diagonal correlation matrix (2.16). It is straightforward to show that $M_t < \infty$, i.e. from Theorem 6.2, $Z_{n_t}(1) \to 0$ as $n_t \to \infty$. Thus, Theorem 4.3 applies in this case. Moreover,

$$\lim_{n_t \to \infty} Z_{n_t}(1) = \frac{\left(1+6|r_t|^2\right)^{1/3}}{\left(1+2|r_t|^2\right)^{1/2}} \cdot \lim_{n_t \to \infty} n_t^{-1/6} = 0, \tag{6.17}$$

i.e. similarly to (6.16), n_0 is an increasing function of $|r_t|$, and higher correlation results in slower convergence. Another important case is the squared-exponential correlation matrix (2.15), which has been proposed for the IEEE 802.11n Wireless LANs standard [22]. While the confirmation of (6.1) is difficult in this case, it is straightforward to show that $M_t < \infty$, $|r_t| < 1$, and hence (6.1) holds.

It can be shown, however, that M_t is unbounded for the popular correlation models which correspond to the uniform or truncated Laplacian angular distributions of the multipath [22]. Hence, Theorem 6.2 does not apply in these cases. Clearly, whether M_t is finite or not is determined by asymptotic behavior of $\mathbf{R}_t$'s tails ($k, m \to \infty$). However, the match between the popular correlation models and real correlation structures for $k, m \to \infty$ has not been thoroughly studied, if studied at all, since (i) in practice n_t is always finite, so that the asymptotic behavior of $\mathbf{R}_t$'s tails had little or no importance, and (ii) measuring these tails is difficult from the technical point of view. Thus, the issue of convergence for practical correlation structures seems to be an open problem. The usefulness of Theorem 6.2, however, is somewhat more general than just with respect to some particular correlation models. It states that Theorem 4.3 applies for all Toeplitz correlation structures for which the correlation decays faster than $1/\sqrt{D}$, where D is the distance between the antenna elements.

6.5. Summary: On Practical Utility of Gaussian Approximation

The practical utility of the asymptotic Gaussian distribution is that it can be used as an approximation to the outage capacity distribution of MIMO channels with finite (realistic) n_t. While the convergence conditions discussed above are important theoretical tools that provide generic guidance, they should be used with caution for practical applications due to the following reasons: (i) Even though condition (6.1) is satisfied for some δ, it does not mean that Δ_{n_t} is sufficiently small for realistic n_t. Consequently, using Gaussian approximation for realistic (finite) n_t may result in inaccurate estimation of the channel capacity. (ii) In the opposite case, when (6.1) is not satisfied, Δ_{n_t} may be still sufficiently small for given realistic n_t, so that the Gaussian approximation can be used. Note also that (6.1) is a sufficient but not necessary condition. (iii) The common generic approach to evaluate Δ_{n_t} is by the upper bound in (6.8), which, in many cases, is very conservative for low to moderate n_t [118]. As we have shown, this bound does not converge faster then $1/\sqrt{n_t}$, which is comparatively slow and requires large n_t to guarantee accurate approximation based on the bound alone. In practice, however, the convergence can be much faster, so that the difference between the true distribution and its Gaussian approximation can be indistinguishably small already for $n_t = 2$, as shown in [101], [32], and in Chapter XI using rigorous statistical methods. This problem arises from the fact that the upper bound on (6.8) applies to a wide class of channel distributions and therefore cannot be further improved unless specific distributions are considered [85]. The mathematical results in this area are rare [118].

The results in this chapter are presented in [45] and [50].

CHAPTER VII: WHAT IS THE BEST ANGULAR DENSITY OF MULTIPATH IN MIMO CHANNELS?

The problem of channel capacity maximization over multipath angular density is solved for uniform linear arrays with a large number of antennas. It is shown that the asymptotic capacity of a broad class of MIMO channels (not necessarily Rayleigh-fading) with an arbitrary correlation structure does not depend on particular channel distribution, but only on the correlation between antennas. The best multipath angular density that eliminates the correlation and thus maximizes the asymptotic capacity is non-uniform, which implies that the popular Clarke's (Jakes) [34] model does not represent the best case scenario. This result provides a number of practical guidelines for antenna design.

7.1. Asymptotic Capacity of MIMO Channels

Consider instantaneous capacity of a MIMO channel with n_t Tx and n_r Rx antennas. The following common assumptions are adopted. (i) The channel state information (CSI) is available at the Rx end but not at the Tx end. (ii) The total transmitted power is constrained to P_T and does not depend on n_t. (iii) The noise at Rx end is spatially uncorrelated circular symmetric Gaussian and has identical power per each Rx antenna. From [25], the instantaneous capacity per Rx antenna of a frequency flat quasi-static MIMO channel in natural units $[nat]$ is given by

$$C_1 = n_r^{-1} \ln \det[\mathbf{I} + \gamma_0 / n_t \cdot \mathbf{H}\mathbf{H}^H], \tag{7.1}$$

where γ_0 is the SNR per Rx antenna. Without loss of generality $\mathbf{H}$ is normalized so that $E\{\|\mathbf{H}\|^2\} = n_t n_r$, where $\| \ \|$ is L_2 norm. The following notations are used below: (i) $\mathbf{\Gamma}_1 = E\{vec(\mathbf{H}) \cdot vec^H(\mathbf{H})\}$, $\mathbf{\Gamma}_2 = E\{vec(\mathbf{H}^H) \cdot vec^H(\mathbf{H}^H)\}$. (ii) $\mathbf{R}_r = n_t^{-1} E\{\mathbf{H}\mathbf{H}^H\}$, $\mathbf{R}_t = n_r^{-1} E\{\mathbf{H}^H\mathbf{H}\}$. Note that due to adopted normalization, $tr\{\mathbf{R}_r\} = n_r$ and $tr\{\mathbf{R}_t\} = n_t$.

Definition 7.1: The total fourth order cumulant of $\mathbf{H}$ is defined as

$$K_4(\mathbf{H}) = \sum_{k,m=1}^{n_t} \sum_{n,l=1}^{n_r} \kappa_4(H_{nm} H_{nk} H_{lk} H_{lm}), \tag{7.2}$$

where $\kappa_4(H_{nm} H_{nk} H_{lk} H_{lm}) = E\{H_{nm}^* H_{nk} H_{lk}^* H_{lm}\} - E\{H_{nm}^* H_{nk}\} E\{H_{lk}^* H_{lm}\} - E\{H_{nm}^* H_{lm}\} E\{H_{nk} H_{lk}^*\}$ is the fourth order cumulant of circular symmetric random variables [88], H_{nm}^* is the complex conjugate of H_{nm}. If $\mathbf{H}$ is complex circular symmetric Gaussian, then $\kappa_4(H_{nm} H_{nk} H_{lk} H_{lm}) = 0$, otherwise, it is in general nonzero [88].

Definition 7.2: The pseudo-norm of $\mathbf{\Gamma}_1$, $\mathbf{\Gamma}_2$:

$$\|\mathbf{\Gamma}_1\|_Q = \left(\sum_{k,l=1}^{n_t} |tr\{\mathbf{Q}_{kl}\}|^2 \right)^{1/2}, \quad \|\mathbf{\Gamma}_2\|_Q = \left(\sum_{k,l=1}^{n_r} |tr\{\mathbf{G}_{kl}\}|^2 \right)^{1/2}, \tag{7.3}$$

where $\mathbf{Q}_{kl} = E\{\mathbf{h}_k \mathbf{h}_l^H\}$ and $\mathbf{G}_{kl} = E\{\mathbf{g}_k \mathbf{g}_l^H\}$ are the blocks of $\mathbf{\Gamma}_1$ and $\mathbf{\Gamma}_2$, $\mathbf{h}_k$ and $\mathbf{g}_k$ are the k^{th} columns of $\mathbf{H}$ and $\mathbf{H}^H$ respectively.

In general, $\| \ \|_Q$ is not a norm in the classic sense, since it is possible that for two matrices $\mathbf{\Gamma}_1 \neq \mathbf{\Gamma}_2$, $\|\mathbf{\Gamma}_1 - \mathbf{\Gamma}_2\|_Q = 0$. However, as we show later, in some cases the pseudo-norm is equivalent to the L_2 norm.

Theorem 7.1: Let $\mathbf{H}$ be a complex circular symmetric random matrix (not necessarily Gaussian), and the following conditions are satisfied:

$$\text{(i)} \lim_{n_t, n_r \to \infty} [n_t^{-2} (\|\mathbf{\Gamma}_1\|_Q^2 + \|\mathbf{\Gamma}_2\|_Q^2) - \|\mathbf{R}_r\|^2] = 0 \tag{7.4}$$

$$\text{(ii)} \lim_{n_t, n_r \to \infty} n_t^{-2} K_4(\mathbf{H}) = 0 \tag{7.5}$$

Then, as n_t or both n_t and n_r go to infinity, the instantaneous capacity per Rx antenna is

$$C_1 \xrightarrow{p} n_r^{-1} \ln(\det[\mathbf{I} + \gamma_0 \mathbf{R}_r]), \tag{7.6}$$

where $\xrightarrow{p}$ denotes convergence in probability.

Proof: see Appendix E.

Theorem 7.1 allows to split the effect of correlation at transmit and receive ends and indicates that in asymptotic approximation the channel capacity does not depend on a particular distribution of $\mathbf{H}$, but

only on $\mathbf{R}_r$. Note that the RHS of (7.6) corresponds to the upper bound on the mean (ergodic) capacity $\bar{C}$ (2.36) for Rayleigh-fading channels with a finite number of antennas, i.e. following Theorem 7.1, the bound is asymptotically tight. Thus, in the small outage probability region

$$C_1 < n_r^{-1}\bar{C} \le n_r^{-1}\ln(\det[\mathbf{I}+\gamma_0\mathbf{R}_r]) \tag{7.7}$$

Moreover, under the conditions of Theorem 7.1, the channel "hardens" as the number of antennas increases, i.e. C_1 converges to a deterministic value equal to the upper bound. As a special case, Theorem 7.1 includes a number of popular channel models for which the result in (7.6) is known:

(i) $\mathbf{H}$ is i.i.d. complex circular symmetric. Based on Definition 7.1, it is straightforward to show that $K_4(\mathbf{H}) = n_t n_r (E\{|H_{km}|^4\} - 2)$. Apparently, if $\mathbf{H}$ is i.i.d. complex circular symmetric Gaussian [103], [25], $(E\{|H_{km}|^4\} = 2)$, then $K_4(\mathbf{H}) \equiv 0$, so that (7.5) always holds true. If $\mathbf{H}$ is not Gaussian, but $E\{|H_{km}|^4\}$ is finite as in [[108], Theorem 2.76], it is straightforward to show that in this case $n_t^{-2}K_4(\mathbf{H})$ behaves as n_r/n_t, and $n_t^{-2}(\|\mathbf{\Gamma}_r\|_Q^2 + \|\mathbf{\Gamma}_t\|_Q^2) - \|\mathbf{R}_r\|^2 = n_r/\sqrt{n_t}$. Thus, Theorem 7.1 holds if $\lim_{n_t,n_t\to\infty} n_r \cdot n_t^{-1/2} = 0$.

(ii) The channel correlation structure is separable and follows Kronecker correlation model (2.9), i.e. $\mathbf{\Gamma}_1 = \mathbf{R}_t^* \otimes \mathbf{R}_r$, $\mathbf{\Gamma}_2 = \mathbf{R}_r^* \otimes \mathbf{R}_t$, where $\mathbf{R}_t^*$ is the complex conjugate of $\mathbf{R}_t$ elementwise. It is straightforward to show, based on Definition 7.2, that in this case $\|\mathbf{\Gamma}_1\|_Q^2 = n_r^2\|\mathbf{R}_t\|^2$, $\|\mathbf{\Gamma}_2\|_Q^2 = n_t^2\|\mathbf{R}_r\|^2$ (the pseudo-norm and the L_2 norm are equivalent), and thereby (7.4) becomes

$$\lim_{n_t,n_r\to\infty}[n_t^{-2}(\|\mathbf{\Gamma}_r\|_Q^2 + \|\mathbf{\Gamma}_t\|_Q^2) - \|\mathbf{R}_r\|^2] = \lim_{n_t,n_r\to\infty}\left(\frac{n_r}{n_t}\|\mathbf{R}_t\|\right)^2 = 0, \tag{7.8}$$

where $n_t^{-1}\|\mathbf{R}_t\|$ is the measure of correlation and power imbalance of a MIMO channel[22] at Tx end introduced in Chapter V.

Consider a Rayleigh-fading and a non Rayleigh-fading MIMO channels (both with the same $\mathbf{R}_r$) such that conditions (7.4) and (7.5) are satisfied. From Theorem 7.1, when the number of antennas is large in both channels, their instantaneous capacity converges to the same value given by the right hand side

[22] If $\lim_{n_t\to\infty} n_t^{-1}\|\mathbf{R}_t\| = 0$, the channel is said to be asymptotically uncorrelated.

(RHS) of (7.6). This motivates the following definition:

Definition 7.3: A MIMO channel is said to be asymptotically Rayleigh-like (in terms of capacity) if it satisfies conditions (7.4) and (7.5).

Note that uncorrelated keyhole channels are not Rayleigh-like, since in this case (7.5) is not satisfied as $\lim_{n_t\to\infty} n_t^{-2}K_4(\mathbf{H}) = n_r^2 \neq 0$.

Corollary 7.1: Consider a MIMO channel that satisfies the conditions of Theorem 7.1 and whose correlation matrix $\mathbf{R}_r$ has a Toeplitz structure, i.e. $R_{nm} = R_{n-m}$, $n,m = 1...n_r$, where R_{nm} is an element of $\mathbf{R}_r$, and R_{n-m} is the matrix-generating vector. Assume that $\mathbf{R}_r$ is non-degenerate and square-summable[23], i.e. $0 < \lim_{n_r\to\infty} \sum_{n=-n_r+1}^{n_r-1} |R_n|^2 < \infty$. Then as both n_t and n_r go to infinity, the instantaneous capacity of the channel per Rx antenna is

$$C_1 \xrightarrow{p} (2\pi)^{-1} \int_{-\pi}^{\pi} \ln[1 + \gamma_0 \lambda(u)] du, \tag{7.9}$$

where $\lambda(u) = \lim_{n_r\to\infty} \sum_{n=-n_r+1}^{n_r-1} R_k e^{jnu}$, $u \in (-\pi;\pi]$ is the spectrum of $\mathbf{R}_r$, $j = (-1)^{1/2}$.

Proof: due to the Szego Theorem [30].

Despite the asymptotic nature, (7.6) and (7.9) approximate reasonably well the instantaneous capacity of MIMO channels with a moderate number of antennas. To demonstrate this, consider, as an example, a correlated Rayleigh-fading channel with the Kronecker correlation structure, when both $\mathbf{R}_t$ and $\mathbf{R}_r$ are given by the exponential correlation model with parameter r (the correlation between two adjacent antennas). It straightforward to show that the spectrum of $\mathbf{R}$ (either $\mathbf{R}_t$ or $\mathbf{R}_r$) in this case is given by $\lambda(u) = (1-|r|^2)/|1-re^{ju}|^2$, $|r|<1$. Note that since $\lambda(u)$ is periodic with the period 2π, the capacity in (7.9) is not affected by the phase of r, but only by its amplitude. Fig. 7.1 shows the capacity of a correlated Rayleigh MIMO channel per Rx antenna with $n_t = 5$ and $n_r = 2$. The solid line represents the "true" mean capacity obtained by the Monte-Carlo (MC) simulation and averaged over 10^3 channel realizations, the error bars illustrate $\pm\sigma$ deviation range of the instantaneous capacity around its mean

[23] If $\mathbf{R}_r$ is non-degenerate and absolutely summable, it also satisfies the condition of Corollary 7.1, since $\sum_{n=-n_t+1}^{n_t-1} |R_n|^2 \le \left(\sum_{n=-n_t+1}^{n_t-1} |R_n|\right)^2$.

value, and the doted lines demonstrate the asymptotic approximations in (7.6) and (7.9). In general, the gap between (7.6) and the "true" mean capacity increases with $|r|$. (7.9) coincides with (7.6) for small $|r| \le 0.2$. In contrast to (7.6), the discrepancy between (7.9) and the "true" mean capacity decreases with $|r|$, so that the two are practically indistinguishable for $|r| \ge 0.7$. Note that in this case, the deviations of the instantaneous capacity around its mean are relatively small. Therefore, the latter can be approximated with reasonable accuracy by the mean capacity, which, in turn, is well approximated by the integral in (7.9), see Fig. 7.1.

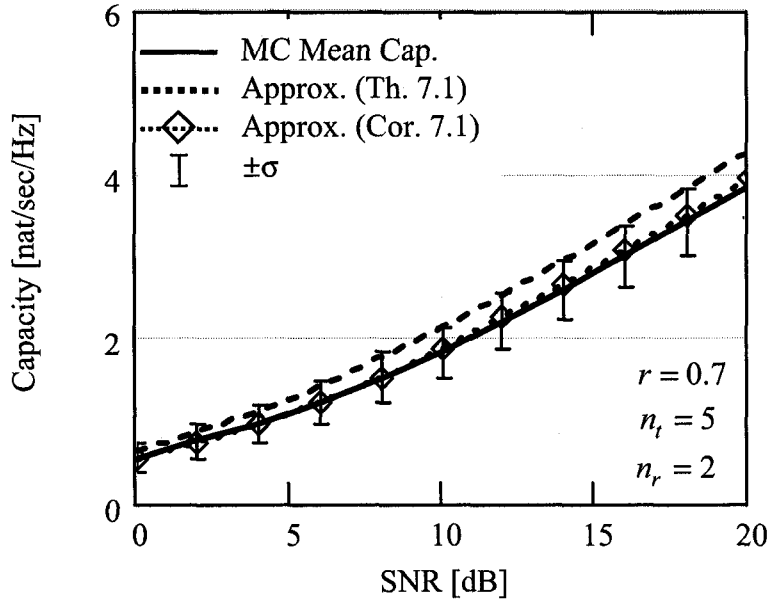

Fig. 7.1 Capacity per Rx antenna of correlated Rayleigh-fading channel.

- *Maximum Asymptotic Capacity*:

From Hadamard inequality [119], it follows that $0 \le \det(\mathbf{R}) \le 1$ for any $n \times n$ correlation matrix $\mathbf{R}$ normalized such that $tr(\mathbf{R}) = n$. Thus, the asymptotic capacity in (7.6) is maximal when $\mathbf{R}_r = \mathbf{I}$, i.e. the channel is uncorrelated at the Rx end. In this case the spectrum of $\mathbf{R}_r$ is

$$\lambda(u) = 1, \; u \in (-\pi; \pi], \tag{7.10}$$

and the corresponding channel capacity per Rx antenna is $C_{max} = \ln(1 + \gamma_0)$, i.e. in the asymptotic

approximation, each additional Rx antenna increases the total capacity by the amount equivalent to the capacity of an 1x1 AWGN channel. The multipath angular density that achieves the maximal capacity $C_{\max}$ for a broad class of MIMO channels is derived in the following sections.

7.2. Best Angular Density in 2-D Space

Consider a channel where the multipath is randomly distributed on the xy plane. Let $R(x)$ denote the spatial correlation between two antennas at spacing x. The multipath wave-number spectrum and the correlation function are related by the Fourier Transform [110]

$$f(k_x) = (2\pi)^{-1} \int_{-\infty}^{\infty} R(x) e^{-jk_x \cdot x} dx , \tag{7.11}$$

where k_x is x component of the wave-vector $\mathbf{k}$. $f(k_x)$ is often referred as the probability density function (PDF) of k_x [110] due to the following properties: (i) $f(k_x)$ is real and non-negative assuming that $R(x)$ is Hermitian, (ii) under normalization $R(0) = 1$, $\int_{-\infty}^{\infty} f(k_x) dk_x = R(0) = 1$.

Consider a receiving ULA of isotropic antennas located along x axis, when the correlation between antennas is given by the Toeplitz matrix $\mathbf{R}_r$, such that $R_n = R(d \cdot n)$, $n \in \mathrm{Z}$ (integer numbers), where R_n is the matrix-generating vector of $\mathbf{R}_r$, and d is the adjacent antenna spacing. From the geometry of the problem [110], the link between k_x and the angle of arrival of a multipath component is $\psi = k_x d = 2\pi d \cos\theta$, $-\pi < \theta \le \pi$, where ψ represents the phase difference between two adjacent antennas, θ is measured from the array axis, and d is in wavelengths. Let $f_\psi(\psi)$ be the PDF of ψ, and $f_\theta(\theta)$ be the PDF of θ or multipath angular density. It is straightforward to show, using the connection between the spectrums of continuous and sampled signals, that there is a direct relationship between the spectrum $\lambda(u)$ of $\mathbf{R}_r$ (see (7.9)) and $f_\psi(\psi)$ as indicated below

$$\lambda(u) = 2\pi \sum_{n=-\infty}^{\infty} f_\psi\left(u - 2\pi n\right), \; u \in (-\pi; \pi], \tag{7.12}$$

where u is the normalized spatial frequency. Hence, by substituting (7.10) in (7.12) one obtains the condition to achieve the maximal capacity $C_{\max}$: $C_1 \xrightarrow{p} C_{\max}$ if

$$2\pi \sum_{n=-\infty}^{\infty} f_\psi(\psi - 2\pi n) = 1, \; \psi \in (-\pi; \pi] \tag{7.13}$$

Theorem 7.2: (i) If $d<1/2$, there is no such $f_\psi(\psi)$ that $C_1 \xrightarrow{p} C_{\max}$.

(ii) If $d>1/2$, there are a number of $f_\psi(\psi)$ such that $C_1 \xrightarrow{p} C_{\max}$.

(iii) If $d=1/2$, the only $f_\psi(\psi)$ such that $C_1 \xrightarrow{p} C_{\max}$ is the uniform PDF given by $f_\psi(\psi)=(2\pi)^{-1}$, $\psi \in (-\pi;\pi]$. The corresponding multipath angular density and correlation function are

$$f_\theta(\theta)=1/4\cdot\left|\sin(\theta)\right|,\ \theta\in(-\pi;\pi], \tag{7.14}$$

$$R(x)=sinc(2x), \tag{7.15}$$

where $sinc(x)=\sin(\pi x)/(\pi x)$.

Proof: see Appendix E.

Statement (i) of Theorem 7.2 implies that placing antennas closer than half a wavelength is not optimal in terms of the capacity C_1 per Rx antenna, which is the measure of efficiency of a single antenna. However, in some cases, it is worthwhile to place antennas closer then half a wavelength, as it may increase the total capacity by way of increasing the capacity per aperture length C_{ap}, which characterizes the efficiency of utilizing the space occupied by the antenna. The following example is the case where the capacity per Rx antenna decreases with d, but the capacity per aperture increases. Consider a ULA with $d<1/2$ when $f_\psi(\psi)$ is uniformly distributed over $[-2\pi d;2\pi d]$. From Corollary 7.1 and using (7.12) for $0<d<1/2$,

$$\begin{aligned} C_1 &\xrightarrow{p} (2\pi)^{-1}\int_{-2\pi d}^{2\pi d}\ln\left[1+2\pi\gamma_0 f_\psi(u)\right]du = 2d\ln\left[1+\frac{\gamma_0}{2d}\right] \\ C_{ap} &= C_1/d \xrightarrow{p} 2\ln\left[1+\frac{\gamma_0}{2d}\right] \end{aligned}, \tag{7.16}$$

i.e. asymptotically C_1 decreases as d decreases, but C_{ap} increases.

When $d>1/2$, it is in general difficult to find out what angular density $f_\theta(\theta)$ corresponds to such $f_\psi(\psi)$ that satisfies condition (7.13) and therefore maximizes the asymptotic capacity C_1, as implied by statement (ii) of Theorem 7.2. However, as $d\to\infty$, the following corollary gives a simple necessary condition that applies to $f_\theta(\theta)$ and indirectly verifies (7.13).

Corollary 7.2: For any multipath angular density that satisfies $f_\theta(\pi/2)<\infty$, i.e. there is no specular component at the broadside direction of a ULA, (7.13) always holds true as $d\to\infty$, and therefore $C_1 \xrightarrow{p} C_{\max}$.

Proof: see Appendix E.

To obtain an insight, consider a case when Corollary 7.2 is not satisfied. Assume that specular multipath arrive at only two equiprobable angles $\pm\pi/2$, i.e.

$$f_\theta(\theta)=[\delta(\theta-\pi/2)+\delta(\theta+\pi/2)]/2, \tag{7.17}$$

where $\delta(x)$ is the Dirac's delta function. Then it is straightforward to show that $\lambda(u)=2\pi\delta(u)$, and therefore from Corollary 7.1

$$C_1 \xrightarrow{p} \lim_{\varepsilon\to 0^+}(2\pi)^{-1}\int_{-\varepsilon}^{\varepsilon}\ln[1+\pi\gamma_0/\varepsilon]du=0, \tag{7.18}$$

i.e. C_1 does not converge to $C_{\max}$. Moreover, this example demonstrates a capacity saturation effect, when the contribution of each single antenna to the total capacity approaches zero as $n_r\to\infty$.

While under the condition of Corollary 7.2, $C_1 \xrightarrow{p} C_{\max}$ as $d\to\infty$, the convergence is generally not monotonic. To demonstrate this, Fig. 7.2 shows the asymptotic capacity per Rx antenna (7.9) vs. d, when the multipath angular density follows Clarke's (Jakes) model [34], i.e. $f_\theta(\theta)$ is uniformly distributed over $(-\pi;\pi]$. The dotted lines represent $C_{\max}$ calculated for $10dB$ and $15dB$ SNR. It can be seen that the asymptotic capacities (solid lines) converge not monotonically to corresponding $C_{\max}$ as d increases. The capacities almost achieve $C_{\max}$ at $d=1.5$. However, due to the capacity oscillations (see Fig. 7.2), a local increase in d may decrease the capacity instead of increasing it. Simulations show that the multipath angular density, not SNR, has a dominant effect on the oscillation amplitude, i.e. $\Delta_1\approx\Delta_2$ (see Fig. 7.2). This implies that for any multipath angular density that satisfies the condition of Corollary 2 and $d>0.5$, the tendency is that relative distance $|\ln C_1-\ln C_{\max}|$ decreases as γ_0 increases, i.e. the relative effectivity of an ULA increases with SNR.

Statement (iii) of Theorem 7.2 indicates that when $d=1/2$, the multipath angular density $f_\theta(\theta)$ that maximizes the asymptotic capacity is non-uniform. Thus, for asymptotically large ULA, the Clarke's

(Jakes) model [34], where $f_\theta(\theta)$ is assumed to be uniform over $(-\pi,\pi]$, does not represent the best case scenario. Since in some cases, the asymptotic capacity approximates well the exact one (see Fig. 7.1), the same conclusion can be made for ULA with a moderate number of antennas.

An intuition behind the result in (7.14) is there are two major effects that influence the channel capacity for given SNR: (i) the multipath angular spread; the larger the spread, the lower the correlation between antennas, the higher the capacity, and (ii) the concentration of the multipath around the broadside direction of a ULA; when the multipath arrive at the angles close to the endfire ($\theta = 0;\pi$), the ULA gain and thus the SNR is low, which results in low capacity. Combining these two effects together suggests that the best multipath angular density is high at broadside direction ($\theta = \pm\pi/2$) and decays toward endfire ($\theta = 0;\pi$).

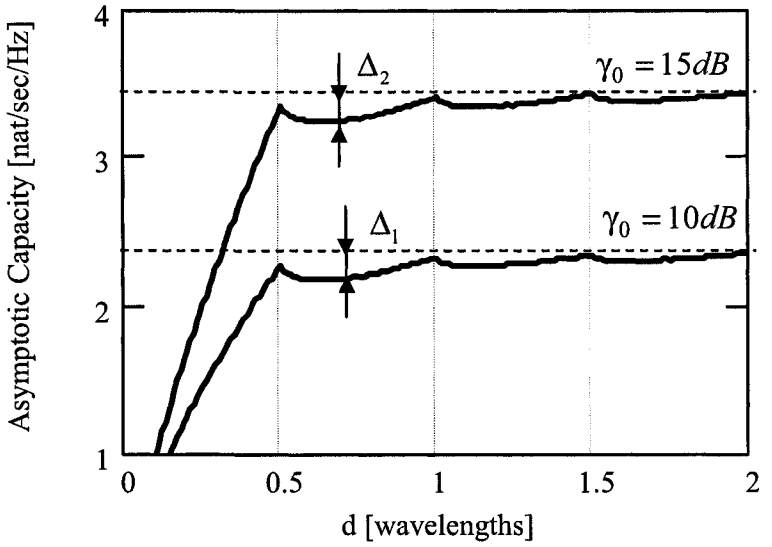

Fig. 7.2 Asymptotic capacity per Rx antenna (7.9) vs. antenna spacing. The multipath angular density follows Clarke's (Jakes) model [34], i.e. $f_\theta(\theta)$ is uniformly distributed over $(-\pi;\pi]$.

- *Measure of Correlation as a function of d* :

When the multipath angular density follows (7.14), the measure of correlation is well approximated, for large $n >> 1/(2d)$, by

$$n^{-1}\|\mathbf{R}\| \approx \frac{1}{\sqrt{n}} \begin{cases} \sqrt{1/(2d)}, & 0 < d \le 1/2 \\ \sqrt{(3d-1)/(2d^2)}, & 1/2 < d \le 1 \end{cases}, \tag{7.19}$$

(see Appendix E for a proof). When d is small ($0 < d \le 1/2$), $n^{-1}\|\mathbf{R}\|$ decreases monotonically as d increases. However, when $1/2 < d \le 1$, an increase in d does not necessarily decreases $n^{-1}\|\mathbf{R}\|$, but can also increase it. Since the asymptotic capacity is determined by the measure of correlation (see Chapters III and IV), this explains the oscillations observed in Fig. 7.2. When $d > 1$, the calculation of $n^{-1}\|\mathbf{R}\|$ is complicated. However under the condition of Corollary 7.2, for $d >> 1$ $\mathbf{R} \approx \mathbf{I}$ (best case in terms of asymptotic capacity), so that $n^{-1}\|\mathbf{R}\| \approx 1/\sqrt{n}$. For both $0 < d \le 1$ and $d >> 1$, $n^{-1}\|\mathbf{R}\| \to 0$ as $n \to \infty$, i.e. if the multipath angular density follows (7.14), the channel is asymptotically uncorrelated. However, if antenna arrays with a fixed aperture length $L = d \cdot n$ and $d \le 1/2$ are considered, $\lim_{n\to\infty} n^{-1}\|\mathbf{R}\| = 1/\sqrt{2L}$ (see (7.19)) does not converge to zero, i.e. the measure of correlation does not vanish asymptotically if $d \to 0$. Interestingly, when $0 < d \le 1/2$, for both arrays with fixed d and with fixed L, $(n^{-1}\|\mathbf{R}\|)^2$ equals to the array null-to-null bandwidth in wavelengths and determines the resolution ability of an array (for more details on array null-to-null bandwidth see [110]).

7.3. Best Angular Density in 3-D Space

Consider a uniform linear array located along z axis in the 3-D space. From the geometry of the problem [110] $\psi = k_z d = 2\pi d \cos\theta$, $0 \le \theta \le \pi$, where k_z is the z component of a random wave-vector $\mathbf{k}$, θ is the elevation angle measured from the array axis.

Theorem 7.3: The 3-D multipath angular density, which maximizes the asymptotic capacity per Rx antenna C_1 for $d = 1/2$, is given by

$$f_{\theta,\phi}(\theta,\phi) = 1/(4\pi) \cdot \sin(\theta),\ \theta \in [0;\pi],\ \phi \in (-\pi;\pi], \tag{7.20}$$

where ϕ is the azimuth angle, and $f_{\theta,\phi}(\theta,\phi)$ is the joint PDF of θ and ϕ.

Proof: due to the same arguments as for Theorem 7.2.

An isometric view of the best multipath angular density (7.20) is shown in Fig. 7.3. The ULA is located along z axis at $x = y = 0$. The density at angles θ and ϕ is represented by the distance between

the origin and the corresponding point on the figure surface. An intuition behind this result is that (i) the best angular density should not depend on ϕ, due to the rotational symmetry of the problem, (ii) given ϕ, $f_{\theta,\phi}(\theta,\phi)$ should coincide (up to a constant) with $f_{\theta}(\theta)$ in (7.14), i.e. in the best case scenario, the multipath angular density is concentrated around broadside direction ($\theta=\pi/2$) and decays toward endfire ($\theta=0,\pi$). Following (7.20), the angles θ and ϕ are statistically independent. Similarly to $f_{\theta}(\theta)$, $f_{\theta,\phi}(\theta,\phi)$ is non-uniform. The last fact has certain practical implications. Consider, for example, a 3-D environment where the multipath is not isotropic, but concentrated around a horizontal plane. Theorem 7.3 suggests that in order to increase the capacity in this case, the ULA should be placed orthogonally to this plane. Note that following the discussion in Section 7.1, this guideline holds for a broad class of MIMO channels with arbitrary correlation structure and not necessarily Rayleigh-fading.

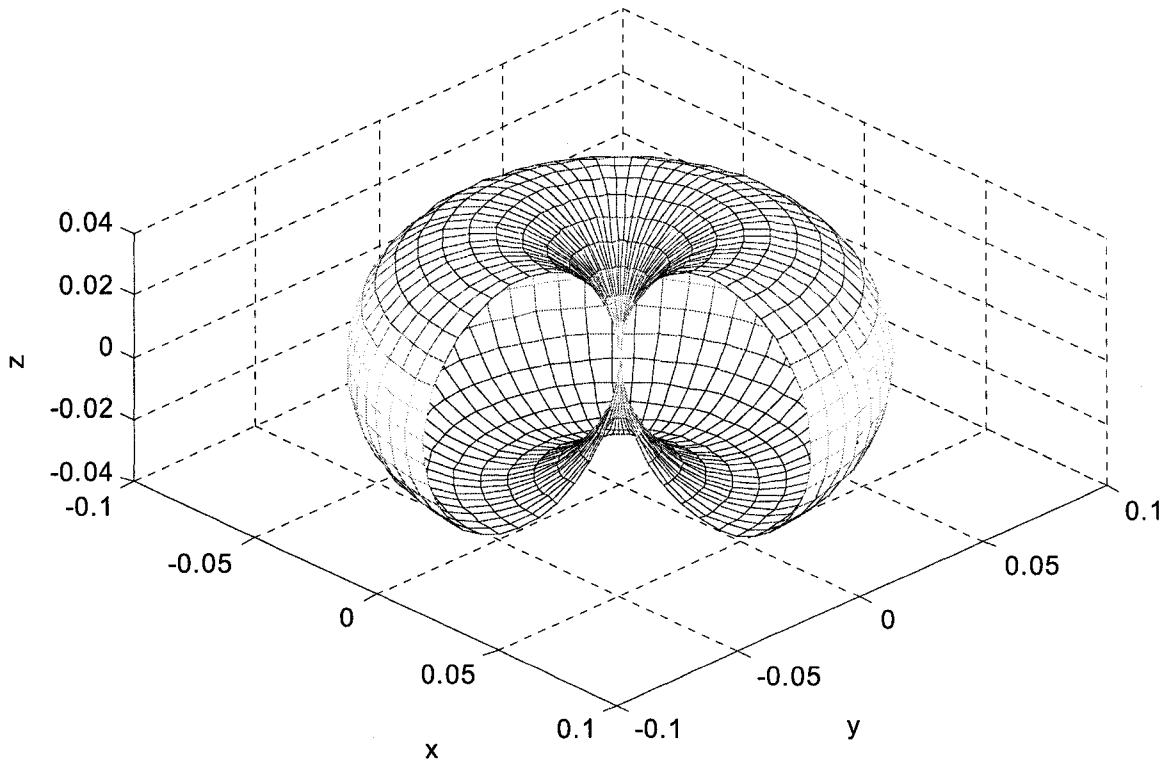

Fig. 7.3 An isometric view of the best multipath angular density in 3-D space (with $\pi/2$ cut). The ULA is located along z axis at $x=y=0$. The density at angles θ and ϕ is represented by the distance between the origin and the corresponding point on the figure surface.

7.4. Summary

The framework proposed in [109] is generalized and it is shown that when the number of antennas is large, the asymptotic outage capacity of a broad class of MIMO channels (not necessarily Rayleigh-fading) with an arbitrary correlation structure (not necessarily UIU [109]) does not depend on a particular channel distribution, but only on the correlation between antennas. Special cases include classic i.i.d. Rayleigh-fading channel [103], [25], Rayleigh-fading channel with separable (Kronecker) correlation structure [37], and i.i.d. zero-mean (not necessarily Rayleigh-fading) channel with finite forth-order statistics considered in [[108], Theorem 2.76].

Using Szego Theorem [30], the multipath angular density that eliminates the correlation between antennas and thus maximizes the asymptotic capacity of this class of MIMO channels is derived, when the receive ULA and the multipath are located on a plane (2-D). The capacity-maximizing density is non-uniform. Since the asymptotic capacity approximates reasonably well the exact one when the number of antennas is moderate, it is concluded that the popular Clarke's (Jakes) model [34] does not represent the best case propagation scenario. For the optimal multipath angular density, a simple expression, that links the measure of correlation and power imbalance to the distance between antennas, has been obtained. The expression explains the oscillatory behavior of the capacity as a function of antenna spacing.

The study is extended to the multipath distributed in the 3-D space (volume). It is shown that the capacity-maximizing angular density in this case is also non-uniform. The latter provides guidelines for an optimal location of a ULA antenna in a 3-D multipath environment.

The results in this chapter are presented in [42].

CHAPTER VIII: APPLICATIONS OF ASYMPTOTIC ANALYSIS

A number of applications of the asymptotic capacity analysis are considered. The fact that the outage capacity distribution of a broad class of MIMO channels is asymptotically Gaussian is used to characterize a finite SNR size-asymptotic diversity multiplexing trade-off (DMT) for keyhole channels in Section 8.1. A simple yet reasonably-accurate estimate of symbol error rate (SER) in a fading keyhole channel for a variety of modulation formats is obtained in Section 8.2. Telatar's Conjecture [103] is proven for multi-keyhole channels with a large number of antennas in Section 8.3. In Section 8.4, a motivation for the Kronecker correlation model (2.9) is provided by considering a Rayleigh-fading channel as a multi-keyhole one with a large number of keyholes. In Section 8.5, scheduling gain and the required feedback rate in wireless networks is evaluated assuming that the propagation environment is described by the multi-keyhole channel with a sufficient number of antennas, so that the asymptotic Gaussian approximation applies.

8.1. Finite SNR Diversity-Multiplexing Tradeoff

Multi-antenna (MIMO) systems are able to provide either high spectral efficiency (spatial multiplexing) or low error rate (high diversity) via exploiting multiple degrees of freedom available in the channel, but not both simultaneously as there is a fundamental tradeoff between the two. This tradeoff (DMT) is best characterized using the concepts of multiplexing and diversity gains [117]. Fundamentally, this is a tradeoff between the outage probability P_{out}, i.e. the probability that the fading channel is not able to support a transmission rate R, and the rate R, which can be expressed via the outage capacity distribution,

$$P_{out}(R) = \Pr[C < R] = F_C(R), \tag{8.1}$$

(see Chapter II, Section 2.1 for details on $F_C(R)$). Defining the multiplexing gain r as

$$r = \lim_{\gamma \to \infty} R / \ln \gamma_0, \tag{8.2}$$

where γ_0 is the average SNR per Rx antenna, and the diversity gain as[24]

$$d = -\lim_{\gamma \to \infty} \frac{\ln P_{out}}{\ln \gamma_0} \tag{8.3}$$

the asymptotic ($\gamma_0 \to \infty$) tradeoff for the independent identically distributed (i.i.d.) Rayleigh fading channel with the coherence time in symbols $l \geq n_t + n_r - 1$ can be compactly expressed as [117],

$$d(r) = (n_t - r)(n_r - r),\ r = 0,1,\ldots \min(n_t, n_r) \tag{8.4}$$

for integer values of r, and using the linear interpolation in-between. While this approach provides a significant insight into MIMO channels and also into performance of various systems that exploit such channels, it has a number of limitations. Specifically, it does not say anything about operational significance of r and d at realistic (i.e. low to moderate) SNR. It was observed in [76], based on a lower bound to P_{out} for Rayleigh and Rician channels, that the finite-SNR DMT lies well below the curve in (8.4). While some results with finite SNR are available in the literature, their complexity prevents any analytical development. To evaluate the DMT for arbitrary SNR, [58], [59] proposes using an asymptotic approximation of the outage capacity distribution, which is Gaussian for a broad class of MIMO channels. The following theorem follows immediately from [58], [59] based on the asymptotic normality of P_{out}.

Theorem 8.1: Consider a correlated keyhole channel (see Fig. 2.2) with a large number of Tx and Rx antennas. Under the conditions of Theorem 3.3, the outage probability of such a channel can be expressed as

$$P_{out} \approx \frac{1}{2}\left(n_r \gamma_0\right)^{-d(r)\Delta(\gamma_0)}, \tag{8.5}$$

where the multiplexing gain $r \leq 1$ is defined as $r = \min(m,n) R / \overline{C}$ to take into account the high-SNR offset[25], and

---

[24] While the original definition in [117] employed the average error rate, since it is dominated by the outage probability, the definition in (8.3) is equivalent to it. This definition has also been adopted in [76].

[25] [66] gives a detailed discussion of the importance of high-SNR offset in the capacity analysis of MIMO systems. Note that this offset is missing in [117].

$$d(r)=(1-r)^2,\ \Delta(\gamma_0)=\frac{\ln(\gamma_0 n_r)}{2(n_t^{-2}\|\mathbf{R}_t\|^2+n_r^{-2}\|\mathbf{R}_r\|^2)} \tag{8.6}$$

The differential diversity gain d'_γ [26] in the keyhole channel is then

$$d'_\gamma=-\frac{\partial \ln P_{out}}{\partial \ln \gamma_0}=\frac{(1-r)^2\ln(\gamma_0 n_r)}{n_t^{-2}\|\mathbf{R}_t\|^2+n_r^{-2}\|\mathbf{R}_r\|^2} \tag{8.7}$$

Proof: follows immediately from the proof of [[58], Theorem 2].

Eq. (8.7) demonstrates the effect of SNR and of the correlation on the finite-SNR DMT. The denominator in (8.7) is in fact the measure of correlation and power imbalance in a MIMO channel introduced in Chapter V. Thus, any correlation or power imbalance, at either Tx or Rx end, reduce the differential diversity gain.

There are notable differences between the asymptotic ($\gamma_0 \to \infty$) DMT of Zheng and Tse and that considered by Theorem 8.1: (i) Neither d nor d'_γ involve linear interpolation for fractional r (see [59] for more details on the properties of the finite SNR DMT). (ii) The diversity gains in (8.7) increase without bound as the SNR increases. This is in sharp contract to the SNR-asymptotic DMT (which is SNR-independent and finite).

Due to the asymptotic nature of the capacity distribution in Theorem 3.3, the results in Theorem 8.1 cannot be extended to $\gamma_0 \to \infty$ for finite n_t, n_r because of slow convergence (with n_t, n_r) of the distribution tail (for more details on this issue see Chapter VI). However, it does provide a good approximation at moderate SNR values [58].

8.2. Outage Capacity and Block Error Rate

Let us consider an application of the outage capacity distribution for estimating symbol error rate (SER). If an M-ary modulation is used to transmit digital data over a pass-band channel, the maximum

[26] The definition of the differential diversity gain was introduced in [76] to capture the differential effect of diversity, i.e. how much increase in SNR is required to decrease P_{out} by certain amount. For high SNR, both diversity and differential diversity gains give the same result.

rate in natural units per unit bandwidth, which satisfies the zero ISI Nyquist criterion, is $R = \ln(M)$. If $C < R$, the channel is in outage and all the received blocks of symbols are in error with high probability. Assuming that the outage events are the dominant contributor to the block error rate (BLER), it can be estimated via the outage probability,

$$P_e(M) \approx \Pr\{C < R\} = F_C(\ln(M)), \tag{8.8}$$

where $F_C(x)$ is given by (3.2). In general, the BLER upper bounds the SER [57]. When the coherence time of the channel significantly exceeds the symbol interval (i.e. long bursts of errors during outage events), the two are close and (8.8) can serve as an estimate of the SER as well. Table VIII-I compares $P_e(M)$ in (8.8) using the exact $F_\alpha(x)$ in (3.4) and the SER of 8-PSK and 16-QAM with Alamouti scheme in the 2x2 uncorrelated keyhole channel given in [98]. As expected, (8.8) indeed upper-bounds the SER and is of the same order of magnitude[27]. Thus, the outage probability provides a simple estimation of the SER, which captures the effect of modulation level *M*, without detailed and complicated analysis usually encountered in such problems. Furthermore, for large systems the asymptotic Gaussian capacity distribution can be used in (8.8) for this purpose, simplifying the estimation even further.

TABLE VIII-I COMPARISON OF BLER (8.8) AND SER [98]. γ_0 DENOTES THE AVERAGE SNR PER RX ANTENNA.

	8-PSK		16-QAM	
	$\gamma_0 = 10dB$	$\gamma_0 = 20dB$	$\gamma_0 = 10dB$	$\gamma_0 = 20dB$
$P_e(M)$	$3\cdot10^{-1}$	$1\cdot10^{-2}$	$6\cdot10^{-1}$	$5\cdot10^{-2}$
SER	$2\cdot10^{-1}$	$8\cdot10^{-3}$	$2\cdot10^{-1}$	$2\cdot10^{-2}$

[27] Note that Alamouti scheme is a capacity achieving strategy in keyhole channels. This fact may explain the close concurrence between $P_e(M)$ and SER.

8.3. Telatar's Conjecture for Large MIMO Channels

Telatar's Conjecture [103]: Consider an i.i.d. Rayleigh fading MIMO channel with full CSI at Rx end but no CSI at the Tx end. The outage capacity is maximized if the Tx covariance matrix is

$$\mathbf{Q}_{n_t \times n_t} = \frac{P_T}{k}\begin{bmatrix} \mathbf{I}_{k\times k} & \mathbf{0} \\ \mathbf{0} & \mathbf{0} \end{bmatrix}, \tag{8.9}$$

where $k = 1...n_t$ is a number of active antennas. The value of k depends on the rate: the higher the rate (i.e. higher the outage probability), the smaller the k.

The following corollary gives a condition for the conjecture to hold in a multi-keyhole channel with a large number of antennas.

Corollary 8.1: As $n_t, n_r \to \infty$, the optimum Tx covariance matrix is as in (8.9), and the optimum number of active Tx antennas is given by

$$n = \arg\min_{1\le k\le n_t} \Psi(k) \tag{8.10}$$

for rates corresponding to outage probability $P_{out} \le 0.5$, and

$$n = \arg\max_{1\le k\le n_t} \Psi(k) \tag{8.11}$$

for rates corresponding to $P_{out} > 0.5$, where $\Psi(k)$ is a total measure of correlation and power imbalance at Tx end. For a RDMK channel $\Psi(k) = k^{-2}\sum_{m=1}^{M} \|\mathbf{R}_{tm}\|^2$, and for a FRMK one, $\Psi(k) = k^{-2}\|\mathbf{R}_t\|^2$ (see Chapter IV for the definitions of $\mathbf{R}_{tm}$ and $\mathbf{R}_t$). If $\Psi(k)$ monotonically decreases with k, then the optimum $n = n_t$ (i.e. all antennas are active) for $P_{out} \le 0.5$, and $n = 1$ (i.e. a single antennas is active) for $P_{out} > 0.5$.

Proof: Following the argument in [103], since there is no CSI at the Tx end and due to the problem symmetry, $\mathbf{Q}_{n_t \times n_t}$ must be diagonal with equal power distribution across the active antennas. (8.10) and (8.11) follow from the fact that an increase of $\Psi(k)$ increases the outage capacity for $P_{out} \le 0.5$, and decreases it for $P_{out} > 0.5$ (see more details on the properties of the measure of correlation and power imbalance in Chapter V). **Q.E.D.**

Consider, for example, a single keyhole channel. Assume that $\mathbf{R}_t$ is the exponential correlation

matrix (2.15) and the outage probability is below 0.5. From (3.17) and Corollary 8.1, the optimum number of Tx antennas is

$$n = \arg\min_{1\le k\le n_t} \frac{1}{k}\cdot\frac{1+|r|^2}{1-|r|^2} = n_t, \tag{8.12}$$

i.e. the outage capacity is maximized when all available antennas are used, since the measure of correlation decreases monotonically with the number of active antennas.[28] Apparently, in asymptotic approximation $P_{out}=0.5$ is a transition point, where the optimal number of antennas changes from all available antennas to a single one. Simulations show that when the number of antennas is finite, such a point does not exist and there is a gradual transition from $n=n_t$ to $n=1$, as P_{out} increases.

8.4. Motivation for Kronecker Correlation Model

Considering a Rayleigh channel as a limiting case of the FRMK channel (see Chapter IV) provides a motivation for the Kronecker correlation model (2.9) by the following arguments. Consider a multi-keyhole channel where $\mathbf{R}_t=\mathbf{R}_{tk}$ and $\mathbf{R}_r=\mathbf{R}_{rk}$, $k=1...M$. It is straightforward to show using (4.1) and (4.2) that

$$\begin{aligned}\mathbf{R}_r &= n_t^{-1}E\{\mathbf{H}\mathbf{H}^H\}\\ \mathbf{R}_t &= n_r^{-1}E\{\mathbf{H}^H\mathbf{H}\}\end{aligned} \tag{8.13}$$

From (4.1), $\mathbf{H}$ can be represented in this case as

$$\mathbf{H} \propto \mathbf{R}_r^{1/2}\mathbf{G}_r\mathbf{A}\mathbf{G}_t^H(\mathbf{R}_t^{1/2})^H, \tag{8.14}$$

where $\propto$ means identically distributed, $\mathbf{A}$ is a $[M\times M]$ diagonal matrix with elements $\mathbf{A}_{kk}=a_k$, a_k, $k=1...M$ is the complex gain of the k-th keyhole, and $\mathbf{G}_t$, $\mathbf{G}_r$ are i.i.d. Gaussian circular symmetric $[n_t\times M]$ and $[n_r\times M]$ matrices with unit variances. Since under the conditions of Theorem 4.1, $\mathbf{H}_w=\mathbf{G}_r\mathbf{A}\mathbf{G}_t^H$ is i.i.d. Gaussian circular symmetric $[n_r\times n_t]$ matrix as $M\to\infty$, the following holds true

[28] In general, $\Psi(k)$ may not be monotonic in k, in which case the global minimum in (8.10) should be found.

$$\mathbf{H} \xrightarrow{d} \mathbf{R}_r^{1/2} \mathbf{H}_w (\mathbf{R}_t^{1/2})^H, \tag{8.15}$$

where $\xrightarrow{d}$ denoted convergence in distribution as $M \to \infty$, and the right side of (8.15) is the Kronecker correlation model for Rayleigh fading channels. Therefore, the Kronecker correlation model is justified, for example, when there is a physical separation (a screen) between correlation-forming mechanisms at Tx and Rx ends, such as in the multi-keyhole channel (see Fig. 4.1).

8.5. Scheduling Gain and Feedback Rate in Multiuser Environment

- *Scheduling Gain:*

Scheduling algorithms have gained recent interest due to the potential to increase the data throughput in multiuser environment. In one possible algorithm, the base station receives a feedback from various users on the conditions of their channels, and then, transmits data to the user with the best channel [32]. Following [32], we adopt the following assumptions: (i) the channels between the base station and the users are i.i.d. and have the same number of antennas, which is large enough to apply the Gaussian approximation of the capacity with reasonable accuracy; (ii) the base station transmits to the channel with the largest instantaneous capacity with rate $R = C$. When the number of users K in the network is large, the average data rate per user is approximately [32]

$$R \approx \mu(1+g), \tag{8.16}$$

where μ is the mean capacity of the channel between the base station and a user, and g is a scheduling gain given by [32] as

$$g = \frac{\sqrt{2\sigma^2 \ln(K)}}{\mu}, \tag{8.17}$$

where σ^2 is the variance of the outage capacity distribution of a base-station-user channel. Note that transmitting data to the best user increases the average throughput from μ, which would be obtained from the simple round-robin algorithm, to $\mu(1+g)$. Let us consider a network where the channels between the base stations and the users are RDMK. Substituting (4.15) in (8.17), one obtains

$$g = \frac{\gamma_0/(1+\gamma_0)\sqrt{2\Upsilon(n_t,n_r)\ln(K)}}{\sum_{k=1}^{M}\ln(1+|a_k|^2\gamma_0)} \approx \frac{\sqrt{2\Upsilon(n_t,n_r)\ln(K)}}{(1+\gamma_0)} \text{ for } |a_k|^2\gamma_0 << 1,\ k=1...M, \tag{8.18}$$

where $\Upsilon(n_t,n_r) = n_t^{-2}\sum_{k=1}^{M}\|\mathbf{R}_{tk}\|^2 + n_r^{-2}\sum_{k=1}^{M}\|\mathbf{R}_{rk}\|^2$ is the total measure of correlation and power imbalance at both Tx and Rx ends. The approximation in (8.18) is accurate when M is large, so that under normalization (4.2) the keyhole gains $|a_k|^2 \to 0$. From (8.18), g increases with $\Upsilon(n_t,n_r)$, which has the following intuition behind it. When there is no or low correlation and/or power imbalance across the antennas, there are less channel fluctuations between the base station and different users. As the result, the scheduling gain decreases. If M is sufficiently large and $|a_k|^2\gamma_0 << 1$, $k=1...M$, g increases with the number of keyholes (as $\Upsilon(n_t,n_r)$ is an increasing function of M (see (4.15))), and decreases with γ_0. When γ_0 is large, the mean capacity significantly exceeds the fluctuations, so that the network does not benefit much from employing the scheduling algorithm

Consider a network where the channels between the base stations and the users are FRMK. Assume that $n_t >> n_r$. Substituting (4.10) and (4.11) in (8.17) one obtains

$$g = \frac{\|\mathbf{R}_t\|}{n_t n_r}\cdot\sqrt{\sum_{k=1}^{n_r}\left(\frac{\lambda_k^r}{1+\gamma_0\lambda_k^r/n_r}\right)^2}\,\frac{\sqrt{2\ln(K)}}{(1-\gamma_0\cdot n_r^{-2}\|\mathbf{R}_r\|^2/2)}, \tag{8.19}$$

where it is assumed that n_r is sufficiently large so that μ in (8.17) can be replaced by the corresponding limit in (4.11). Clearly, g increases with $\|\mathbf{R}_t\|$. Moreover, in high SNR regime, $\gamma_0 >> 1$,

$$g \approx \frac{n_t^{-1}\|\mathbf{R}_t\|\sqrt{2n_r\ln(K)}}{\gamma_0(1-\gamma_0\cdot n_r^{-2}\|\mathbf{R}_r\|^2/2)}, \tag{8.20}$$

i.e. g decreases as $\|\mathbf{R}_r\|$ increases. In low SNR regime, $\gamma_0 << 1$

$$g \approx n_t^{-1}\|\mathbf{R}_t\|n_r^{-1}\|\mathbf{R}_r\|\sqrt{2\ln(K)} \tag{8.21}$$

Here g increases with $\|\mathbf{R}_r\|$.

- *Feedback Rate:*

In situations such as in the scheduling algorithm described above, the receiver upon request

measures the channel condition and computes the transmission rate R. But rather than to send an exact value of R back to the base station, the receiver, in practice, quantizes the rate and sends this quantized value to the transmitter. The selection of quantized transmission rates is kept in a predetermined list, and the receiver simply chooses the closest list entry that is less than C. An efficient way to estimate the number of bits for a given outage probability P_{out} (the probability that no entry in the list will have a value less than C) is proposed by [32]. In particular, the number of nats b required to be sent to the transmitter for $P_{out} \approx 2.5 \cdot 10^{-2}$ is [32]

$$b = \ln\left(\frac{4\sigma}{\mu\nu}\right) \text{ [nats per feedback channel use]}, \tag{8.22}$$

where ν is the spacing between adjacent list entries normalized to the mean capacity μ (ν is also termed granularity).

Substitution (4.15) in (8.22), one obtains the feedback rate required for the RDMK channel

$$b = \ln\left(\frac{4\gamma_0/(1+\gamma_0)\sqrt{\Upsilon(n_t,n_r)}}{\nu \cdot \sum_{k=1}^{M} \ln(1+|a_k|^2\gamma_0)}\right) \approx \ln\left(\frac{4\sqrt{\Upsilon(n_t,n_r)}}{\nu(1+\gamma_0)}\right) \text{ for } |a_k|^2\gamma_0 << 1,\ k=1...M, \tag{8.23}$$

where the approximation holds under normalization (4.2) for $M >> 1$. In turn, substituting (4.10) and (4.11) in (8.22) results in the feedback rate required for the FRMK channel

$$b = \ln\left(\frac{4\|\mathbf{R}_t\|(n_t n_r)^{-1}}{\nu \cdot (1-\gamma_0 \cdot n_r^{-2}\|\mathbf{R}_r\|^2/2)} \cdot \sqrt{\sum_{k=1}^{n_r}\left(\frac{\lambda_k^r}{1+\gamma_0\lambda_k^r/n_r}\right)^2}\right) \tag{8.24}$$

In (8.23), b increases with $\Upsilon(n_t,n_r)$, decreases with γ_0, and increases with M, if M is sufficiently large, so that under normalization (4.2), $|a_k|^2\gamma_0 << 1$, $k=1..M$. In (8.24), b increases with $\|\mathbf{R}_t\|$, and decreases with $\|\mathbf{R}_r\|$ for $\gamma_0 >> 1$, since in this case

$$b \approx \ln\left(\frac{4n_t^{-1}\|\mathbf{R}_t\|\sqrt{n_r}}{\nu \cdot \gamma_0 \cdot (1-\gamma_0 \cdot n_r^{-2}\|\mathbf{R}_r\|^2/2)}\right) \tag{8.25}$$

In low SNR regimes, b increases with $\|\mathbf{R}_r\|$, as

$$b \approx \ln\left(4\|\mathbf{R}_t\|\|\mathbf{R}_r\|(\nu n_t n_r)^{-1}\right) \tag{8.26}$$

An intuitive explanation follows the same arguments as for the scheduling gain: when the channel fluctuations are small compared to the mean capacity, given the same outage probability and the granularity, the rate list may have fewer entries, or equivalently one needs less bits to encoder it.

8.6. Summary

It has been demonstrated that the Gaussian approximation of MIMO channel capacity significantly reduces the mathematical complexity of a number of problems. In particular, based on the Gaussian approximation, (i) it became possible to find the DMT in the keyhole channels, (ii) to provide a simple yet accurate estimation of SER, which captures the effect of modulation level without detailed and complicated analysis usually encountered in this kind of problems., (iii) to prove Telatar's conjecture for the multi-keyhole channels, and (iv) to estimate scheduling gain and the required feedback rate in wireless networks. Finally, it has been shown that the multi-keyhole channel model with a large number of keyholes provides a motivation for the Kronecker correlation model. The model is justified when, for example, there is a physical separation, such as a screen, between correlation-forming mechanisms at Tx and Rx ends.

The results in this chapter are presented in [47], [58].

CHAPTER IX: STATISTICAL ANALYSIS OF MEASURED MIMO CHANNELS

While the asymptotic analysis of the capacity distribution is a mathematically rigorous one, the validation of the asymptotic approximations via empirical data is usually done by visual comparison of the graphs only. The mean and outage capacity of many measured MIMO channels are reported without accompanying statistically-rigorous analysis leaving the question as to whether the measured channel capacity distribution is close to the theoretical one not being answered in a satisfactory way. In this chapter we address this problem by developing a statistically-rigorous procedure (in terms of statistical hypothesis testing) for the analysis of the mean and outage capacity of MIMO channels (both theoretical models and measured) with the main goal being to compare the theoretical and measured channel capacity distribution. We demonstrate that there is a tight lower bound on the amount of measured data necessary to provide a unique answer with high confidence probability. Based on the procedure above, we develop guidelines for measurements and Monte-Carlo simulations in terms of accuracy, and show that the outage capacity of some measured 5.2GHz indoor MIMO channels [79], [80] is statistically Gaussian with a reasonable significance level already for two antennas at each end.

9.1. Introduction to Statistical Analysis

In general, there are two hypotheses considered against each other in any statistical test: an assumption on some property of the measured data (the null hypothesis H_0) against the possibility that this assumption is not true (the alternative hypothesis H_1). For this purpose, a test statistics T_n (a function applied on the measured data) is calculated using n observations and compared to some critical value ε. The meaning of ε depends on the meaning of T_n in each particular test. If $|T_n| \le \varepsilon$, H_0 is accepted; otherwise, it is rejected. It should be stressed, that if H_0 is accepted it does not mean that the measured data possesses the assumed property; it simply means that the test performed does not find any statistically significant difference between the observed and assumed properties. Apparently, there are two probabilities associated with T_n and ε:

$$\alpha = P\{|T_n| > \varepsilon | H_0\}, \tag{9.1}$$

where α is the miss probability or significance level; i.e. the probability to reject H_0 given it is true.

$$\beta = P\{|T_n| \le \varepsilon | H_1\} \tag{9.2}$$

is the false alarm probability; i.e. the probability to accept H_0 given it is not true.

Unlike the computer-based Monte-Carlo simulations, the common problem of any measurement is a limited number of observations available. Therefore, it is important to choose α and β (test parameters) properly with accordance to the data size, especially when the size is small.

To show how α and β should be chosen, let us consider T_n of a monotonically consistent statistical test, such that the following is true: i) for any ε $\lim_{n\to\infty} P\{|T_n| > \varepsilon | H_0\} = 0$ and ii) for any given α and ε there is only one n, which satisfies (9.1) [21]. As follows from i) and ii), α decreases as n increases. Moreover, due to the additive property of the probability measure for any n, $P\{|T_n| > \varepsilon | H_0\}$ is a non-increasing function of ε. Therefore, if ε is small, either α or n should be large. This is a general conclusion that is true regardless of any specifics.

On the other hand, let us consider β. Its exact value depends on the actual distribution of the measured data, which is unknown in most practical cases. In general, due to the additive property of the probability measure, β is a non-decreasing function of ε (see (9.2)). Thus, if β is low, the corresponding α would be high for given n. Therefore, the only way to keep the equality in (9.1), when both α and β are small, would be to increase the size of the acquired data. While the relationship given in (9.1) between n, ε and α is general for any monotonically consistent statistical test, specific values of n, ε and α depend on a particular test to be used. Below, we use three statistical tests to analyze the measured MIMO channel: 1) Pearson χ^2 test [36], for channel and outage capacity distribution hypothesis testing; 2) generalization of the T-test [36] of correlation coefficients, to check whether the measured channel correlation is statistically different from zero; and 3) generalization of the F-test (variance ratio test) [36], to check whether the variances of two sample sets are statistically identical. It is straightforward to show that all three tests are monotonically consistent. Moreover, since the distributions of T_n given H_0 is true are known for all three test, and they do not depend on the measured data distribution [21], it is

straightforward to show that: i) for the χ^2 test (9.1) is given by

$$\alpha = 1 - \gamma(0.5(K-m-1), 0.5n \cdot \varepsilon) \cdot \Gamma^{-1}(0.5(K-m-1)), \tag{9.3}$$

where $\gamma(a,x) = \int_0^x t^{a-1}e^{-t}dt$ is the incomplete Gamma function [119], $\Gamma(a) = \gamma(a,\infty)$ is the Gamma function, K is the number of intervals in the χ^2 test, and m is the number of statistical moments to be estimated. The meaning of ε in (9.3) is a critical mean relative deviation of the observed histogram from the expected one. For the generalized T-test, (9.1) is

$$\alpha = \exp\left\{-0.5 \cdot \varepsilon^2 \cdot (2n-2)/(1-\varepsilon^2)\right\}, \tag{9.4}$$

where ε is a critical value for sample correlation. For the generalized F-test, (9.1) is given by the following integral

$$\alpha = 1 - \frac{\Gamma(2n-1)}{\Gamma^2(n-0.5)} \cdot \int_{1-\varepsilon}^{1+\varepsilon} \frac{w^{(n-1.5)}}{(1+w)^{(2n-1)}} dw, \tag{9.5}$$

where ε is a critical value for the deviation of a ratio of two sample variances from one. To demonstrate the general relationship between n, ε and α, Fig. 9.1 shows α vs. n for different ε. Clearly, decreasing α for given n results in increasing ε, which, in turn, increases β following the above arguments. The only way to decrease α while keeping β low is to increase n. This is a statistically-rigorous representation of error due to the limited amount of the data available.

9.2. Statistical Analysis of Rayleigh-fading Channels

The subject of this section is to describe the rigorous statistical analysis of the outage capacity distribution of a computer simulated correlated flat-fading Rayleigh MIMO channel. To account for the correlation, the channel matrix $\mathbf{H}$ is given by the Kronecker model (2.9) with exponentially correlated matrices (2.14).

We generated the sets of 100, 300 and 1000 channel matrices $\mathbf{H}$ with orders up to 8x8 for different correlation parameters r_t and r_r at Tx and Rx ends respectively. The χ^2 test with $K = 10$ intervals was then applied on the standardized outage capacity (i.e. capacity shifted by its mean and normalized by its

standard deviation). $\alpha = 0.05$ was chosen as the miss probability, which corresponds to ε 0.141, 0.047 and 0.014 for n 100, 300 and 1000 respectively (see (9.3) and also Fig. 9.1). As the null hypothesis, we assumed as that the standardized outage capacity distribution is Gaussian with zero mean and unit variance. To distinguish between the Gaussian distribution and a channel distribution that is well approximated by the Gaussian one by means of a statistical test, we introduce below the following definition.

Definition 9.1: A distribution is called Gaussian in statistical sense given test parameters n, ε and α, if a statistical test does not find any significant difference between the distribution and the corresponding Gaussian curve.

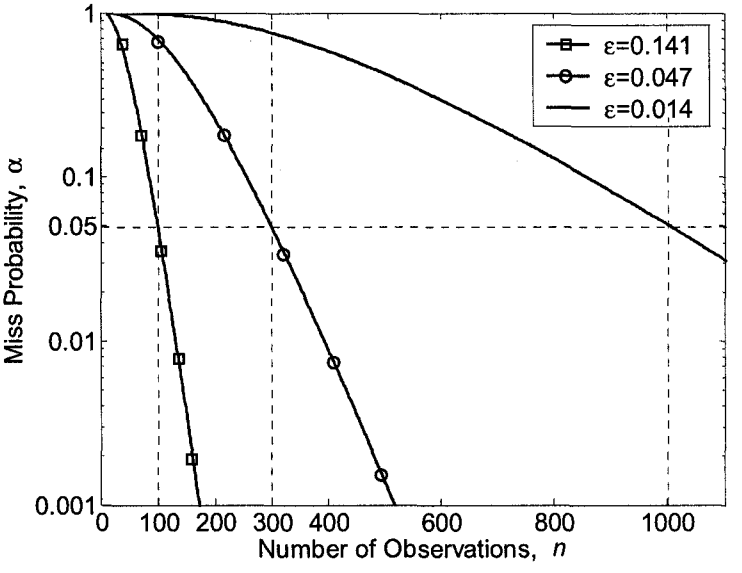

Fig. 9.1 α vs. n in the χ^2 test (K=10, m=2)

For the sets of 100 realizations, the χ^2 test did not provide any credible conclusions. For the wide range of tested SNR values and regardless of r_t and r_r, H_0 was accepted already for a 1x1 channel. In fact, the critical value $\varepsilon = 0.141$ is too large resulting in high false alarm probability. On the contrary, for $n = 300$ the test results are more consistent. Some of these results are given in Table IX-I. Each cell in the table contains the value of the χ^2 test statistics $|T_n|$. If $|T_n| \le \varepsilon$, the H_0 is accepted and the corresponding

cell is shadowed. The table rows (n_t) and columns (n_r) represent the number of receive and transmit antennas of the tested channel, i.e. the MIMO order. The χ^2 test results for $n=1000$ were found quite similar to those of $n=300$ and, therefore, are not shown.

As follows from Table IX-I, the Gaussian distribution is a good approximation of the outage capacity of the correlated Rayleigh channel starting from MIMO orders 2x2 and 3x3.

TABLE IX-I RESULTS OF THE χ^2 TEST FOR DIFFERENT MIMO ORDERS ($n_t \times n_r$) PERFORMED ON 300 SPATIAL REALIZATIONS (ε=0.047)

$n_r \setminus n_t$	1.	2.	3.	4.	5.	6.	7.	8.
1.	*0.11*	*0.11*	*0.04*	*0.06*	*0.05*	*0.05*	*0.07*	*0.11*
2.	*0.11*	*0.07*	*0.05*	*0.06*	*0.03*	*0.02*	*0.01*	*0.02*
3.	*0.05*	*0.04*	*0.01*	*0.01*	*0.01*	*0.01*	*0.05*	*0.06*
4.	*0.06*	*0.12*	*0.03*	*0.02*	*0.03*	*0.01*	*0.06*	*0.04*
5.	*0.05*	*0.04*	*0.02*	*0.03*	*0.02*	*0.04*	*0.01*	*0.05*
6.	*0.05*	*0.02*	*0.03*	*0.05*	*0.01*	*0.03*	*0.01*	*0.01*
7.	*0.07*	*0.04*	*0.02*	*0.03*	*0.06*	*0.03*	*0.02*	*0.04*
8.	*0.12*	*0.04*	*0.07*	*0.02*	*0.04*	*0.02*	*0.01*	*0.01*

a) $\gamma_0 = 15dB$, $r_t = r_r = 0$

$n_r \setminus n_t$	1.	2.	3.	4.	5.	6.	7.	8.
1.	*0.07*	*0.05*	*0.04*	*0.01*	*0.04*	*0.08*	*0.01*	*0.04*
2.	*0.05*	*0.06*	*0.02*	*0.06*	*0.01*	*0.04*	*0.01*	*0.01*
3.	*0.07*	*0.03*	*0.02*	*0.03*	*0.01*	*0.02*	*0.02*	*0.04*
4.	*0.02*	*0.04*	*0.01*	*0.03*	*0.03*	*0.01*	*0.04*	*0.02*
5.	*0.02*	*0.03*	*0.03*	*0.02*	*0.01*	*0.02*	*0.02*	*0.03*
6.	*0.05*	*0.03*	*0.02*	*0.02*	*0.01*	*0.02*	*0.05*	*0.02*
7.	*0.01*	*0.01*	*0.03*	*0.03*	*0.02*	*0.03*	*0.02*	*0.02*
8.	*0.03*	*0.03*	*0.02*	*0.02*	*0.03*	*0.01*	*0.05*	*0.01*

b) $\gamma_0 = 10dB$, $r_t = r_r = 0.8$

Following Definition 9.1 and from Table IX-I, the outage capacity distribution of the correlated Rayleigh channel considered above is Gaussian in statistical sense given $n=300$, $\varepsilon=0.047$ and $\alpha=0.05$ starting from orders 2x2 and 3x3.

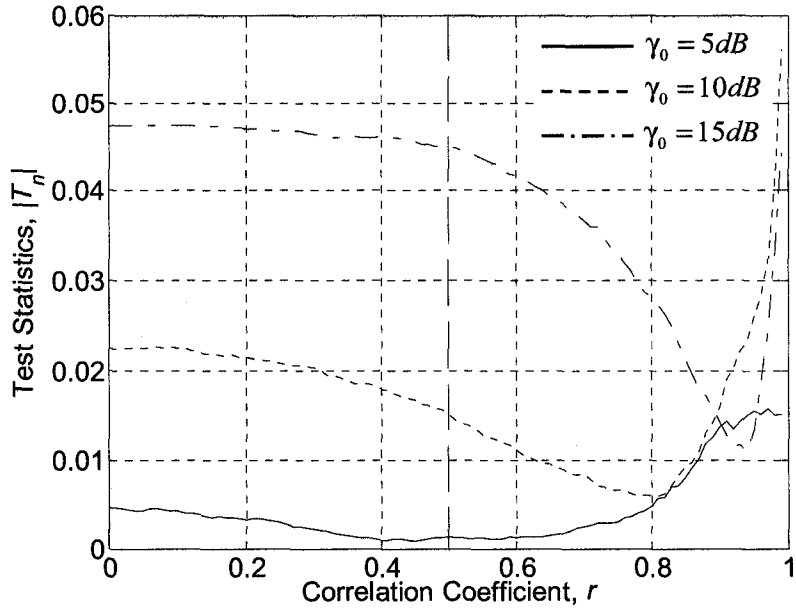

Fig. 9.2 χ^2 statistics of 2x2 MIMO channel vs. correlation parameter $r = r_t = r_r$

Fig. 9.2 shows the χ^2 statistics of the 2x2 MIMO channel vs. correlation parameter. It follows that the convergence rate to the Gaussian distribution with respect to the MIMO order is faster for low SNR, since for low correlations $|T_n|$ is smaller for lower γ_0. Similar observations have been reported in [101]. Fig. 9.2 does not reveal any significant change in the outage capacity statistics for correlation parameter < 0.5. When the correlation parameter increases (0.5 and up) the corresponding $|T_n|$ for $\gamma_0 = 10dB$ and $15dB$ decreases and approaches that of $\gamma_0 = 5dB$, i.e. an increase in correlation has a similar effect on the capacity distribution with respect to the Gaussian distribution as a decrease in SNR. Similarly, from Table IX-I the 3x3 MIMO channel outage capacity distribution is statistically Gaussian in both tables a) and b), where we deliberately decreased γ_0 and simultaneously increased correlation parameters r_t and r_r. This fact is with an analogy to the results reported in [101], where it was analytically shown that the effect of an increase in correlation on the mean capacity is equivalent to decrease in SNR[29]. Another observation, which follows from Fig. 9.2, is that when the correlation parameter is close to unity, $|T_n|$ sharply

[29] Similar effect has been observed in correlated keyhole channels with a small number of antennas (see (3.10)).

increases regardless of γ_0. Indeed, when the spatial correlation is very high, the MIMO channel degenerates, i.e. its order reduces to 1x1. As the result, the outage capacity distribution of that channel is far from Gaussian.

In many cases the behavior of the real physical channel is different from the theoretical models. Hence, in the next section, we apply the same rigorous statistical analysis as above on a measured channel and assess the validity of the Gaussian approximation on it.

9.3. Statistical Analysis of the Measured Channel

In this section we analyze the experimental data based on the measurements of the 8x8 5.2 GHz indoor MIMO channel reported in [79], [80]. However, the procedure is general enough to be applied to any channel. The MIMO channel was measured at $F = 193$ frequency bins equally spread over 120MHz frequency band at the central frequency of 5.2GHz. At each frequency bin, $n = 130$ spatial realizations of the 8x8 MIMO complex channel matrix were taken at 8 different locations (Rx1, Rx2,..., Rx7, and Rx9) and 3 different directions (D1, D2, and D3) in each location. As a result a (3x8x130x193x8x8) 6-dimensional complex channel transfer matrix was obtained (for details see [79]).

Below we compare the outage capacity distribution of the measured channel to the Gaussian approximation in a statistically-rigorous way. We start with MIMO channel identification.

a. *Channel Gain Distribution:*

The χ^2 test was applied on the sets of the measured complex channel gains. As H_0, it was assumed that the gains are Rayleigh distributed. As a compromise between low α and not very big ε, $\alpha = 0.05$, which corresponds to $\varepsilon = 0.119$ for $n = 130$ (9.3). $K = 10$ intervals were used in the test.

For every considered configuration, H_0 was accepted. We also noticed that the measured channel does not have line-of-sight (LOS) component, since the estimated LOS factors were very low (around $-30dB$) in each considered configuration.

b. Tx and Rx correlation:

In order to test Tx and Rx correlations, we estimated sample correlations between different Tx and Rx antennas at different frequencies, locations and directions. Then, the generalized T-test was applied, as the null hypothesis we assumed that the measured channel is uncorrelated. The miss probability was chosen $\alpha = 0.05$, which corresponded to $\varepsilon = 0.054$ (9.4).

In most of the considered cases H_0 was rejected. The test showed that there is a statistically significant correlation (in some cases >0.75). We also observed much more severe correlation at the Rx end than at the Tx end. This can be explained by the fact that the angular spread was smaller at the transmitter rather than at the receiver [79].

c. Channel frequency response:

To test the channel frequency response, we considered the ratio of the channel power gains measured at different frequencies in each location and direction. As H_0 the channel was assumed frequency-flat. The generalized F-test of the variance ratio was applied with $\alpha = 0.1$ ($\varepsilon = 0.205$ for $n = 130$, see (9.5)). For all considered configurations, H_0 was rejected, i.e. the channel has different power gains at different frequencies. Therefore, the channel is statistically frequency selective within the considered frequency band and the measurements at different frequencies had to be analyzed separately.

d. Outage Capacity Distribution:

First, the measured channel rank was determined to be eight. That means that the measured channel is non-degenerated or it has no "keyholes". The χ^2 test with 10 intervals was applied to the standardized outage capacity distribution computed in different locations, directions, SNR, different channel orders and at all frequency bins. To test different MIMO orders the right-upper corners with appropriate size were picked up from the 8x8 measured channel matrices.

As the null hypothesis it was assumed that the standardized outage capacity distribution is Gaussian distributed with zero mean and unit variance. Since the number of spatial observations in each tested location and direction is $n = 130$, $\alpha = 0.1$ was chosen, which corresponds to $\varepsilon = 0.092$ in (9.3). Some of

the results are presented in Table IX-II, where the χ^2 test statistics $|T_n|$ in Rx6D2 computed at the central frequency bin for different orders. As above, if $|T_n| \leq \varepsilon$, H_0 was accepted and the corresponding cell is shadowed.

TABLE IX-II RESULTS OF χ^2 TEST IN RX6D2 FOR DIFFERENT MIMO ORDERS ($n_t \times n_r$), $\gamma_0 = 5dB$, $\varepsilon = 0.092$.

$n_r \backslash n_t$	1.	2.	3.	4.	5.	6.	7.	8.
1.	*0.14*	*0.06*	*0.10*	*0.12*	*0.13*	*0.03*	*0.06*	*0.13*
2.	*0.10*	*0.02*	*0.07*	*0.07*	*0.06*	*0.05*	*0.06*	*0.10*
3.	*0.11*	*0.05*	*0.03*	*0.11*	*0.17*	*0.08*	*0.06*	*0.07*
4.	*0.04*	*0.05*	*0.06*	*0.14*	*0.08*	*0.07*	*0.05*	*0.11*
5.	*0.04*	*0.02*	*0.06*	*0.11*	*0.16*	*0.18*	*0.13*	*0.11*
6.	*0.05*	*0.14*	*0.14*	*0.08*	*0.08*	*0.13*	*0.09*	*0.05*
7.	*0.04*	*0.03*	*0.10*	*0.03*	*0.01*	*0.03*	*0.05*	*0.04*
8.	*0.06*	*0.03*	*0.05*	*0.06*	*0.07*	*0.03*	*0.06*	*0.06*

Following the asymptotic analysis given in the previous chapters, H_0 is expected to be more frequently accepted for higher MIMO orders, as well as, for lower SNR, as suggested in [101]. However, as Table IX-II demonstrates, as the order of the MIMO channel increases the χ^2 test does not follow systematically this expectation. The same was observed when γ_0 was decreased. Since $\alpha = 0.1$, on average in 6.4 tests out of 64 H_0 should be rejected given it is true. However, we were encountering significantly more test fails in the high order regions, i.e. after the orders for which H_0 was first accepted. It does not mean, however, that H_0 is not true, since the probability to get more than 6.4 failures in the test is significant due to the high α. Another reason for the observed inconsistency could be a result of the large ε, as in our case for $n = 130$. As indicated above, the only way to reduce α and ε simultaneously is to increase n. Thus, to avoid insufficient statistics, we split each 8x8 spatial realization of the channel into four spatially independent 2x2 realizations. This allowed us to get in total $n = 520$ realizations, which following (9.3) corresponds to $\varepsilon = 0.012$ for $\alpha = 0.05$ against $\varepsilon = 0.092$ for $\alpha = 0.1$ in the preceding test. Then the χ^2 test was applied once again. We found that as the outage capacity distribution of all measured 2x2 channels strongly depends on γ_0 and it is Gaussian in the statistical sense

for $\gamma_0 < 10dB$. We also noticed that the average 2x2 outage capacity measured over all 120MHz frequency band is statistically Gaussian for $\gamma_0 < 30dB$.

The χ^2 test gives an integral evaluation of the discrepancy between measured and expected distributions (i.e. for the entire range). This has some disadvantages for the outage capacity analysis, as it includes the contribution of high outage probability region, which is not of interest from practical viewpoint (since this is low quality of service region). From the practical perspective, it is more important to know the outage capacity distribution on the distribution tales, where the outage probability P_{out} is low, i.e. in the region of high quality of service. In order to compare the measured capacity to its Gaussian approximation in low P_{out} region, we plot the 2x2 MIMO standardized outage capacities for $n = 520$ and $\gamma_0 = 5dB$ computed at the central frequency bin in Fig. 9.3 together with $\pm\sigma$ confidence intervals, which corresponds to $\alpha \approx 0.3$. Despite the fact that the measured capacity distributions are statistically Gaussian, as affirmed by the χ^2 test, in some locations the difference between the measured capacity distribution and the Gaussian approximation exceeds the $\pm\sigma$ error range for low P_{out}. This deviation is especially large on the tales where $P_{out} < 0.02$.

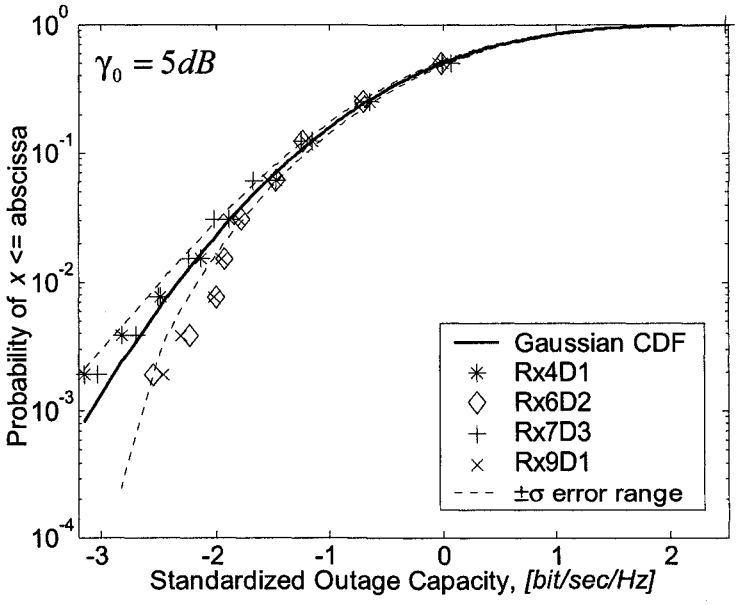

Fig. 9.3 Standardized outage capacity distribution of 2x2 MIMO channel measured in different locations and directions.

9.4. Summary

Based on the rigorous statistical analysis, the outage capacity distribution of some 5.2GHz measured indoor MIMO channels has been found to be statistically Gaussian with significance level 5% starting already from two antennas at each end and $\gamma_0 < 10dB$. However, the discrepancy between the measured capacity and the Gaussian curve on the distribution tails may be still significant and should be taken in account when low outage probabilities are important. The presented study shows that in order to avoid insufficient statistics, future experiments should make at least $n = 300$ measurements at the same frequency and environment. For the χ^2 test this will grant $\alpha = 0.05$ and $\varepsilon = 0.047$ (see (9.3)), which are shown to be small enough to provide credible conclusions. Although this chapter does not aim to verify the multi-keyhole channels model proposed in Chapter IV, the presented study shows that the asymptotic analysis with respect to the number of antennas not only offers a significant insight, but also can be applied to realistic systems of a moderate size.

The results of this chapter are presented in [53], [52].

CONCLUSION AND FURTHER RESEARCH

10.1. Conclusion

Throughout this thesis, we have presented analytical characterization of the outage capacity distribution of asymptotically large MIMO channels. We started with the analysis of rare but analytically well-tractable single keyhole MIMO channels, where the channel rank is one regardless of a number of Tx and Rx antennas (the worst case propagation scenario). Then, the analysis has been expanded to the channels with multiple statistically-independent keyholes, named the multi-keyholes channels, which serve a transition model between the rank-one single keyhole and full-rank classic Rayleigh-fading channels. The asymptotic analysis of single and multi-keyhole channels has provided a number of analytical tools and allowed for a significant insight into the capacity behavior of a broad class of MIMO channels. The main observations are:

- The Gaussian distribution is a common asymptotic property of the outage capacity of a broad class of MIMO channels.
- When the correlation among antennas decreases faster than $1/\sqrt{D}$, where D is the distance between a pair of antennas, the convergence rate toward asymptotic normality, in many cases, is not slower than $1/\sqrt{n}$, where n is the number of antennas at either Tx or Rx end.
- When the number of antennas is large, the impact of correlation on the outage capacity is always detrimental for outage probabilities < 0.5. The L_2 norm of correlation matrices represents, in this case, a simple scalar measure of correlation and power imbalance, which does not only quantify the correlation between multiple antennas, but also compactly describes the impact of correlation on the asymptotic outage capacity of a broad class of MIMO channels.
- The popular Kronecker correlation model, which has been used in numerous analytical analyses due to its simplicity, is justified, when, for example, there is a physical separation (a screen) between correlation-forming mechanisms at Tx and Rx ends, such as in the keyhole channels.
- The best multipath angular density, which removes the correlation between the antennas of uniform

linear arrays and thus maximizes the asymptotic instantaneous capacity of a broad class of MIMO channels is non-uniform. This implies that the popular Clarke's (Jakes) model does not represent the best case propagation scenario.

A number of applications have been considered based on the asymptotic Gaussian distribution of the outage capacity.

- A closed-form expression of the size-asymptotic, finite-SNR diversity-multiplexing trade-off has been obtained for multi-keyhole channels.
- A simple yet reasonably accurate estimate of symbol error rate (SER) in MIMO channels has been suggested. The estimate captures the effect of modulation level, without detailed and complicated analysis usually encountered in this kind of problems.
- Telatar's conjecture has been proven for the multi-keyhole channels with a large number of antennas. A transition rate where the impact of correlation on the outage capacity changes from detrimental to beneficial has been found.
- Simple algorithms for calculation of scheduling gain and feedback rate in the wireless networks, where the propagation environment is well described by multi-keyhole channel model, and the asymptotic approximation of outage capacity is reasonably accurate, has been proposed.

Finally, using rigorous methods of hypothesis testing, the outage capacity distribution of some measured 5.2GHz indoor MIMO channels has been analyzed. It has been found that the capacity is statistically Gaussian with a reasonable significance level already for two antennas at each end. The latter can serve as an empirical validation of the theoretical results presented in this thesis and implies that the asymptotic analysis with respect to the number of antennas not only offers a significant insight and simplification, but can also be applied to realistic systems of a moderate size.

10.2. Further Research

There are a number of directions for possible research that arise from this thesis. These directions can be divided in three main categories: (i) capacity analysis of generic MIMO channels that cannot be

represented by the multi-keyhole model, (ii) extension of the results obtained in this thesis, and (iii) development of new mathematical tools necessary for further research in this area.

- *Capacity analysis of generic MIMO channels*:

A lot of the research activity today is dedicated to generalization of asymptotic normality of outage capacity distribution for a generic type of channel regardless of a particular channel distribution, or specific correlation structure (Kronecker, UIU etc'). While we have shown that the Gaussian distribution is a common asymptotic property of a broad class of MIMO channels: from a single keyhole channel to a Rayleigh-fading one, the presented analysis is based on the "multi-keyhole" structure. Channels that do not have such a structure fall beyond the scope of this investigation and require additional attention.

- *Extension of the results obtained in this thesis:*

Due to the tremendous variety of wireless channels, practically important results could stem from considering single and multi-keyhole channels with generic, not necessarily Rayleigh-fading subchannels, and subchannels with line-of-sight (LOS). Finding the capacity of these channels, and the relationship between the latter and canonic Rayleigh and Rice MIMO channels could reveal the impact of parameters, other than considered in this thesis, on the channel capacity. This, in turn would allow developing new, more efficient coding techniques that would be robust in the presence of different kinds of multipath and LOS.

The multi-keyhole model proposed in this thesis could be also be useful to model analogue relay networks [39], where the keyhole may represent a relay node rather than a propagation effect. This apparent similarity between the network structure and the keyhole propagation environment has not been elaborated in the literature yet.

Another open problem, which has not been addressed in this thesis, is the capacity of keyhole channels with perfect or partial channel state information available not only at the Rx end but also at the Tx end. Despite the complexity in providing such information to the transmitter, solution of this kind of problems has certain practical value, as in some scenarios CSI is available at the Tx end via e.g. a control

channel end.

The results presented in Chapter VII could be extended for additional, other than ULA, types of antennas such as, for example, multi-dimensional uniform and circular antennas. Finding the best multipath angular density in these cases might provide useful design guidelines, and possibly to imply the optimal antenna structures for arbitrary multipath density.

- *Development of new mathematical tools necessary for further research in this area*:

Novel statistical hypothesis tests are required to examine the outage capacity distribution of measured MIMO channels. These tests should have the following properties: (i) be sufficiently powerful under the limited number of channel measurements[30], and (ii) be able to provide a differential (over some sub-intervals), not integral (over a whole range of outage probabilities) characteristic of the outage capacity, as in many cases, the fit between the measured outage capacity and the analytical model (such as Gaussian) is important at low outage probabilities (high quality of service).

While the limiting (Gaussian) distribution of the outage capacity is known in many cases, much less attention has been paid to the rigorous analytical evaluation of the accuracy of the asymptotic approximation when the number of antennas is finite. Existing methods do not allow obtaining sufficiently tight bounds that can be used in practical systems. This problem arises from the fact that the bounds apply to a wide class of channel distributions and therefore cannot be further improved unless specific distributions are considered [85]. The mathematical results in this area are rare [119].

[30] The usefulness of a test depends on its ability to discriminate against the alternative hypothesis (see Section 9.1, Chapter IX). The measure of this usefulness is the power of the test, defined as the probability $1-\beta$, where β is given by (9.2) [21].

APPENDIX A: KEYHOLE CHANNELS

Proof of Theorem 3.1:

Let β be either $\beta_t = \|\mathbf{h}_t\|^2$, $\beta_r = \|\mathbf{h}_r\|^2$. Under the adopted assumptions, the distribution of β is generalized χ^2 with the characteristic function $\Phi_\beta(\omega) = \det^{-1}[\mathbf{I} - j\omega\mathbf{R}]$, where $\mathbf{R}$ is either $\mathbf{R}_t$ or $\mathbf{R}_r$ [70]. When $\mathbf{R}$ is non-singular and has n distinct eigenvalues λ_k, $k = 1...n$. The characteristic function (CF) of β can be represented as:

$$\Phi_\beta(\omega) = \prod_{k=1}^{n}(1 - j\omega\lambda_k)^{-1} = \sum_{k=1}^{n} A_k (1 - j\omega\lambda_k)^{-1}, \tag{10.1}$$

where A_k are the coefficients of the partial fraction decomposition of $\Phi_\beta(\omega)$, such that $\sum_{k=1}^{n} A_k = 1$ [119]. From (10.1),

$$\sum_{k=1}^{n} A_k \prod_{\substack{m=1 \\ m\neq k}}^{n}(1 - j\omega\lambda_m) = 1 \tag{10.2}$$

Since the equality in (10.2) holds for every ω, let $\omega = -j\lambda_k^{-1}$, $k = 1...n$ (10.2), then

$$A_k \prod_{\substack{m=1 \\ m\neq k}}^{n}(1 - \lambda_m/\lambda_k) = 1, \tag{10.3}$$

which proves (3.5).

Based on (10.1), the PDF and the CDF of β are given respectively by:

$$f_\beta(x) = \frac{1}{2\pi}\int_{-\infty}^{\infty}\Phi_\beta(\omega)e^{-j\omega x}d\omega = \sum_{k=1}^{n}\frac{A_k}{\lambda_k}\exp\{-x/\lambda_k\},\ x \geq 0 \tag{10.4}$$

$$F_\beta(x) = \int_0^x f_\beta(t)dt = 1 - \sum_{k=1}^{n} A_k \exp\{-x/\lambda_k\},\ x \geq 0 \tag{10.5}$$

Since α is a product $\beta_t \cdot \beta_r$, and β_t, β_r are assumed to be independent, the PDF $f_\alpha(z)$ and the CDF $F_\alpha(z)$ of α are given by [83]:

$$f_\alpha(z) = \int_0^\infty f_{\beta_t}(z/x) f_{\beta_r}(x) d\ln(x), \tag{10.6}$$

$$F_\alpha(z) = \int_0^\infty F_{\beta_t}(z/x) f_{\beta_r}(x) dx, \tag{10.7}$$

where $F_{\beta_t}(x), f_{\beta_t}(x)$ and $F_{\beta_r}(x)$, $f_{\beta_r}(x)$ are the CDF and the PDF of β_t and β_r respectively. Thus, by substituting (10.4) and (10.5) in (10.6) and (10.7) one obtains (3.3) and (3.4). **Q.E.D.**

Lemma A1: Let β be a generalized χ^2 random variable with the CF $\Phi_\beta(\omega) = \det^{-1}[\mathbf{I} - j\omega\mathbf{R}]$ [70]. If $\lim_{n\to\infty} n^{-1}tr\{\mathbf{R}\} < \infty$ and $\lim_{n\to\infty} n^{-2}\|\mathbf{R}\|^2 = 0$, then, as $n \to \infty$, the distribution of $n^{-1}\beta$ is Gaussian with the mean $\mu = n^{-1}tr\{\mathbf{R}\}$ and the variance $\sigma^2 = n^{-2}\|\mathbf{R}\|^2$.

Proof: Since β is a generalized χ^2 random variable with CF $\Phi_\beta(\omega) = \det^{-1}[\mathbf{I} - j\omega\mathbf{R}]$, the characteristic function of $n^{-1}\beta$ is $\Phi(\omega) = \prod_{k=1}^{n}(1 - j\omega\lambda_k / n)^{-1}$, where λ_k are the eigenvalues of $\mathbf{R}$. Or equivalently $\ln(\Phi(\omega)) = -\sum_{k=1}^{n}\ln(1 - j\omega\lambda_k / n)$. Assume that n is large enough such that for every λ_k, $|\omega\lambda_k / n| < 1$, then the expansion of $\ln(\Phi(\omega))$ in Maclaurin series gives

$$\ln(\Phi(\omega)) = \sum_{k=1}^{n}\sum_{m=1}^{\infty}\frac{(j\omega\lambda_k)^m}{n^m m} \tag{10.8}$$

Define $L_m = n^{-m}\sum_{k=1}^{n}\lambda_k^m$, $m = 1,2,...$ By changing the order of summation, (10.8) can be rewritten as:

$$\ln(\Phi(\omega)) = \ln(\Phi_g(\omega)) + \sum_{m=3}^{\infty}(j\omega)^m L_m / m, \tag{10.9}$$

where $\Phi_g(\omega) = \exp(j\omega L_1 - \omega^2 L_2 / 2)$ is the CF of a Gaussian random variable with the mean $\mu = L_1$ and the variance $\sigma^2 = L_2$. Note that $L_1 = n^{-1}tr(\mathbf{R})$ and $L_2 = n^{-2}\|\mathbf{R}\|^2$. Therefore, the necessary conditions for $\lim_{n\to\infty}\Phi(\omega) = \Phi_g(\omega)$ are:

$$\lim_{n\to\infty} L_1 < \infty,\ \lim_{n\to\infty} L_2 < \infty \text{ and } \lim_{n\to\infty} L_m / L_2 = 0 \text{ for } m \geq 3 \tag{10.10}$$

Below we show in two steps that the sufficient condition to ensure $\lim_{n\to\infty} L_m / L_2 = 0$ for $m \geq 3$ is $\lim_{n\to\infty} L_2 = 0$. Note that $|\omega\lambda_k / n| < 1$ follows from $\lim_{n\to\infty} L_2 = 0$, and hence it holds true under the conditions of Lemma A1.

1. If $\lim_{n\to\infty} L_2 = 0$ then $\lim_{n\to\infty} L_{2m} / L_2 = 0$ for $m = 2,3,...$:

$$\lim_{n\to\infty} L_{2m} / L_2 = \lim_{n\to\infty} L_2^{-1} n^{-2m}\sum_{k=1}^{n}\lambda_k^{2m} \leq \lim_{n\to\infty} L_2^{-1}\left(n^{-2}\sum_{k=1}^{n}\lambda_k^2\right)^m = \lim_{n\to\infty} L_2^{m-1} = 0 \tag{10.11}$$

The inequality is because all λ_k are non-negative. Thereby, since $\lim_{n\to\infty} L_m / L_2 \geq 0$,

$$\lim_{n\to\infty} L_{2m} / L_2 = 0\,,\ m \geq 2 \tag{10.12}$$

2. Based on (10.12) and Cauchy-Schwarz's inequality [119], for $m \geq 2$:

$$\begin{aligned}\lim_{n\to\infty} L_{m+1} / L_2 = \lim_{n\to\infty} L_2^{-1} n^{-(m+1)} \sum_{k=1}^{n} \lambda_k^{m+1} \leq \lim_{n\to\infty} L_2^{-1} \sqrt{n^{-2m} \sum_{k=1}^{n} \lambda_k^{2m}} \cdot \sqrt{n^{-2} \sum_{k=1}^{n} \lambda_k^{2}} = \\ = \lim_{n\to\infty} L_2^{-1} \sqrt{L_{2m}} \cdot \sqrt{L_2} = \lim_{n\to\infty} \sqrt{L_{2m} / L_2} = 0\end{aligned} \tag{10.13}$$

Using the same argument as for (10.12)

$$\lim_{n\to\infty} L_{m+1} / L_2 = 0\,,\ m \geq 2 \tag{10.14}$$

Therefore, if $\lim_{n\to\infty} n^{-1} tr(\mathbf{R}) < \infty$ and $\lim_{n\to\infty} n^{-2} \|\mathbf{R}\|^2 = 0$, $\lim_{n\to\infty} \Phi(\omega) = \Phi_g(\omega)$, i.e. $n^{-1}\beta$ is asymptotically Gaussian in distribution. **Q.E.D.**

Corollary A1: Under the conditions of Lemma A1

$$n^{-1}\beta \xrightarrow{p} 1 \text{ as } n \to \infty\,, \tag{10.15}$$

where $\xrightarrow{p}$ denotes convergence in probability.

Proof: From Chebyshev inequality [83], for any $\varepsilon > 0$:

$$\Pr\left\{\left|n^{-1}\beta - E\{n^{-1}\beta\}\right| \geq \varepsilon\right\} \leq Var\{n^{-1}\beta\} / \varepsilon^2\,, \tag{10.16}$$

where Var denotes variance. Since under the adopted normalization $E\{n^{-1}\beta\} = 1$ and following Lemma A1, $Var\{n^{-1}\beta\} \to 0$ as $n_t \to \infty$, using the continuity property of probability measure, one obtains

$$\Pr\left\{\left|\lim_{n\to\infty} n^{-1}\beta - 1\right| \geq \varepsilon\right\} \leq \lim_{n\to\infty} Var\{n^{-1}\beta\} / \varepsilon^2 = 0 \ \textbf{Q.E.D.} \tag{10.17}$$

Proof of Theorem 3.2:

(i) $n_t \to \infty$, $n_r < \infty$: From Lemma A1 and Corollary A1, $n_t^{-1}\beta_t \xrightarrow{p} 1$ as $n_t \to \infty$. Thus, from Slutsky Theorem [[23], Theorem 6a], $C \xrightarrow{d} \ln(1 + \gamma_0 \beta_r / n_r)$ as $n_t \to \infty$, where, under the adopted assumptions, $\ln(1 + \gamma_0 \beta_r / n_r)$ is the instantaneous capacity of an $1 \times n_r$ Rayleigh fading channel.

(ii) $n_t < \infty$, $n_r \to \infty$: Due to the symmetry, the proof follows the same arguments when the Tx and

Rx ends exchanged. **Q.E.D.**

Proof of Corollary 3.2:

(i) $n_t \to \infty$, $n_r < \infty$: Let $J = \ln(1+\gamma_0\beta_r / n_r)$. Since J is a continuous monotonically increasing function of β_r, its CDF is $F_J(x) = F_{\beta_r}\left(n_r(e^x - 1)/\gamma_0\right)$. Thus, from Theorem 3.2, as $n_t \to \infty$

$$F_C(x) \to F_J(x) = F_{\beta_r}\left(n_r(e^x - 1)/\gamma_0\right) \tag{10.18}$$

If $\mathbf{R}_r$ is non-singular and has distinct eigenvalues λ_t^r, $k = 1...n_t$, $F_{\beta_r}(x)$ is given by (10.5) **Q.E.D.**

(ii) $n_t < \infty$, $n_r \to \infty$: Due to the symmetry, the proof follows the same arguments when the Tx and Rx ends exchanged. **Q.E.D.**

Proof of Theorem 3.3:

Define a function $f(x,y) = \ln(1+\gamma_0 x \cdot y)$. From (3.1) $C = f(n_t^{-1}\beta_t, n_r^{-1}\beta_r)$. From Lemma A1, as $n_t \to \infty$ and $n_r \to \infty$, $n_t^{-1}\beta_t$ and $n_r^{-1}\beta_r$ are asymptotically Gaussian in distribution with the means $E(n_t^{-1}\beta_t) = E(n_r^{-1}\beta_r) = 1$ and the variances $n_t^{-2}\|\mathbf{R}_t\|^2$, $n_r^{-2}\|\mathbf{R}_r\|^2$ both converge to zero. Since the derivative of $f(x,y)$ is continuous in the neighborhood of $x=1$ and $y=1$, using Cramer Theorem [19], C is asymptotically Gaussian with the mean

$$\mu = f(1,1) = \ln(1+\gamma_0), \tag{10.19}$$

and the variance

$$\sigma^2 = \left[\left.\frac{\partial f(x,y)}{\partial x}\right|_{\substack{x=1\\y=1}}\right]^2 \frac{1}{n_t^2}\|\mathbf{R}_t\|^2 + \left[\left.\frac{\partial f(x,y)}{\partial y}\right|_{\substack{x=1\\y=1}}\right]^2 \frac{1}{n_r^2}\|\mathbf{R}_r\|^2 = \left(\frac{\gamma_0}{1+\gamma_0}\right)^2\left(\frac{1}{n_t^2}\|\mathbf{R}_t\|^2 + \frac{1}{n_r^2}\|\mathbf{R}_r\|^2\right) \quad \textbf{Q.E.D.} \tag{10.20}$$

Proof of (3.17):

Consider an $n \times n$ exponential correlation matrix $\mathbf{R}$ whose elements are defined in (2.14). Then

$$n^{-1}tr\{\mathbf{R}\} = 1 < \infty \tag{10.21}$$

For a finite n and $|r| \neq 1$, $\|\mathbf{R}\|^2$ is

$$\|\mathbf{R}\|^2 = tr\{\mathbf{RR}\} = 2\sum_{k=0}^{n-1}\sum_{m=0}^{n-k-1}|r|^{2m} - n =$$
$$= 2\sum_{k=0}^{n-1}\frac{1-|r|^{2(n-k)}}{1-|r|^2} - n = \frac{2}{1-|r|^2}\left[n - \sum_{m=1}^{n}|r|^{2m}\right] - n = \frac{n(1+|r|^2)}{1-|r|^2} + \frac{2\left(|r|^{2(n+1)} - |r|^2\right)}{(1-|r|^2)^2} \tag{10.22}$$

Therefore

$$\lim_{n\to\infty} n^{-1}\|\mathbf{R}\|^2 = \frac{1+|r|^2}{1-|r|^2};\ |r|<1 \quad \textbf{Q.E.D.} \tag{10.23}$$

Proof of (3.20):

Consider an $n\times n$ quadratic exponential correlation matrix $\mathbf{R}$ whose elements are defined in (2.15). Then:

$$n^{-1}tr\{\mathbf{R}\} = 1 < \infty \tag{10.24}$$

For a finite n, $\|\mathbf{R}\|^2$ is

$$\|\mathbf{R}\|^2 = tr\{\mathbf{RR}\} = 2\sum_{k=0}^{n-1}\sum_{m=0}^{n-k-1}|r|^{2m^2} - n \tag{10.25}$$

$\|\mathbf{R}\|^2$ can be bounded using Cauchy convergence test [119] based on the following: Let a_k be a decreasing sequence of $k \in Z$ (a set of integer numbers) and $a(x)$ be a monotonically decreasing function such that $a(x) = a_k$ at $x = k$, then:

$$\int_0^{n+1} a(x)dx \le \sum_{k=0}^{n} a_k \le \int_{-1}^{n} a(x)dx \tag{10.26}$$

Let b_k be an increasing sequence of $k \in Z$ and $b(x)$ be a monotonically increasing function such that $b(x) = b_k$ at $x = k$, then:

$$\int_{-1}^{n} b(x)dx \le \sum_{k=0}^{n} b_k \le \int_{0}^{n+1} b(x)dx \tag{10.27}$$

(i) Upper bound on $n^{-1}\|\mathbf{R}\|^2$ for $n\to\infty$: Let $a_k=\sum_{m=0}^{n-k-1}|r|^{2m^2}$. Since for $|r|<1$, a_k is a sum of the decreasing sequence $|r|^{2m^2}$, we use (10.26) to obtain

$$a_k=1+\sum_{m=1}^{n-k-1}|r|^{2m^2}\le 1+\int_0^{n-k-1}|r|^{2x^2}dx=1+\frac{\sqrt{\pi}}{2}\cdot\frac{erf\left[(n-k-1)\sqrt{-2\ln|r|}\right]}{\sqrt{-2\ln|r|}}, \quad (10.28)$$

where $erf(x)$ is the error function [119]. From (10.25),

$$\|\mathbf{R}\|^2=2\sum_{k=0}^{n-1}a_k-n\le n+\frac{\sqrt{\pi}}{\sqrt{-2\ln|r|}}\sum_{k=0}^{n-1}erf\left[(n-k-1)\sqrt{-2\ln|r|}\right]=$$

$$=n+\frac{\sqrt{\pi}}{\sqrt{-2\ln|r|}}\sum_{m=0}^{n-1}erf\left[m\cdot\sqrt{-2\ln|r|}\right]\le \quad (10.29)$$

$$\le n+\frac{\sqrt{\pi}}{\sqrt{-2\ln|r|}}\int_0^n erf\left[x\cdot\sqrt{-2\ln|r|}\right]dx=n+\frac{n\sqrt{\pi}}{\sqrt{-2\ln|r|}}erf\left[n\cdot\sqrt{-2\ln|r|}\right]+\frac{1-\exp\left[2n^2\ln|r|\right]}{2\ln|r|}$$

The second inequality is due to (10.27), since $erf\left[m\cdot\sqrt{-2\ln|r|}\right]$ is an increasing sequence of m, and $\lim_{x\to\infty}erf[x]=1$. Thus

$$\lim_{n\to\infty}n^{-1}\|\mathbf{R}\|^2\le\left[1+\sqrt{\frac{\pi}{-2\ln|r|}}\right],\ |r|<1 \quad (10.30)$$

(ii) Lower bound on $n^{-1}\|\mathbf{R}\|^2$ for $n\to\infty$: From (10.26) and $|r|<1$:

$$a_k=1+\sum_{m=1}^{n-k-1}|r|^{2m^2}\ge 1+\int_1^{n-k}|r|^{2x^2}dx=1+\frac{\sqrt{\pi}}{2\sqrt{-2\ln|r|}}\left(erf\left[(n-k)\sqrt{-2\ln|r|}\right]-erf\left[\sqrt{-2\ln|r|}\right]\right) \quad (10.31)$$

Then using (10.25)

$$\|\mathbf{R}\|^2=2\sum_{k=0}^{n-1}a_k-n\ge n+\frac{\sqrt{\pi}}{\sqrt{-2\ln|r|}}\sum_{k=0}^{n-1}erf\left[(n-k)\sqrt{-2\ln|r|}\right]-\frac{n\sqrt{\pi}}{\sqrt{-2\ln|r|}}erf\left[\sqrt{-2\ln|r|}\right]=$$

$$=n+\frac{\sqrt{\pi}}{\sqrt{-2\ln|r|}}\sum_{m=1}^{n}erf\left[m\sqrt{-2\ln|r|}\right]-\frac{n\sqrt{\pi}}{\sqrt{-2\ln|r|}}erf\left[\sqrt{-2\ln|r|}\right]\ge \quad (10.32)$$

$$\geq n+\frac{\sqrt{\pi}}{\sqrt{-2\ln|r|}}\int_0^n erf\left[x\cdot\sqrt{-2\ln|r|}\right]dx-\frac{n\sqrt{\pi}}{\sqrt{-2\ln|r|}}erf\left[\sqrt{-2\ln|r|}\right]=$$

$$=n+\frac{n\sqrt{\pi}}{\sqrt{-2\ln|r|}}\left(erf\left[n\cdot\sqrt{-2\ln|r|}\right]-erf\left[\sqrt{-2\ln|r|}\right]\right)+\frac{1-\exp\left[2n^2\ln|r|\right]}{2\ln|r|}$$

i.e. as $n\to\infty$

$$\lim_{n\to\infty}n^{-1}\|\mathbf{R}\|^2\geq\left[1+\sqrt{\frac{\pi}{-2\ln|r|}}\cdot erfc\left[\sqrt{-2\ln|r|}\right]\right],\ |r|<1\ \textbf{Q.E.D.}\qquad(10.33)$$

Lemma A2: Let $\mathbf{h}\propto\mathbf{R}^{1/2}\mathbf{g}$, where $\mathbf{R}$ is an $n\times n$ correlation matrix, and $\mathbf{g}$ is an $n\times 1$ zero mean complex random vector invariant under unitary transformation. The entries of $\mathbf{g}$ are independent. As $n\to\infty$, $n^{-1}\|\mathbf{h}\|^2$ is asymptotically normal in distribution if: (i) $m_{2+\delta}(k)<\infty$ and $m_2(k)>0$ for all k and some $\delta>0$, where $m_\delta(k)=E\{(|g_k|^2-E\{|g_k|^2\}^\delta\}$ is the central moment of $|g_k|^2$ of order δ, and g_k is the k^{th} entry of $\mathbf{g}$, and (ii)

$$Z(\delta)=\lim_{n\to\infty}\|\lambda\|_{2+\delta}/\|\lambda\|_2=0,\qquad(10.34)$$

where $\|\lambda\|_m=\left(\sum_{i=1}^n(\lambda_i)^m\right)^{1/m}$ is the L_m norm of the eigenvalues of $\mathbf{R}$.

Proof: Under the adopted assumptions,

$$n^{-1}\|\mathbf{h}\|^2\propto n^{-1}\sum_{k=1}^n\lambda_k|g_k|^2\qquad(10.35)$$

From Lyapounov Theorem [[28], p. 310], $n^{-1}\|\mathbf{h}\|^2$ is asymptotically normal in distribution as $n\to\infty$, if for some $\delta>0$

$$\lim_{n\to\infty}\frac{\left(\sum_{k=1}^n\lambda_k^{2+\delta}m_{2+\delta}(k)\right)^{1/(2+\delta)}}{\left(\sum_{k=1}^n\lambda_k^2\cdot m_2(k)\right)^{1/2}}=0\qquad(10.36)$$

Let $M=\max_k\{m_{2+\delta}(k)\}<\infty$, and $m=\min_k\{m_2(k)\}>0$, then

$$\lim_{n\to\infty}\frac{\left(\sum_{k=1}^{n}\lambda_k^{2+\delta}m_{2+\delta}(k)\right)^{1/(2+\delta)}}{\left(\sum_{k=1}^{n}\lambda_k^2\cdot m_2(k)\right)^{1/2}}\le\lim_{n\to\infty}\frac{M^{1/(2+\delta)}}{m^{1/2}}\frac{\left(\sum_{k=1}^{n}\lambda_k^{2+\delta}\right)^{1/(2+\delta)}}{\left(\sum_{k=1}^{n}\lambda_k^2\right)^{1/2}}=\frac{M^{1/(2+\delta)}}{m^{1/2}}Z(\delta) \tag{10.37}$$

Under the conditions of the lemma, $M^{1/(2+\delta)}/m^{1/2}<\infty$. Thus, from (10.37), if $Z(\delta)=0$, the limit in (10.36) holds, i.e. $n^{-1}\|\mathbf{h}\|^2$ is asymptotically normal in distribution. **Q.E.D.**

Proof of Theorem 3.4:

Under the conditions of Lemma A2, as $n_t\to\infty$ and $n_r\to\infty$, $n_t^{-1}\beta_t$ and $n_r^{-1}\beta_r$ are asymptotically Gaussian in distribution with means $E(n_t^{-1}\beta_t)=E(n_r^{-1}\beta_r)=1$. From (3.1), the instantaneous capacity C is a continuous function of $n_t^{-1}\beta_t$ and $n_r^{-1}\beta_r$, and it has a continuous derivative in the neighborhood of $E(n_t^{-1}\beta_t)$ and $E(n_r^{-1}\beta_r)$. Thus, using Cramer Theorem [19], C is asymptotically Gaussian. **Q.E.D.**

Proof of Corollary 3.4:

Let $\mathbf{R}$ (either $\mathbf{R}_t$ or $\mathbf{R}_r$) be a Toeplitz correlation matrix with vector eigenvalues $\boldsymbol{\lambda}$. Let t_{k-m} be the k,m element of $\mathbf{R}$. From Lyapounov Theorem [[28], p.310], $Z(\delta)=\lim_{n_t\to\infty}\|\boldsymbol{\lambda}\|_{2+\delta}/\|\boldsymbol{\lambda}\|_2=0$ for any $\delta>0$ if

$$\lim_{n\to\infty}\sum_{k=-n+1}^{n-1}|t_k|^2<\infty, \tag{10.38}$$

i.e. $\mathbf{R}$ is square-summable. From [30]

$$\lim_{n\to\infty}\sum_{k=-n+1}^{n-1}|t_k|^2=\lim_{n\to\infty}n^{-1}\sum_{k=0}^{n-1}\lambda_k^2=\lim_{n\to\infty}n^{-1}\|\mathbf{R}\|^2, \tag{10.39}$$

where λ_k are the eigenvalues of $\mathbf{R}$. Thus, if $\lim_{n\to\infty}n^{-1}\|\mathbf{R}\|^2<\infty$, then $Z(\delta)=0$ for any $\delta>0$. **Q.E.D.**

Proof of (3.25):

From (3.1) and following the approach proposed in [20],

$$\overline{C}=E\left\{\ln\left(1+\frac{\gamma_0}{n_tn_r}\cdot\alpha\right)\right\}\ge\ln\left(1+\frac{\gamma_0}{n_tn_r}\cdot\exp\left[E\{\ln\alpha\}\right]\right), \tag{10.40}$$

where, the inequality is due to the convexity of $\ln\left(1+\gamma_0 \exp[x]/n_t\right)$. The generalized moments of α are

$$E\{\alpha^u\} = \int_0^\infty x^u dF_\alpha(x) = \Gamma^2[u+1]\cdot \sum_{k=1}^{n_t} A_k^t(\lambda_k^t)^u \cdot \sum_{m=1}^{n_r} A_m^r(\lambda_m^r)^u \,, \qquad (10.41)$$

where $F_\alpha(x)$ is given by (3.4), $\Gamma(x)$ is the Gamma function [119], λ_k^t, λ_m^r are the eigenvalues of the correlation matrices $\mathbf{R}_t$ and $\mathbf{R}_r$, and both A_k^t, A_m^r are given by (3.5) for distinct and non-zero λ_k^t, λ_m^r. Thus, since $E\{\ln\alpha\} = (d/du)E\{\alpha^u\}\big|_{u=0}$,

$$E\{\ln\alpha\} = \Theta(\mathbf{R}_t) + \Theta(\mathbf{R}_r)\,, \qquad (10.42)$$

where $\Theta(\mathbf{R}_t) = -\gamma_e + \sum_{k=1}^{n_t} A_k^t \ln(\lambda_k^t)$ and $\Theta(\mathbf{R}_t) = -\gamma_e + \sum_{m=1}^{n_r} A_m^r \ln(\lambda_m^r)$. Substituting (10.42) in (10.40) gives the lower bound in (3.25). **Q.E.D.**

Denote the upper and lower bounds in (3.24) and (3.25) by C_u and C_l respectively. From (10.40), as $\gamma_0 \to \infty$, $\bar{C} \to \ln(\gamma_0/(n_t n_r)) + E\{\ln\alpha\}$, and so $C_l \to \ln(\gamma_0/(n_t n_r)) + E\{\ln\alpha\}$, thus, $C_l \to \bar{C}$ as $\gamma_0 \to \infty$. On the other hand, as $\gamma_0 \to 0$, $\bar{C} \to (\gamma_0/(n_t n_r))E\{\alpha\} = \gamma_0$, and $C_u \to \gamma_0$, where $E\{\alpha\} = n_t n_r$ due to the adopted normalization. Therefore $C_u \to \bar{C}$ as $\gamma_0 \to 0$ **Q.E.D.**

APPENDIX B: MULTI-KEYHOLE CHANNELS

Lemma B1: Let $\mathbf{H}$ be an $[n\times M]$ random matrix with M mutually independent columns $\mathbf{h}_1...\mathbf{h}_M$, such that $\mathbf{h}_k$, $k=1...M$, is a Gaussian circularly symmetric vector with the correlation matrix $\mathbf{R}_k=E\{\mathbf{h}_k\mathbf{h}_k^H\}$. If $n^{-1}tr\{\mathbf{R}_k\}=1$ and $n^{-2}tr[\mathbf{R}_k\mathbf{R}_m]\to 0$ as $n\to\infty$, then $\mathbf{H}^H\mathbf{H}/n\xrightarrow{p}\mathbf{I}$ as $n\to\infty$, where $\mathbf{I}$ is an $[M\times M]$ identity matrix.

Proof: Under the adopted normalization, $E\{\mathbf{H}\mathbf{H}^H/n\}=\mathbf{I}$, since $\mathbf{h}_1...\mathbf{h}_M$ are mutually independent. From Chebyshev inequality [119], for any $\varepsilon>0$

$$\Pr\left\{\left\|\mathbf{H}^H\mathbf{H}/n-\mathbf{I}\right\|\geq\varepsilon\right\}\leq\varepsilon^{-2}\cdot E\left\{\left\|\mathbf{H}^H\mathbf{H}/n-\mathbf{I}\right\|^2\right\}, \tag{11.1}$$

where

$$E\left\{\left\|\mathbf{H}^H\mathbf{H}/n-\mathbf{I}\right\|^2\right\}=n^{-2}tr[E\{\mathbf{H}\mathbf{H}^H\mathbf{H}\mathbf{H}^H\}]-M=n^{-2}\sum_{m=1}^{M}\sum_{k=1}^{M}tr[E\{\mathbf{h}_m\mathbf{h}_m^H\mathbf{h}_k\mathbf{h}_k^H\}]-M \tag{11.2}$$

For $k=m$, $\sqrt{tr\{\mathbf{h}_k\mathbf{h}_k^H\mathbf{h}_k\mathbf{h}_k^H\}}=\|\mathbf{h}_k\|^2$ is a generalized χ^2 random variable with $2n$ degrees of freedom. Thus, from Lemma A1 (see Appendix A):

$$n^{-2}tr[E\{\mathbf{h}_m\mathbf{h}_m^H\mathbf{h}_k\mathbf{h}_k^H\}]=\begin{cases}n^{-2}\|\mathbf{R}_k\|^2+1;\ k=m\\ n^{-2}tr[\mathbf{R}_m\mathbf{R}_k];\ k\neq m\end{cases} \tag{11.3}$$

By substituting (11.3) in (11.2), one obtains

$$E\left\{\left\|\mathbf{H}^H\mathbf{H}/n-\mathbf{I}\right\|^2\right\}=n^{-2}\sum_{m=1}^{M}\sum_{k=1}^{M}tr[\mathbf{R}_m^H\mathbf{R}_k] \tag{11.4}$$

Therefore, if $n^{-2}tr[\mathbf{R}_k^H\mathbf{R}_m]\to 0$ as $n\to\infty$, then from (11.1) for any $\varepsilon>0$

$$\Pr\left\{\left\|\mathbf{H}^H\mathbf{H}/n-\mathbf{I}\right\|\geq\varepsilon\right\}\to 0,\ \text{as } n\to\infty\ \textbf{Q.E.D.} \tag{11.5}$$

Proof of Theorem 4.1:

(i) Under the conditions of Lemma B1, for $\mathbf{H}=\mathbf{H}_t$ and $n=n_t$

$$\mathbf{H}_t^H \mathbf{H}_t / n_t \xrightarrow{p} \mathbf{I}, \text{ as } n_t \to \infty \tag{11.6}$$

Since (4.3) is a continuous function of $\mathbf{H}_t$, from Slutsky Theorem [[23], Theorem 6'(a)]

$$C \xrightarrow{p} \ln\det[\mathbf{I} + \gamma_0 \mathbf{B}_r \mathbf{A}\mathbf{A}^H] = \ln\det[\mathbf{I} + \gamma_0 \mathbf{H}_r \mathbf{A}\mathbf{A}^H \mathbf{H}_r^H / n_r] \text{ as } n_t \to \infty, \tag{11.7}$$

where the RHS is the instantaneous capacity of an $[M \times n_r]$ semicorrelated Rayleigh channel with the channel matrix $\mathbf{H}_r$ and the Tx covariance matrix $\mathbf{A}\mathbf{A}^H$.

(ii) By the same argument as for (i)

$$\mathbf{H}_r^H \mathbf{H}_r / n_r \xrightarrow{p} \mathbf{I}, \text{ as } n_r \to \infty \tag{11.8}$$

Thus, from Slutsky Theorem [[23], Theorem 6'(a)]

$$C \xrightarrow{p} \ln\left(\det[\mathbf{I} + \gamma_0 \mathbf{A}^H \mathbf{A}\mathbf{B}_t]\right) = \ln\left(\det[\mathbf{I} + \gamma_0 \mathbf{H}_t \mathbf{A}^H \mathbf{A}\mathbf{H}_t^H / n_r]\right) \text{ as } n_r \to \infty, \tag{11.9}$$

where the right side is the instantaneous capacity of an $[n_t \times M]$ semicorrelated Rayleigh channel with the channel matrix $\mathbf{H}_t$. **Q.E.D.**

Theorem B1 [7]: Let $\mathbf{s} = \sum_{k=1}^{n} \mathbf{x}_k$, where $\mathbf{x}_1 ... \mathbf{x}_n$ are mutually independent random vectors taking values in $\mathbf{R}^d$ such that $E\{\mathbf{x}_k\} = 0$ for all k, and $\mathbf{C} = E\{\mathbf{s} \cdot \mathbf{s}^T\}$ is invertible. Then, as $n \to \infty$, $\mathbf{s}$ is asymptotically normal in distribution with zero mean and covariance matrix $\mathbf{C}$ if

$$\lim_{n \to \infty} \sum_{k=1}^{n} E\left\{\left\|\mathbf{C}^{-1/2} \mathbf{x}_k\right\|^3\right\} = 0 \tag{11.10}$$

Moreover, let $\Delta_n(\mathbf{x}) = \left|F_n(\mathbf{x}) - \Phi(\mathbf{x})\right|$, where $F_n(\mathbf{x})$ is the CDF of $\mathbf{s}$, and $\Phi(\mathbf{x})$ is a normal CDF with the same mean and variance as of $\mathbf{s}$, then $\Delta_n(\mathbf{x}) \to 0$ with the same rate as $\sum_{k=1}^{n} E\left\{\left\|\mathbf{C}^{-1/2} \mathbf{x}_k\right\|^3\right\}$.

Corollary B1 (Generalization of Theorem B1 for a complex case): Let $\mathbf{s} = \sum_{k=1}^{n} \mathbf{x}_k$, where $\mathbf{x}_1 ... \mathbf{x}_n$ are mutually independent circularly symmetric random vectors taking values in $\mathbf{C}^d$ such that $E\{\mathbf{x}_k\} = 0$ for all k, and $\mathbf{C} = E\{\mathbf{s} \cdot \mathbf{s}^H\}$ is invertible. Then Theorem B1 holds

Proof: A proof is standard, based on $\mathbf{R}^{2d} \to \mathbf{C}^d$ mapping, and follows immediately from the

properties of circular symmetric random vectors, see [[103], Lemma 1].

Proof of Theorem 4.2:

Consider $vec(\mathbf{H})$, where $\mathbf{H}$ is a matrix of a multi-keyhole channel defined in (4.1). It is straightforward to show that

$$vec(\mathbf{H}) = \sum_{k=1}^{M} \mathbf{x}_k , \tag{11.11}$$

where $\mathbf{x}_k = a_k vec(\mathbf{h}_{rk}\mathbf{h}_{tk}^H)$. Under the adopted assumptions, $\mathbf{x}_k$ are mutually independent circular symmetric random vectors, so that following Theorem B1 Corollary B1, $vec(\mathbf{H})$ is asymptotically circular symmetric Gaussian as $M \to \infty$, if

$$\lim_{M\to\infty} \sum_{k=1}^{M} E\left\{\left\|\mathbf{C}^{-1/2}\mathbf{x}_k\right\|^3\right\} = 0 , \tag{11.12}$$

where

$$\mathbf{C} = E\left\{vec(\mathbf{H}) \cdot vec(\mathbf{H})^H\right\} = \sum_{k=1}^{M} |a_k|^2 \boldsymbol{\Gamma}_k , \tag{11.13}$$

and $\boldsymbol{\Gamma}_k = \mathbf{R}_{tk}^T \otimes \mathbf{R}_{rk}$. Consider the following upper bounds

$$\begin{aligned} &\sum_{k=1}^{M} E\left\{\left\|\mathbf{C}^{-1/2}\mathbf{x}_k\right\|^3\right\} \le \sum_{k=1}^{M}\left(E\left\{\left\|\mathbf{C}^{-1/2}\mathbf{x}_k\right\|^4\right\}\right)^{3/4} \le \left\|\mathbf{C}^{-1/2}\right\|^3 \cdot \sum_{k=1}^{M}\left(E\left\{\left\|\mathbf{x}_k\right\|^4\right\}\right)^{3/4} = \\ &= \left\|\mathbf{C}^{-1/2}\right\|^3 \cdot \sum_{k=1}^{M} |a_k|^3 \left(E\left\{\left\|\mathbf{h}_{tk}\right\|^4\right\} \cdot E\left\{\left\|\mathbf{h}_{rk}\right\|^4\right\}\right)^{3/4} \le \left\|\mathbf{C}^{-1/2}\right\|^3 \cdot \max_k\left(E\left\{\left\|\mathbf{h}_{tk}\right\|^4\right\} \cdot E\left\{\left\|\mathbf{h}_{rk}\right\|^4\right\}\right)^{3/4} \sum_{k=1}^{M} |a_k|^3 \end{aligned} , \tag{11.14}$$

where the first inequality is due to Lyapounov Inequality [[24], Theorem 3.4.1]. Note that under the adopted assumptions, $\left\|\mathbf{C}^{-1/2}\right\|$ and $\max_k\left(E\left\{\left\|\mathbf{h}_{tk}\right\|^4\right\} \cdot E\left\{\left\|\mathbf{h}_{rk}\right\|^4\right\}\right)^{3/4}$ exist. Therefore, if

$$\lim_{M\to\infty} \sum_{k=1}^{M} |a_k|^3 = 0 , \tag{11.15}$$

then necessarily from (11.14) $\lim_{M\to\infty} \sum_{k=1}^{M} E\left\{\left\|\mathbf{C}^{-1/2}\mathbf{x}_k\right\|^3\right\} = 0$.

(ii) Let $\Delta_M(\mathbf{x}) = \left|F_M(\mathbf{x}) - \Phi(\mathbf{x})\right|$, where $F_M(\mathbf{x})$ is the CDF of $vec(\mathbf{H})$, and $\Phi(\mathbf{x})$ is a normal CDF with the same mean and variance as of $vec(\mathbf{H})$, then from Theorem B1, Corollary B1, $\Delta_M(\mathbf{x}) \to 0$ with the same rate as $\sum_{k=1}^{M} E\left\{\left\|\mathbf{C}^{-1/2}\mathbf{x}_k\right\|^3\right\}$. Under the assumption that $\mathbf{C}$ does not depend on M, then from

(11.14), $\sum_{k=1}^{M} E\left\{\left\|\mathbf{C}^{-1/2}\mathbf{x}_k\right\|^3\right\}$ converges to zero with at least the same rate as $\sum_{k=1}^{M}|a_k|^3$ **Q.E.D.**

Proof of Corollary 4.2.1:

Assume that there is a finite set of k largest $|a_i|$, $i=1...k$, which is not dominated by the rest as $M\to\infty$, i.e. if $S_1=\sum_{i=1}^{k}|a_i|^3\neq 0$ and $S_2=\sum_{i=k+1}^{M}|a_i|^3$, then

$$\lim_{M\to\infty}\frac{S_2}{S_1}=\lim_{n_t\to\infty}\frac{\sum_{i=k+1}^{M}|a_i|^3}{\sum_{i=1}^{k}|a_i|^3}=c<\infty \tag{11.16}$$

Thus

$$\lim_{M\to\infty}\sum_{i=1}^{M}|a_i|^3=\lim_{M\to\infty}S_1(1+S_2/S_1)=S_1(1+c)>0 \quad \textbf{Q.E.D.} \tag{11.17}$$

Proof of Corollary 4.2.2:

For $\mathbf{C}^{-1/2}$ to exist, $\mathbf{C}$ must be positive-definite, i.e. $\lambda_k(\mathbf{C})>0$ for every $k=1...n_t n_r$, where $\lambda_k(\mathbf{C})$ is the k-th eigenvalue of matrix $\mathbf{C}$, $\lambda_1(\mathbf{C})\le\lambda_2(\mathbf{C})\le...\le\lambda_{n_t n_r}(\mathbf{C})$. It is straightforward to show that

$$\lambda_1(\mathbf{C})\ge\sum_{k=1}^{M}|a_k|^2\lambda_1(\mathbf{\Gamma}_k)=\sum_{k=1}^{M}|a_k|^2\lambda_1(\mathbf{R}_{tk})\lambda_1(\mathbf{R}_{rk}) \tag{11.18}$$

(i) If for every $k=1...M$, $\lambda_1(\mathbf{R}_{tk}),\lambda_1(\mathbf{R}_{rk})>0$, i.e. all $\mathbf{R}_{tk}$, $\mathbf{R}_{tk}$ are non-singular, then $\lambda_k(\mathbf{C})>0$.

(ii) Let S be a finite subset of all singular keyholes as $M\to\infty$. As follows from (4.2) and (4.5), $\lim_{M\to\infty}\sum_{k\notin S}|a_k|^2=1$. Thus, from (11.18)

$$\lambda_1(\mathbf{C})\ge\min_{k\notin S}(\lambda_1(\mathbf{R}_{tk})\lambda_1(\mathbf{R}_{rk}))\sum_{k\notin S}|a_k|^2\to\min_{k\notin S}(\lambda_1(\mathbf{R}_{tk})\lambda_1(\mathbf{R}_{rk}))>0 \text{ as } M\to\infty \tag{11.19}$$

(iii) If S has infinite size, then

$$\lambda_1(\mathbf{C})\ge\min_{k\notin S}(\lambda_1(\mathbf{R}_{tk})\lambda_1(\mathbf{R}_{rk}))\sum_{k\notin S}|a_k|^2>0 \tag{11.20}$$

if $\sum_{k\notin S}|a_k|^2>0$ **Q.E.D.**

Lemma B2: Let $\mathbf{H}$ be an $[n_r \times n_t]$ channel matrix of a Rayleigh fading channel with the Kronecker correlation structure, i.e. $\mathbf{H} \sim \mathbf{R}_r^{1/2}\mathbf{H}_w(\mathbf{R}_t^{1/2})^H$, where $\mathbf{H}_w$ is an $[n_r \times n_t]$ i.i.d. Gaussian circular symmetric matrix, and $\mathbf{R}_t$, $\mathbf{R}_r$ are correlation matrices normalized such that $n_t^{-1}tr\{\mathbf{R}_t\}=1$ and $n_r^{-1}tr\{\mathbf{R}_r\}=1$. (i) if $\lim_{\substack{n_t\to\infty \\ n_r\to\infty}} n_r\|\mathbf{R}_t\|/n_t = 0$, then $\mathbf{H}\mathbf{H}^H/n_t \xrightarrow{q.m.} \mathbf{R}_r$ as both $n_t, n_r \to \infty$, where $\xrightarrow{q.m.}$ denotes convergence in quadratic mean, i.e. $\lim_{\substack{n_t\to\infty \\ n_r\to\infty}} E\left\{\left\|\mathbf{H}\mathbf{H}^H/n_t - \mathbf{R}_r\right\|^2\right\} = 0$. (ii) If $\lim_{\substack{n_t\to\infty \\ n_r\to\infty}} n_t\|\mathbf{R}_r\|/n_r = 0$, then $\mathbf{H}^H\mathbf{H}/n_r \xrightarrow{q.m.} \mathbf{R}_t$ as both $n_t, n_r \to \infty$.

Proof: (i) First note that $E\{\mathbf{H}\mathbf{H}^H/n_t\} = \mathbf{R}_r$. Thus

$$E\left\{\left\|\mathbf{H}\mathbf{H}^H/n_t - \mathbf{R}_r\right\|^2\right\} = n_t^{-2}tr[E\{\mathbf{H}\mathbf{H}^H\mathbf{H}\mathbf{H}^H\}] - \|\mathbf{R}_r\|^2 \tag{11.21}$$

Consider the trace in (11.21)

$$\begin{aligned} tr[E\{\mathbf{H}\mathbf{H}^H\mathbf{H}\mathbf{H}^H\}] = tr[E\{\mathbf{H}^H\mathbf{H}\mathbf{H}^H\mathbf{H}\}] = \sum_{m=1}^{n_t}\sum_{k=1}^{n_t} E\{\mathbf{h}_m^H\mathbf{h}_k\mathbf{h}_k^H\mathbf{h}_m\} = \\ = \sum_{m=1}^{n_t}\sum_{k=1}^{n_t}\sum_{i=1}^{n_r}\sum_{j=1}^{n_r} E\{H_{im}^* H_{ik} H_{jk}^* H_{jm}\} \end{aligned}, \tag{11.22}$$

where $\mathbf{h}_k$ is the k-th column of $\mathbf{H}$, and H_{ik} is an i,k-th element of $\mathbf{H}$. Since all H_{ik}, $k=1...n_t$, $i=1...n_r$ are Gaussian circular symmetric, their four-order cumulant is zero [88], and thus

$$\begin{aligned} \sum_{m=1}^{n_t}\sum_{k=1}^{n_t}\sum_{i=1}^{n_r}\sum_{j=1}^{n_r} E\{H_{im}^* H_{ik} H_{jk}^* H_{jm}\} = \\ = \sum_{m=1}^{n_t}\sum_{k=1}^{n_t}\sum_{i=1}^{n_r}\sum_{j=1}^{n_r} [E\{H_{im}^* H_{ik}\}E\{H_{jk}^* H_{jm}\} + E\{H_{ik}H_{jk}^*\}E\{H_{im}^* H_{jm}\}] \end{aligned} \tag{11.23}$$

As follows from the Kronecker correlation model $E\{H_{ik}H_{jk}^*\} = T_{jm}^* R_{ik}$, where T_{jm} and R_{ik} are j,m-th and i,k-th elements of $\mathbf{R}_t$ and $\mathbf{R}_r$ respectively. Thus

$$\begin{aligned} \sum_{m=1}^{n_t}\sum_{k=1}^{n_t}\sum_{i=1}^{n_r}\sum_{j=1}^{n_r} E\{H_{im}^* H_{ik} H_{jk}^* H_{jm}\} = \sum_{m=1}^{n_t}\sum_{k=1}^{n_t}\sum_{i=1}^{n_r}\sum_{j=1}^{n_r}\left(T_{km}^* R_{ii}^* T_{km} R_{jj} + T_{kk}^* R_{ij} T_{mm} R_{ij}^*\right) = \\ = \sum_{m=1}^{n_t}\sum_{k=1}^{n_t}\left(n_r^2|T_{km}|^2 + T_{kk}^* T_{mm}\|\mathbf{R}_r\|^2\right) = n_r^2\|\mathbf{R}_t\|^2 + n_t^2\|\mathbf{R}_r\|^2 \end{aligned} \tag{11.24}$$

Substituting (11.24) in (11.21), one obtains

$$E\left\{\left\|\mathbf{H}\mathbf{H}^H/n_t - \mathbf{R}_r\right\|^2\right\} = \left(\frac{n_r}{n_t}\|\mathbf{R}_t\|\right)^2,$$

i.e. if $\lim_{\substack{n_t\to\infty \\ n_r\to\infty}} n_r\|\mathbf{R}_t\|/n_t = 0$, then

$$\lim_{\substack{n_t\to\infty \\ n_r\to\infty}} E\left\{\left\|\mathbf{H}\mathbf{H}^H/n_t-\mathbf{R}_r\right\|^2\right\}=0 \tag{11.25}$$

(ii) If $\lim_{\substack{n_t\to\infty \\ n_r\to\infty}} n_t\|\mathbf{R}_r\|/n_r=0$, then $\lim_{\substack{n_t\to\infty \\ n_r\to\infty}} E\left\{\left\|\mathbf{H}^H\mathbf{H}/n_r-\mathbf{R}_t\right\|^2\right\}=0$. A proof is the same due to the symmetry of the problem.

Definition B1: Let g be a function $\mathbb{C}^{n\times n}\to\Re$. The derivative $\dot{g}$ is an $n\times n$ matrix with elements $\dot{g}_{ij}(\mathbf{H})=\partial g(\mathbf{H})/\partial\mathbf{H}_{ij}$, $i,j=1...n$.

Lemma B3: Let g be a function $\mathbb{C}^{n\times n}\to\Re$, such that $\dot{g}$ is continuous. Then, if $\mathbf{H}_k$ is a sequence of random matrices such that $\mathbf{H}_k\xrightarrow{q.m.}\mathbf{H}$, as $k\to\infty$, where $\mathbf{H}$ is a random matrix of an appropriate size, $\lim_{k\to\infty} E\{g(\mathbf{H}_k)\}\to E\{g(\mathbf{H})\}$.

Proof: First show that $\lim_{k\to\infty} E\left\{\left|g(\mathbf{H}_k)-g(\mathbf{H})\right|^2\right\}=0$. Using the Mean-Value Theorem [[23], p. 20], for some $n\times n$ matrix $\mathbf{G}_k$, such that $\|\mathbf{G}_k\|\le\|\mathbf{H}_k-\mathbf{H}\|$

$$g(\mathbf{H}_k)=g(\mathbf{H})+tr\left\{\int_0^1\dot{g}(\mathbf{H}+u\cdot\mathbf{G}_k)du\cdot\mathbf{G}_k\right\} \tag{11.26}$$

Thus,

$$E\left\{\left|g(\mathbf{H}_k)-g(\mathbf{H})\right|^2\right\}=E\left\{\left|tr\left\{\int_0^1\dot{g}(\mathbf{H}+u\cdot\mathbf{G}_k)du\cdot\mathbf{G}_k\right\}\right|^2\right\}\le E\left\{\left\|\int_0^1\dot{g}(\mathbf{H}+u\cdot\mathbf{G}_k)du\right\|^2\right\}E\left\{\|\mathbf{G}_k\|^2\right\}, \tag{11.27}$$

where the inequality is due to [[30], Lemma 2.2], and using the fact that $\sqrt{E\left\{\|\mathbf{H}\|^2\right\}}$ is a norm. Since $\|\mathbf{G}_k\|\le\|\mathbf{H}_k-\mathbf{H}\|$ and due to the continuity property of $\dot{g}$

$$\lim_{k\to\infty} E\left\{\left\|\int_0^1\dot{g}(\mathbf{H}+u\cdot\mathbf{G}_k)du\right\|^2\right\}\le M_0<\infty \tag{11.28}$$

Thus, from (11.27)

$$0\le\lim_{k\to\infty} E\left\{\left|g(\mathbf{H}_k)-g(\mathbf{H})\right|^2\right\}\le\lim_{k\to\infty} M_0E\left\{\left\|\mathbf{H}_k-\mathbf{H}\right\|^2\right\}=0 \tag{11.29}$$

The equality is because $E\left\{\|\mathbf{G}_k\|^2\right\}\le E\left\{\left\|\mathbf{H}_k-\mathbf{H}\right\|^2\right\}\to 0$, as $k\to\infty$. Due to Cauchy-Schwarz's inequality [119],

$$E\left\{\left|g(\mathbf{H}_k)-g(\mathbf{H})\right|^2\right\}\geq\left|E\{g(\mathbf{H}_k)-g(\mathbf{H})\}\right|^2=\left|E\{g(\mathbf{H}_k)\}-E\{g(\mathbf{H})\}\right|^2, \quad (11.30)$$

i.e. from (11.29) and (11.30)

$$\lim_{k\to\infty}E\{g(\mathbf{H}_k)\}\to E\{g(\mathbf{H})\}\ \textbf{Q.E.D.} \quad (11.31)$$

Proof of Corollary 4.3:

(i) First note that following the proof of Theorem 4.2, see Eq. (11.14), if $\left\|\mathbf{C}^{-1/2}\right\|^3\cdot\sum_{k=1}^{M}|a_k|^3\left(E\left\{\left\|\mathbf{h}_{tk}\right\|^4\right\}\cdot E\left\{\left\|\mathbf{h}_{rk}\right\|^4\right\}\right)^{3/4}\to 0$ as $n_t,n_r,M\to\infty$, the corresponding FRMK channel is Rayleigh-fading in distribution, and thus Theorem 4.3 applies. Assume that $\lim_{\substack{n_t\to\infty\\ n_r\to\infty}} n_r\left\|\mathbf{R}_t\right\|/n_t=0$. From Lemma B2 part (i), $\mathbf{HH}^H/n_t\xrightarrow{q.m.}\mathbf{R}_r$, as both $n_t,n_r\to\infty$. Thus from Lemma B3, for any function g $\mathbb{C}^{n\times n}\to\Re$ with a continuous derivative, $E\{g(\mathbf{HH}^H/n_t)\}\to g(\mathbf{R}_r)$ as $n_t,n_r\to\infty$. Since the instantaneous capacity is a function of $\mathbf{HH}^H/n_t$ with a continuous derivative (see (4.3)) and based on Theorem 4.3

$$E\{\ln\left(\det[\mathbf{I}+\gamma_0\cdot\mathbf{HH}^H/(n_tn_r)]\right)\}\to\ln\left(\det[\mathbf{I}+\gamma_0\cdot\mathbf{R}_r/n_r]\right)=\mu \text{ as } n_t,n_r\to\infty \quad (11.32)$$

Consider λ_k^r/n_r, $k=1...n_r$. Since $\lim_{n_r\to\infty}n_r\left\|\mathbf{R}_r\right\|=0$, there is such n_0, so that for all $n_r>n_0$ $\lambda_k^r/n_r\leq\left\|\mathbf{R}_r\right\|/n_r\leq 1$. Using the Taylor series [119]

$$\mu=\sum_{k=1}^{n_r}\ln\left(1+\gamma_0\cdot\lambda_k^r/n_r\right)=\gamma_0n_r^{-1}\sum_{k=1}^{n_r}\lambda_k^r-\gamma_0^2n_r^{-2}\sum_{k=1}^{n_r}(\lambda_k^r)^2/2+o(n_r^{-2}) \quad (11.33)$$

Finally, under the adopted normalization $n_r^{-1}\sum_{k=1}^{n_r}\lambda_k^r=1$

$$\mu\to\gamma_0(1-\gamma_0n_r^{-2}\left\|\mathbf{R}_r\right\|^2/2) \text{ as both } n_t,n_r\to\infty \quad (11.34)$$

(ii) If $\lim_{\substack{n_t\to\infty\\ n_r\to\infty}} n_t\left\|\mathbf{R}_r\right\|/n_r=0$, then $\mu\to\gamma_0(1-\gamma_0\cdot n_t^{-2}\left\|\mathbf{R}_t\right\|^2/2)$ as both $n_r,n_t\to\infty$. A proof is the same due to the symmetry of the problem **Q.E.D.**

Lemma B4: Let $\mathbf{H}$ be an $n\times M$ random matrix with M mutually independent columns $\mathbf{h}_1...\mathbf{h}_M$, and $\mathbf{\Lambda}$ is an $M\times M$ diagonal matrix with elements $\Lambda_{kk}=n^{-1}\left\|\mathbf{h}_k\right\|^2$, where $\mathbf{h}_k$, $k=1...M$, is a Gaussian circularly symmetric vector with the correlation matrix $\mathbf{R}_k=E\{\mathbf{h}_k\mathbf{h}_k^H\}$. $\mathbf{H}^H\mathbf{H}/n$ and $\mathbf{\Lambda}$ are

asymptotically equivalent, i.e. $\mathbf{H}^H\mathbf{H}/n \xrightarrow{p} \mathbf{\Lambda}$ as $n \to \infty$, if $n^{-1}tr\{\mathbf{R}_k\} = 1$ and $n^{-2}tr[\mathbf{R}_k\mathbf{R}_m] \to 0$, $k,m = 1...M$, as $n \to \infty$.

Proof: Under the adopted normalization, $E\{\mathbf{H}^H\mathbf{H}/n\} = E\{\mathbf{\Lambda}\} = \mathbf{I}$, where $\mathbf{I}$ is the $M \times M$ identity matrix, since $\mathbf{h}_1...\mathbf{h}_M$ are mutually independent. From Chebyshev inequality [119], for any $\varepsilon > 0$

$$\Pr\left\{\left\|\mathbf{H}^H\mathbf{H}/n - \mathbf{\Lambda}\right\| \geq \varepsilon\right\} \leq \varepsilon^{-2} \cdot E\left\{\left\|\mathbf{H}^H\mathbf{H}/n - \mathbf{\Lambda}\right\|^2\right\}, \tag{11.35}$$

where

$$\begin{aligned} E\left\{\left\|\mathbf{H}^H\mathbf{H}/n - \mathbf{\Lambda}\right\|^2\right\} &= n^{-2}tr[E\{\mathbf{H}^H\mathbf{H}\mathbf{H}^H\mathbf{H}\}] - 2tr[E\{\mathbf{H}^H\mathbf{H}/n \cdot \mathbf{\Lambda}\}] + tr[E\{\mathbf{\Lambda}\mathbf{\Lambda}\}] = \\ &= n^{-2}tr[E\{\mathbf{H}\mathbf{H}^H\mathbf{H}\mathbf{H}^H\}] - tr[E\{\mathbf{\Lambda}\mathbf{\Lambda}\}] = \\ &= n^{-2}\sum_{m=1}^{M}\sum_{k=1}^{M} tr[E\{\mathbf{h}_m\mathbf{h}_m^H\mathbf{h}_k\mathbf{h}_k^H\}] - n^{-2}\sum_{m=1}^{M} tr[E\{\mathbf{h}_m\mathbf{h}_m^H\mathbf{h}_m\mathbf{h}_m^H\}] = \\ &= n^{-2}\sum_{m=1}^{M}\sum_{\substack{k=1 \\ k\neq m}}^{M} tr[E\{\mathbf{h}_m\mathbf{h}_m^H\mathbf{h}_k\mathbf{h}_k^H\}] = n^{-2}\sum_{m=1}^{M}\sum_{\substack{k=1 \\ k\neq m}}^{M} tr[\mathbf{R}_m\mathbf{R}_k] \end{aligned}, \tag{11.36}$$

where the second equality is since $tr[E\{\mathbf{H}^H\mathbf{H}/n \cdot \mathbf{\Lambda}\}] = tr[E\{\mathbf{\Lambda}\mathbf{\Lambda}\}]$. By substituting (11.36) in (11.35),

$$\Pr\left\{\left\|\mathbf{H}^H\mathbf{H}/n - \mathbf{\Lambda}\right\| \geq \varepsilon\right\} \leq \varepsilon^{-2} \cdot n^{-2}\sum_{m=1}^{M}\sum_{\substack{k=1 \\ k\neq m}}^{M} tr[\mathbf{R}_m\mathbf{R}_k] \tag{11.37}$$

Therefore, if $n^{-2}\sum_{m=1}^{M}\sum_{\substack{k=1 \\ k\neq m}}^{M} tr[\mathbf{R}_m\mathbf{R}_k] \to 0$, $k,m = 1...M$, as $n \to \infty$, then from (11.37) using the continuity property of the probability measure, for any $\varepsilon > 0$

$$\Pr\left\{\left\|\mathbf{H}^H\mathbf{H}/n - \mathbf{\Lambda}\right\| \geq \varepsilon\right\} \to 0, \text{ as } n \to \infty \textbf{ Q.E.D.} \tag{11.38}$$

Proof of Theorem 4.4:

From Lemma B4, $\mathbf{B}_t \xrightarrow{p} \mathbf{\Lambda}_t$ and $\mathbf{B}_r \xrightarrow{p} \mathbf{\Lambda}_r$, where $\mathbf{\Lambda}_t$ and $\mathbf{\Lambda}_r$ are diagonal matrices with elements $n_t^{-1}\left\|\mathbf{h}_{tk}\right\|^2$ and $n_r^{-1}\left\|\mathbf{h}_{rm}\right\|^2$, $k,m = 1...M$ respectively. Thus, from Slutsky Theorem [[23], Theorem 6a]

$$C \xrightarrow{d} \ln\left(\det[\mathbf{I} + \gamma_0\mathbf{\Lambda}_r\mathbf{A}\mathbf{\Lambda}_t\mathbf{A}^H]\right) = \sum_{k=1}^{M}\ln(1 + |a_k|^2\gamma_0\left\|\mathbf{h}_{tk}\right\|^2\left\|\mathbf{h}_{rk}\right\|^2/[n_t n_r]) \text{ as both } n_t, n_r \to \infty \textbf{ Q.E.D.} \tag{11.39}$$

APPENDIX C: MEASURE OF CORRELATION AND POWER IMBALANCE

Proof of Theorem 5.1:

Let f be a scalar function defined on $\mathbf{R} \in \Re_M$. f is called Schur-convex if for any $\mathbf{R}_1, \mathbf{R}_2 \in \Re_M$ such that $\mathbf{R}_1 \succ \mathbf{R}_2$, $f(\mathbf{R}_1) \geq f(\mathbf{R}_2)$ [10]. From [[68], Theorem 3.A.4], f is Schur-convex iff

$$(\lambda_i - \lambda_j)\left(\frac{\partial f(\mathbf{R})}{\partial \lambda_i} - \frac{\partial f(\mathbf{R})}{\partial \lambda_j}\right) \geq 0, \tag{12.1}$$

where λ_i, $i = 1...n$ are the eigenvalues of $\mathbf{R}$. Let $f(\mathbf{R}) = \|\mathbf{R}\|^2$, then

$$(\lambda_i - \lambda_j)\left(\frac{\partial \|\mathbf{R}\|^2}{\partial \lambda_i} - \frac{\partial \|\mathbf{R}\|^2}{\partial \lambda_j}\right) = (\lambda_i - \lambda_j)\left(\frac{\partial}{\partial \lambda_i}\sum_{k=1}^{n}\lambda_k^2 - \frac{\partial}{\partial \lambda_j}\sum_{k=1}^{n}\lambda_k^2\right) = 2(\lambda_i - \lambda_j)^2 \geq 0, \tag{12.2}$$

i.e. $\|\ \|^2$ is Schur-convex. Therefore, $\mathbf{R}_1 \succ \mathbf{R}_2$ iff $\|\mathbf{R}_1\|^2 \geq \|\mathbf{R}_1\|^2$ **Q.E.D.**

APPENDIX D: ASYMPTOTIC NORMALITY

Proof of Corollary 6.1:

Consider a lower bound on $Z_{n_t}(\delta)$:

$$Z_{n_t}(\delta)=\frac{\|\lambda\|_{2+\delta}}{\|\lambda\|_2}=\frac{\|\mu\|_{2+\delta}}{\|\mu\|_2}\geq\|\mu\|_2^{-1}, \tag{13.1}$$

where $\mu=\{\lambda_i^t/\lambda_1^t,\ i=1...n_t\}$. Assume that there is a finite set of k largest eigenvalues which is not dominated by the rest as $n_t\to\infty$, i.e. if $S_1=\sum_{i=1}^{k}(\mu_i)^2$ and $S_2=\sum_{i=k+1}^{n_t}(\mu_i)^2$, then

$$\lim_{n_t\to\infty}\frac{S_2}{S_1}=\lim_{n_t\to\infty}\sum_{i=k+1}^{n_t}\left(\lambda_i^t\right)^2\Big/\sum_{i=1}^{k}\left(\lambda_i^t\right)^2=c<\infty \tag{13.2}$$

From (13.1),

$$\lim_{n_t\to\infty}Z_{n_t}(\delta)\geq\lim_{n_t\to\infty}\left(S_1(1+S_2/S_1)^{-1/2}\geq(k\cdot[1+c])^{-1/2}>0,\right. \tag{13.3}$$

where the second inequality is since $S_1\leq k$ **Q.E.D.**

Proof of Theorem 6.2:

Since M_t is finite, from Szego Theorem [30], the following holds true

$$\lim_{n_t\to\infty}n_t^{-1}\|\lambda\|_p^p=(2\pi)^{-1}\int_0^{2\pi}f^p(x)dx=I_p<\infty,\ \text{for}\ \forall p>0, \tag{13.4}$$

where $f(x)=\sum_{k=-\infty}^{\infty}t_k\cdot e^{jkx}$ is a spectrum of $\mathbf{R}_t$. Note that since $\mathbf{R}_t$ is a correlation matrix, $f(x)$ is non-negative and real. By substituting (13.4) in (3.22), one obtains

$$\lim_{n_t\to\infty}Z_{n_t}(\delta)=\left(I_{2+\delta}\right)^{1/(2+\delta)}\left(I_2\right)^{-1/2}\cdot\lim_{n_t\to\infty}n_t^{\frac{-\delta}{2(2+\delta)}} \tag{13.5}$$

Note that both I_2 and $I_{2+\delta}$ are finite (see (13.4)) and positive, since $I_2=M_t>0$ due to Parseval's Theorem [119], and $\left(I_{2+\delta}\right)^{1/(2+\delta)}\geq\left(I_2\right)^{1/2}>0$ due to Lyapounov's Inequality [[28], Theorem p. 228] Using (13.5) for $\forall\delta>0$,

$$\lim_{n_t \to \infty} Z_{n_t}(\delta) = 0 \text{ , } \textbf{Q.E.D.} \tag{13.6}$$

Proof of (6.15):

Below we adopt the normalization $tr(\mathbf{R}_t) = n_t$.

Lower Bound: First, note that $\|\lambda\|_3^3 \geq n_t^{-1} \|\mathbf{R}_t\|^4$:

$$\|\lambda\|_3^3 = n_t^{-1} \sum_{i=1}^{n_t} \left((\lambda_i^t)^{1/2}\right)^2 \cdot \sum_{i=1}^{n_t} \left((\lambda_i^t)^{3/2}\right)^2 \geq n_t^{-1} \left(\sum_{i=1}^{n_t} (\lambda_i^t)^2\right)^2 = n_t^{-1} \|\mathbf{R}_t\|^4, \tag{13.7}$$

where the inequality is due to Cauchy-Schwarz inequality [119]. Thus,

$$\|\lambda\|_3 / \|\lambda\|_2 \geq \left(n_t^{-1} \|\mathbf{R}_t\|^4\right)^{1/3} \Big/ \left(\|\mathbf{R}_t\|^2\right)^{1/2} = \left(n_t^{-1} \|\mathbf{R}_t\|\right)^{1/3} \tag{13.8}$$

Upper Bound: First, note that $\|\lambda\|_3^3 \leq \|\mathbf{R}_t\|^3$:

$$\|\lambda\|_3^3 = \sum_{i=1}^{n_t} (\lambda_i^t)^2 \cdot \lambda_i^t \leq \left(\sum_{i=1}^{n_t} (\lambda_i^t)^4\right)^{1/2} \left(\sum_{i=1}^{n_t} (\lambda_i^t)^2\right)^{1/2} \leq \sum_{i=1}^{n_t} (\lambda_i^t)^2 \cdot \left(\sum_{i=1}^{n_t} (\lambda_i^t)^2\right)^{1/2} = \|\mathbf{R}_t\|^3, \tag{13.9}$$

where the first inequality is due to Cauchy-Schwarz inequality, and the second one follows from $\left(\sum_{i=1}^{n_t} (\lambda_i^t)^4\right)^{1/2} \leq \sum_{i=1}^{n_t} (\lambda_i^t)^2$. Thus,

$$\frac{\|\lambda\|_3}{\|\lambda\|_2} \leq \frac{\|\mathbf{R}_t\|}{\|\mathbf{R}_t\|} = 1 \textbf{ Q.E.D.} \tag{13.10}$$

APPENDIX E: BEST ANGULAR DENSITY

Proof of Theorem 7.1:

Part I: First show that under the conditions of the Theorem, $\mathbf{HH}^H / n_t \xrightarrow{p} \mathbf{R}_r$ as $n_t, n_r \to \infty$. From Chebyshev inequality [83], for any $\varepsilon > 0$

$$\Pr\left\{\left\|\mathbf{HH}^H / n_t - \mathbf{R}_r\right\| \geq \varepsilon\right\} \leq \varepsilon^{-2} \cdot E\left\{\left\|\mathbf{HH}^H / n_t - \mathbf{R}_r\right\|^2\right\}, \tag{14.1}$$

where

$$E\left\{\left\|\mathbf{HH}^H / n_t - \mathbf{R}_r\right\|^2\right\} = n_t^{-2} tr[E\{\mathbf{HH}^H \mathbf{HH}^H\}] - \left\|\mathbf{R}_r\right\|^2 \tag{14.2}$$

The equality is since $E\{\mathbf{HH}^H / n_t\} = \mathbf{R}_r$. Consider the trace in (14.2)

$$\begin{aligned} tr[E\{\mathbf{HH}^H \mathbf{HH}^H\}] &= tr\left[\sum_{k=1}^{n_t}\sum_{m=1}^{n_t} E\{\mathbf{h}_k \mathbf{h}_k^H \mathbf{h}_m \mathbf{h}_m^H\}\right] = \sum_{k=1}^{n_t}\sum_{m=1}^{n_t} E\{\mathbf{h}_m^H \mathbf{h}_k \mathbf{h}_k^H \mathbf{h}_m\} = \\ &= \sum_{k=1}^{n_t}\sum_{m=1}^{n_t}\sum_{n=1}^{n_r}\sum_{l=1}^{n_r} E\{H_{nm}^* H_{nk} H_{lk}^* H_{lm}\} \end{aligned} \tag{14.3}$$

From [88]

$$\begin{aligned} &\sum_{k=1}^{n_t}\sum_{m=1}^{n_t}\sum_{n=1}^{n_r}\sum_{l=1}^{n_r} E\{H_{nm}^* H_{nk} H_{lk}^* H_{lm}\} = \\ &= \sum_{k=1}^{n_t}\sum_{m=1}^{n_t}\sum_{n=1}^{n_r}\sum_{l=1}^{n_r}\left[\kappa_4(H_{nm} H_{nk} H_{lk} H_{lm}) + E\{H_{nm}^* H_{nk}\} E\{H_{lk}^* H_{lm}\} + E\{H_{nm}^* H_{lm}\} E\{H_{nk} H_{lk}^*\}\right] = \\ &= \mathbf{K}_4(\mathbf{H}) + \sum_{k=1}^{n_t}\sum_{m=1}^{n_t}\left|E\{\mathbf{h}_m^H \mathbf{h}_k\}\right|^2 + \sum_{n=1}^{n_r}\sum_{l=1}^{n_r}\left|E\{\mathbf{g}_n^H \mathbf{g}_l\}\right|^2 = \\ &= \mathbf{K}_4(\mathbf{H}) + \sum_{k=1}^{n_t}\sum_{m=1}^{n_t}\left|tr\{\mathbf{Q}_{km}\}\right|^2 + \sum_{n=1}^{n_r}\sum_{l=1}^{n_r}\left|tr\{\mathbf{G}_{ln}\}\right|^2 = \mathbf{K}_4(\mathbf{H}) + \left\|\mathbf{\Gamma}_r\right\|_B^2 + \left\|\mathbf{\Gamma}_t\right\|_B^2 \end{aligned} \tag{14.4}$$

By substituting (14.4) in (14.2), one obtains

$$E\left\{\left\|\mathbf{HH}^H / n_t - \mathbf{R}_r\right\|^2\right\} = n_t^{-2}\left[\mathbf{K}_4(\mathbf{H}) + \left\|\mathbf{\Gamma}_r\right\|_B^2 + \left\|\mathbf{\Gamma}_t\right\|_B^2\right] - \left\|\mathbf{R}_r\right\|^2 \tag{14.5}$$

Thus, if $\lim_{n_t, n_r \to \infty}[n_t^{-2}(\left\|\mathbf{\Gamma}_r\right\|_B^2 + \left\|\mathbf{\Gamma}_t\right\|_B^2) - \left\|\mathbf{R}_r\right\|^2] = 0$ and $\lim_{n_t, n_r \to \infty} n_t^{-2} K_4(\mathbf{H}) = 0$, then for any $\varepsilon > 0$

$$\Pr\left\{\left\|\mathbf{HH}^H / n_t - \mathbf{R}_r\right\| \geq \varepsilon\right\} \to 0 \text{ as both } n_t, n_r \to \infty, \tag{14.6}$$

i.e. $\mathbf{HH}^H / n_t \xrightarrow{p} \mathbf{R}_r$.

Part II: Since $\mathbf{HH}^H / n_t \xrightarrow{p} \mathbf{R}_r$ and C_1 in (7.1) is a continuous function of $\mathbf{HH}^H / n_t$, from Slutsky Theorem [[23], Theorem 6']

$$C_1 \xrightarrow{p} n_r^{-1} \ln(\det[\mathbf{I} + \gamma_0 \mathbf{R}_r]) \quad \textbf{Q.E.D.} \tag{14.7}$$

Proof of Theorem 7.2:

Statement (i): Since $f_\psi(x)$ is defined over $[-2\pi d; 2\pi d]$, then if $d < 1/2$, $f_\psi(x - 2\pi k)$, $k \in Z$ the function $\sum_{k=-\infty}^{\infty} f_\psi(x - 2\pi k)$ has intervals of zeros over $(-\pi, \pi]$. Therefore, condition (7.13) cannot be satisfied.

Statement (ii): If $d > 1/2$, $f_\psi(x - 2\pi k)$, $k \in Z$ generally overlap. Thereby, there are many possible $f_\psi(x)$ that satisfy condition (7.13).

Statement (iii): If $d = 1/2$, from the Nyquist Sampling Theorem [78] there is only one (uniform) $f_\psi(x)$ that satisfies (7.13), which is given by

$$f_\psi(x) = \begin{cases} (2\pi)^{-1}, -\pi < x \le \pi \\ 0, \quad otherwise \end{cases}, \tag{14.8}$$

From the geometry of the problem, it follows that

$$f_\psi(x) = \frac{1}{2\pi d} \cdot \frac{f_\theta(\cos^{-1}[x/(2\pi d)]) + f_\theta(-\cos^{-1}[x/(2\pi d)])}{\sqrt{1 - (x/(2\pi d)^2}} = \\ = \frac{1}{\pi d} \cdot \frac{f_\theta(\cos^{-1}[x/(2\pi d)])}{\sqrt{1 - (x/(2\pi d)^2}} \quad , \; x \in [-2\pi d; 2\pi d], \tag{14.9}$$

where it is assumed that $f_\theta(x) = f_\theta(-x)$ (a symmetric function). By substituting (14.8) in (14.9) for $d = 1/2$ one obtains

$$\frac{f_\theta(\cos^{-1}[x/\pi])}{\sqrt{1 - (x/\pi)^2}} = \frac{1}{4}, \; x \in (-\pi; \pi], \tag{14.10}$$

which holds true if

$$f_\theta(\theta) = 1/4 \left|\sin(\theta)\right|, \; \theta \in (-\pi; \pi] \tag{14.11}$$

This proves (7.14). Finally, using (7.11) for $d = 1/2$

$$R(t) = \int_{-\pi}^{\pi} f_{\psi}(x) e^{-j2x \cdot t} dx = (2\pi)^{-1} \int_{-\pi}^{\pi} e^{-j2x \cdot t} dx = \frac{\sin(2\pi t)}{2\pi t} \tag{14.12}$$

This proves (7.15). **Q.E.D.**

Proof of Corollary 7.2:

From the Final Value Theorem [78] and using (14.13), (14.14)

$$\lim_{t \to \infty} R(t) = \lim_{x \to 0} j2\pi x f_{\psi}(x) = \lim_{x \to 0} j \frac{2x}{d} \cdot \frac{f_{\theta}(\cos^{-1}[x/(2\pi d)])}{\sqrt{1 - [x/(2\pi d)]^2}} = \lim_{x \to 0} j2x f_{\theta}(\pi/2)/d \tag{14.15}$$

Thus, if $\lim_{x \to 0} x f_{\theta}(\pi/2) = 0$, which imply $f_{\theta}(\pi/2) < \infty$, then $\lim_{t \to \infty} R(t) = 0$. Therefore, as $d \to \infty$

$$R_k = R(d \cdot k) = \begin{cases} 1, & k = 0 \\ 0, & k \neq 0 \end{cases}, \tag{14.16}$$

with corresponding spectrum

$$\lambda(x) = 1, \; x \in (-\pi; \pi], \tag{14.17}$$

i.e. $\mathbf{R}$ is always uncorrelated results in $C_{\mathrm{I}} \xrightarrow{p} C_{\max}$ **Q.E.D.**

Proof of (7.19):

Based on Szego Theorem [30]

$$\lim_{n \to \infty} n^{-1} \|\mathbf{R}\|^2 = (2\pi)^{-1} \int_{-\pi}^{\pi} \lambda^2(x) dx = (2\pi)^{-1} \int_{-\pi}^{\pi} \left(\sum_{k=-\infty}^{\infty} f_{\psi}(x - 2\pi k) \right)^2 dx, \tag{14.18}$$

where $\lambda(x) = \lim_{n_r \to \infty} \sum_{k=-n_r+1}^{n_r-1} R_k e^{jkx}$, $x \in (-\pi; \pi]$ is the spectrum of $\mathbf{R}$.

1. For $0 < d \leq 1/2$:

$$(2\pi)^{-1} \int_{-\pi}^{\pi} \left(\sum_{k=-\infty}^{\infty} f_{\psi}(x - 2\pi k) \right)^2 dx = 2\pi \int_{-2\pi d}^{2\pi d} f_{\psi}^2(x) dx = 2\pi \int_{-2\pi d}^{2\pi d} \frac{dx}{(4\pi d)^2} = 1/(2d) \tag{14.19}$$

2. For $1/2 < d \le 1$

$$(2\pi)^{-1}\int_{-\pi}^{\pi}\left(\sum_{k=-\infty}^{\infty} f_{\psi}(x-2\pi k)\right)^2 dx =$$

$$= 2\pi\left\{\int_{-\pi+\Delta}^{\pi-\Delta} f_{\psi}^2(x)dx + \int_{\pi+\Delta}^{\pi}[f_{\psi}(x)+f_{\psi}(x+2\pi)]^2 dx + \int_{\pi-\Delta}^{\pi}[f_{\psi}(x)+f_{\psi}(x-2\pi)]^2 dx\right\} = , \qquad (14.20)$$

$$= 2\pi\left\{\int_{-\pi+\Delta}^{\pi-\Delta}\frac{dx}{(4\pi d)^2} + \int_{\pi-\Delta}^{\pi}\frac{dx}{2(\pi d)^2}\right\} = \frac{3d-1}{2d^2}$$

where $\Delta = 2\pi d - \pi$ is the interval where $f_{\psi}(x)$ and $f_{\psi}(x-2\pi)$ overlap. Thus, for large $n >> 1/(2d)$, and using (14.19) and (14.20), (7.19) follows. **Q.E.D.**

BIBLIOGRAPHY

[1] F. Adachi, M. T. Freeney, A. G. Williamson, J. D. Parsons, "Crosscorrelation between the envelopes of 900MHz signals received at a mobile radio base station site", *IEE Proceedings*, vol. 133, no. 6, pp. 506-512, Oct. 1986.

[2] S. M. Alamouti, "A simple transmit diversity technique for wireless communications," *IEEE Journal on Selected Areas in Communications*, vol.16, no.8, pp.1451-1458, Oct 1998.

[3] N. Al-Dhahir, G. B. Giannakis, B. Hochwald, B. L. Hughes, T. L. Marzetta, "Guest editorial," *IEEE Transactions on Signal Processing,* (see also *IEEE Trans. on Acoustics, Speech, and Signal Processing*), vol.50, no.10, pp. 2381-2384, Oct 2002.

[4] P. Almers, F. Tufvesson, A. F. Molisch, "Keyhole effect in MIMO wireless channels: measurements and theory," *IEEE Transactions on Wireless Communications*, vol.5, no.12, pp.3596-3604, December 2006.

[5] P. Almers, F. Tufvesson, A. F. Molisch, "Measurement of keyhole effect in a wireless multiple-input multiple-output (MIMO) channel," *IEEE Communications Letters*, vol.7, no.8, pp. 373-375, Aug. 2003.

[6] V. Bentkus, *Private Communication*, 2007.

[7] V. Bentkus, "A Lyapunov-Type Bound in $\mathbf{R}^d$", *Theory Probab. Appl.*, vol. 49, no. 2, pp. 311-323, 2005.

[8] D. S. Bernstein, *Matrix Mathematics: Theory, Facts, and Formulas with Applications to Linear Systems Theory*, Princeton University Press, 2005.

[9] E. Biglieri J. Proakis, S. Shamai, "Fading channels: information-theoretic and communications aspects," *IEEE Transactions on Information Theory*, vol.44, no.6, pp.2619-2692, Oct 1998.

[10] H. Boche, E. A. Jorswieck, "On the ergodic capacity as a function of the correlation properties in systems with multiple transmit antennas without CSI at the transmitter," *IEEE Transactions on Communications*, vol.52, no.10, pp. 1654-1657, Oct. 2004.

[11] R. M. Buehrer, "The impact of angular energy distribution on spatial correlation", *in Proc. VTC 2002-Fall, IEEE 56th Vehicular Technology Conference*, vol. 2, pp. 1173-1177, 2002.

[12] C. Chen-Nee, D. N. C. Tse, J. M. Kahn, R. A. Valenzuela, "Capacity scaling in MIMO wireless systems under correlated fading ," *IEEE Transactions on Information Theory*, vol.48, no.3, pp.637-650, Mar 2002.

[13] M. Chiani, M. Z. Win, A. Zanella, "On the capacity of spatially correlated MIMO Rayleigh-fading channels," *IEEE Transactions on Information Theory,* , vol.49, no.10, pp. 2363-2371, Oct. 2003.

[14] D. Chizhik, G. J. Foschini, M. J. Gans, R. A. Valenzuela, "Keyholes, correlations, and capacities of multielement transmit and receive antennas," *IEEE Transactions on Wireless Communications*, vol.1, no.2, pp.361-368, Apr 2002.

[15] D. Chizhik, G. J. Foschini, R. A. Valenzuela, "Capacities of multi-element transmit and receive antennas: Correlations and keyholes," *Electronics Letters*, vol.36, no.13, pp.1099-1100, 22 Jun 2000.

[16] D. Chizhik, J. Ling, P. W. Wolniansky, R. A. Valenzuela, N. Costa, K. Huber, "Multiple-input-multiple-output measurements and modeling in Manhattan," *IEEE Journal on Selected Areas in Communications*, vol.21, no.3, pp. 321-331, Apr 2003.

[17] T. S. Chu, L. J. Greenstein, "A semi-empirical representation of antenna diversity gain at cellular and PCS base stations," *IEEE Transactions on Communications*, vol.45, no.6, pp.644-646, Jun 1997.

[18] T. M. Cover, J. A. Thomas, *Elements of Information Theory*, John-Wiley & Sons, Inc., 1991.

[19] H. Cramer, *Mathematical Methods of Statistics*, Princeton University Press, Eleventh Printing, 1966.

[20] X. W. Cui, Z. M. Feng, "Lower capacity bound for MIMO correlated fading channels with keyhole", *IEEE Communications Letters*, vol. 8, no. 8, pp. 500-5002, Aug. 2004.

[21] W. T. Eadie, D. Drijard, F. E. James, M. Roos, B. Sadoulet, *Statistical Methods in Experimental Physics*, North-Holland, 2nd Reprint, 1982.

[22] V. Erceg, *et al*, "TGn channel models", *Proposal for IEEE P802.11 Wireless LANs*, Doc. IEEE 802.11-03/940r4, May 2004.

[23] T. S. Ferguson, *A Course in Large Sample Theory*, Chapman & Hall/CRC, 1st Ed. Reprint, 2002.

[24] M. Fisz, *Probability Theory and Mathematical Statistics*, 3d Edition, John Willey & Sons, Inc., New York, London, 1963.

[25] G. J. Foschini, M. J. Gans, "On limits of wireless communications in a fading environment when using multiple antennas", *Wireless Personal Commun.*, vol. 6, no. 3, pp. 311-335, March 1998.

[26] R. G. Gallagher, *Information Theory and Reliable Communication*, New York: Wiley, 1968.

[27] D. Gesbert, H. Bolcskei, D. A. Gore, A. J. Paulraj, "Outdoor MIMO wireless channels: models and performance prediction," *IEEE Transactions on Communications*, vol.50, no.12, pp. 1926-1934, Dec 2002.

[28] B. V. Gnedenko, *The Theory of Probability*, Nauka, Moscow, 1988.

[29] A. Goldsmith, S. A.; Jafar, N. Jindal, S. Vishwanath, "Capacity limits of MIMO channels," *IEEE Journal on Selected Areas in Communications*, vol.21, no.5, pp. 684-702, June 2003.

[30] R. M. Gray, , "On the asymptotic eigenvalue distribution of Toeplitz matrices", *IEEE Trans. on Information Theory*, vol. IT-18, no. 6, pp. 725-730, Nov. 1972.

[31] B. M. Hochwald., G. Caire, B. Hassibi, T. L. Marzetta, "The academic and industrial embrace of space-time methods," *IEEE Journal on Information Theory*, vol.49, no.10, pp. 2329-2331, Oct. 2003.

[32] B. M. Hochwald, T. L. Marzetta, V. Tarokh, "Multiple-antenna channel hardening and its implications for rate feedback and scheduling," *IEEE Transactions on Information Theory*, vol.50, no.9, pp. 1893-1909, Sept. 2004.

[33] M. T. Ivrlac, J.A. Nossek, "Diversity and correlation in Rayleigh fading MIMO channels," *Vehicular Technology Conference, 2005. VTC 2005-Spring. 2005 IEEE 61st*, vol.1, pp. 151-155 Vol. 1, 30 May-1 June 2005.

[34] W. C. Jakes, *Microwave Mobile Communications*, Willey, NY, 1974.

[35] M. Kang, M. S. Alouini, "Capacity of MIMO Rician channels," *IEEE Transactions on Wireless Communications*, vol.5, no.1, pp. 112-122, Jan. 2006.

[36] G. K. Kanji, *100 Statistical Tests*, London, Newbury Park, CA, Sage Publications, 1993.

[37] J. P. Kermoal, L. Schumacher, K. I. Pedersen, P. E. Mogensen, F. Frederiksen, "A stochastic MIMO radio channel model with experimental validation," *IEEE Journal on Selected Areas in Communications*, vol.20, no.6, pp. 1211-1226, Aug 2002.

[38] S. Khatalin, J. P. Fonseka, "Capacity of correlated Nakagami-m fading channels with diversity combining techniques," *IEEE Transactions on Vehicular Technology*, vol.55, no.1, pp. 142-150, Jan. 2006.

[39] J. N. Laneman, D. N. C. Tse, G. W. Wornell, "Cooperative diversity in wireless networks: Efficient protocols and outage behavior," *IEEE Transactions on Information Theory*, vol.50, no.12, pp. 3062-3080, Dec. 2004.

[40] A. Lapidoth, S. M. Moser, "Capacity bounds via duality with applications to multiple-antenna systems on flat-fading channels," *IEEE Transactions on Information Theory,* vol.49, no.10, pp. 2426-2467, Oct. 2003

[41] G. Lebrun, M. Faulkner, M. Shafi, P. J. Smith, "MIMO Ricean channel capacity: an asymptotic analysis," *IEEE Transactions on Wireless Communications*, vol.5, no.6, pp. 1343-1350, June 2006.

[42] G. Levin, S. Loyka, "What is the best angular density of multipath in MIMO channels?", *submitted to IEEE International Symposium on Information Theory (ISIT2008).*

[43] G. Levin, S. Loyka, "Correlated keyhole MIMO channels: SNR and outage capacity distributions," *IEEE Canadian Conference on Electrical and Computer Engineering, 2006. CCECE '06*, pp.908-911, May 2006.

[44] G. Levin, S. Loyka, "Capacity distribution of a correlated keyhole channel", *in Proc. CWIT'05, Canadian Workshop on Information Theory*, Montréal, QC, June 2005.

[45] G. Levin, S. Loyka, "Comments on asymptotic eigenvalue distributions and capacity for MIMO channels under correlated fading", *IEEE Transactions on Wireless Communications*, vol.7, no.2, pp.475-479, February 2008.

[46] G. Levin, S. Loyka, "From multi-keyholes to measure of correlation and power imbalance in MIMO channels", *submitted to IEEE Trans. on Inform. Theory*, 2007.

[47] G. Levin, S. Loyka, "On the outage capacity distribution of correlated keyhole MIMO channels", *IEEE Trans. on Inform. Theory*, vol.54, no.7, pp.3232-3245, July 2008.

[48] G. Levin, S. Loyka, "Multi-keyhole MIMO channels: Asymptotic analysis of outage capacity," *2006 IEEE International Symposium on Information Theory*, pp.1305-1309, July 2006.

[49] G. Levin, S. Loyka, "Multi-keyholes and measure of correlation in MIMO channels," *2006 23rd Biennial Symposium on Communications*, pp. 22-25, May 29 - June 1, 2006.

[50] G. Levin, S. Loyka, "On asymptotic outage capacity distribution of correlated MIMO channels," *ISSSE '07. International Symposium on Signals, Systems and Electronics, 2007.*, pp.283-286, July 30 2007-Aug. 2 2007.

[51] G. Levin, S. Loyka, "On the outage capacity distribution of correlated keyhole MIMO channels," *IEEE Wireless Communications and Networking Conference, WCNC 2006*, vol.2, pp.745-750, 3-6 April 2006.

[52] G. Levin, S. Loyka, "Statistical analysis of a measured MIMO channel," *IEEE Canadian Conference on Electrical and Computer Engineering,* vol.2, pp. 875-878 Vol.2, 2-5 May 2004.

[53] G. Levin, S. Loyka, "Statistical approach to MIMO capacity analysis in a fading channel," *2004 IEEE 60th Vehicular Technology Conference, VTC2004-Fall.*, vol.3, pp. 1548-1552 Vol. 3, 26-29 Sept. 2004.

[54] A. M. Liapounoff, "A new form of the theorem on probability limit", *Proceedings of the Russian Imperial Academy of Sciences*, series VIII, vol. 12, no. 5, pp. 1-24, 1901 (also appears in A. M. Liapounoff, *Collected Works, the USSR Academy of Sciences*, vol. 1, pp. 157-176, Moscow, 1954).

[55] S. Loyka, "Dimensionality loss in MIMO communication systems, *The 3rd IASTED International Conference on Wireless and Optical Communications (WOC 2003)*, pp. 138-143, Banff, Alberta, Canada, July 14-16, 2003.

[56] S. Loyka, "Information Theory and Electromagnetism: Are they related?", *The Joint COST 273/284 Workshop on Antennas and Related System Aspects in Wireless Communications*, Chalmers University of Technology (Gothenburg, Sweden, June 2004); University of Missouri (Rolla, USA, 03.2004); Swiss Federal Institute of Technology (Lausanne and Zurich, 02.2003).

[57] S. Loyka, F. Gagnon, "V-BLAST without optimal ordering: Analytical performance evaluation for Rayleigh-fading channels", *IEEE Transactions on Communications*, vol. 54, no. 6, pp. 1109-1120, June 2006.

[58] S. Loyka, G. Levin, "Diversity-multiplexing tradeoff via asymptotic analysis of large MIMO systems", *in Proc. 2007 IEEE International Symposium on Information Theory (ISIT2007)*, Nice, France, June 2007.

[59] S. Loyka, G. Levin, "On finite-SNR diversity-multiplexing tradeoff", *in Proc. 2007 IEEE Global Communications Conference (Globecom2007)*, Washington, DC, Nov. 2007.

[60] S. Loyka, G. Levin, "On physically-based normalization of MIMO channel matrices", *submitted to IEEE Trans. on Inform. Theory*, 2006.

[61] S. Loyka, A. Kouki, "New compound upper bound on MIMO channel capacity," *IEEE Communications Letters*, vol.6, no.3, pp.96-98, Mar 2002.

[62] S. Loyka, A. Kouki, "On MIMO channel capacity, correlations, and keyholes: analysis of degenerate channels," *IEEE Transactions on Communications,* , vol.50, no.12, pp. 1886-1888, Dec 2002

[63] S. Loyka, J. Mosig, "Channel capacity of N-antenna BLAST architecture," *Electronics Letters*, vol.36, no.7, pp.660-661, 30 Mar 2000.

[64] S. Loyka, G. Tsoulos, "Estimating MIMO system performance using the correlation matrix approach," *IEEE Communications Letters*, vol.6, no.1, pp.19-21, Jan 2002.

[65] S. L. Loyka, "Channel capacity of MIMO architecture using the exponential correlation matrix," *IEEE Communications Letters*, vol.5, no.9, pp.369-371, Sep 2001.

[66] A. Lozano, A. M. Tulino, S. Verdu, "High-SNR power offset in multiantenna communication," *IEEE Transactions on Information Theory*, vol.51, no.12, pp. 4134-4151, Dec. 2005.

[67] A. Lozano, A. M. Tulino, S. Verdu, "Multiple-antenna capacity in the low-power regime," *IEEE Transactions on Information Theory*, vol.49, no.10, pp. 2527-2544, Oct. 2003.

[68] A. W. Marshall, I. Olkin, *Inequalities: Theory of Majorization and Its Applications*, Mathematics in Science and Engineering, London, U.K.: Academic, vol. 143, 1979.

[69] C. Martin, B. Ottersten, "Asymptotic eigenvalue distributions and capacity for MIMO channels under correlated fading," *IEEE Transactions on Wireless Communications*, vol.3, no.4, pp. 1350-1359, July 2004.

[70] A. M. Mathai, S. B. Provost, *Quadratic Forms in Random Variables*, Marcel Dekker, Inc., New York, Basel, Hong Kong, 1992.

[71] M. R. McKay, I. B. Collings, "General capacity bounds for spatially correlated Rician MIMO channels," *IEEE Transactions on Information Theory*, vol.51, no.9, pp. 3121-3145, Sept. 2005.

[72] A. F. Molisch, M. Steinbauer, M. Toeltsch, E. Bonek, R. S. Thoma, "Capacity of MIMO systems based on measured wireless channels," *IEEE Journal on Selected Areas in Communications*, vol.20, no.3, pp.561-569, Apr 2002.

[73] A. L. Moustakas, H. U. Baranger, L. Balents, A. M. Sengupta, S. H. Simon, "Communication through a diffusive medium: coherence and capacity", *Science*, vol. 287, pp. 287-290, Jan. 2000.

[74] A. L. Moustakas, S. H.Simon, "On the outage capacity of correlated multiple-path MIMO channels," *IEEE Transactions on Information Theory*, vol.53, no.11, pp.3887-3903, Nov. 2007.

[75] A. L. Moustakas, S. H. Simon, A.M. Sengupta, "MIMO capacity through correlated channels in the presence of correlated interferers and noise: a (not so) large N analysis," *IEEE Transactions on Information Theory,* vol.49, no.10, pp. 2545-2561, Oct. 2003.

[76] R. Narasimhan, "Finite-SNR diversity–multiplexing tradeoff for correlated Rayleigh and Rician MIMO channels," *IEEE Transactions on Information Theory*, vol.52, no. 9, pp. 3965-3979, 2006.

[77] C. Oestges, A. J. Paulraj, "Beneficial impact of channel correlations on MIMO capacity," *Electronics Letters*, vol.40, no.10, pp. 606-608, 13 May 2004.

[78] A. V. Oppenheim, A. S. Willsky, *Signals and Systems*, Prentice-Hall Inc., New Jersey, 1983.

[79] H. Ozcelik, M. Herdin, H. Hofstetter, E. Bonek, "A comparison of measured 8x8 MIMO systems with a popular stochastic channel model at 5.2 GHz," *ICT 2003. 10th International Conference on Telecommunications*, vol.2, pp. 1542-1546 vol.2, 23 Feb.-1 March 2003.

[80] H. Ozcelik, M. Herdin, H. Hofstetter, E. Bonek,, "Capacity of different MIMO systems based on indoor measurements at 5.2 GHz," *2003. 5th European Personal Mobile Communications Conference, (Conf. Publ. No. 492)*, pp. 463-466, 22-25 April 2003.

[81] H. Ozcelik, M. Herdin, W. Weichselberger, J. Wallace, E. Bonek, "Deficiencies of 'Kronecker' MIMO radio channel model," *Electronics Letters*, vol.39, no.16, pp. 1209-1210, 7 Aug. 2003.

[82] H. Ozcelik, C. Oestges, "Some remarkable properties of diagonally correlated MIMO channels," *IEEE Transactions on Vehicular Technology*, vol.54, no.6, pp. 2143-2145, Nov. 2005.

[83] A. Papoulis, S. U. Pillai, *Probability, Random Variables and Stochastic Processes*, 4th Ed., McGraw-Hill, 2002.

[84] A. Paulraj, R. Nabar, D. Gore, *Introduction to Space-Time Wireless Communications*, Cambridge University Press, 2003.

[85] V. V. Petrov, *Limit Theorems of Probability Theory: Sequences of Independent Random Variables*, Oxford University Press, NY, 1996.

[86] J. N. Pierce, S. Stein, "Multiple diversity with non-independent fading", *Proc. of the IRE*, vol. 48, pp. 89-104, Jan. 1960.

[87] T. S. Pollock, T. D. Abhayapala, R. A. Kennedy, "Antenna saturation effects on dense array MIMO capacity", *in Proc. ICASSP 2003, IEEE International Conference on Acoustics, Speech, and Signal Processing*, vol.4, no. 6-10, pp. IV-361-4, 2003.

[88] B. Porat, *Digital Processing of Random Signals: Theory and Methods*, Prentice-Hall Inc., New-Jersey, 1994.

[89] D. Porrat, P. Kyritsi, D. C. Cox, "MIMO capacity in hallways and adjacent rooms," *IEEE Global Telecommunications Conference, 2002. GLOBECOM '02*, vol.2, pp. 1930-1934 vol.2, 17-21 Nov. 2002.

[90] V. Raghavan, A. M. Sayeed, "Weak convergence and rate of convergence of MIMO capacity random variable," *IEEE Transactions on Information Theory*, vol.52, no.8, pp.3799-3809, Aug. 2006.

[91] S. Sanayei, A. Hedayat, A. Nosratinia, "Space time codes in keyhole channels: analysis and design," *IEEE Transactions on Wireless Communications*, vol.6, no.6, pp.2006-2011, June 2007.

[92] S. Sanayei, A. Nosratinia, "Antenna selection in keyhole channels," *IEEE Transactions on Communications*, vol.55, no.3, pp.404-408, March 2007.

[93] A. M. Sayeed, "Deconstructing multiantenna fading channels," *IEEE Transactions on Signal Processing, [see also IEEE Transactions on Acoustics, Speech and Signal Processing]*, vol.50, no.10, pp. 2563-2579, Oct 2002.

[94] A. M. Sayeed, V. Raghavan, "Maximizing MIMO capacity in sparse multipath with reconfigurable antenna arrays," *IEEE Journal of Selected Topics in Signal Processing*, vol.1, no.1, pp.156-166, June 2007.

[95] M. Shafi, D. Gesbert, D. Shiu, P. J. Smith, W. H. Tranter, "Guest editorial: MIMO systems and applications I," *IEEE Journal on Selected Areas in Communications,* vol.21, no.3, pp. 277-280, Apr 2003.

[96] M. Shafi, D. Gesbert, D. Shiu, P. J. Smith, W. H. Tranter, "Guest editorial MIMO systems and applications. II," *IEEE Journal on Selected Areas in Communications*, vol.21, no.5, pp. 681-683, June 2003.

[97] H. Shin, J. H. Lee, "Capacity of multiple-antenna fading channels: spatial fading correlation, double scattering, and keyhole," *IEEE Transactions on Information Theory*, vol.49, no.10, pp. 2636-2647, Oct. 2003.

[98] H. Shin, J. H. Lee, "Performance analysis of space-time block codes over keyhole Nakagami-m fading channels," *IEEE Transactions on Vehicular Technology*, vol.53, no.2, pp. 351-362, March 2004.

[99] H. Shin, M. Z. Win, J. H. Lee, M. Chiani, "On the capacity of doubly correlated MIMO channels," *IEEE Transactions on Wireless Communications*, vol.5, no.8, pp. 2253-2265, Aug. 2006.

[100] D. Shiu, G. J. Foschini, M. J. Gans, J. M. Kahn, "Fading correlation and its effect on the capacity of multielement antenna systems," *IEEE Transactions on Communications*, vol.48, no.3, pp.502-513, Mar 2000.

[101] P. J. Smith, M. Shafi, "An approximate capacity distribution for MIMO systems," *IEEE Transactions on Communications*, vol.52, no.6, pp. 887-890, June 2004.

[102] P. J. Smith, S. Roy, M. Shafi, "Capacity of MIMO systems with semicorrelated flat fading," *IEEE Transactions on Information Theory*, vol.49, no.10, pp. 2781-2788, Oct. 2003.

[103] I. E. Telatar, "Capacity of multi-antenna Gaussian channels", *AT&T Bell Labs, Internal Tech. Memo*, pp. 1-28, June 1995, (see also *European Trans. Telecom.*, v.10, no. 6, pp. 585-595, Dec. 1999).

[104] The Bluetooth Special Interest Group (SIG), http://www.bluetooth.com/Bluetooth/SIG/, retrieved on 25 Jan. 2008.

[105] N.H. Tran, H. H. Nguyen, T. Le-Ngoc, "Performance bounds of orthogonal space-time block codes over keyhole Nakagami-m channels," *IEEE Signal Processing Letters*, vol.14, no.9, pp.605-608, Sept. 2007

[106] D. N. C. Tse, P. Viswanath. *Fundamentals of Wireless Communication*, Cambridge: Cambridge University Press, 2005.

[107] D. N. C. Tse, P. Viswanath, L. Zheng, "Diversity-multiplexing tradeoff in multiple-access channels," *IEEE Transactions on Information Theory*, vol.50, no.9, pp. 1859-1874, Sept. 2004.

[108] A. M. Tulino, S. Verdu, "Random Matrix Theory and wireless Communications", *Foundations and Trends in Commun. and Inform. Theory*, vol. 1, pp. 1-182, 2004.

[109] A. M. Tulino, A. Lozano, S. Verdu, "Impact of antenna correlation on the capacity of multiantenna channels," *IEEE Transactions on Information Theory*, vol.51, no.7, pp. 2491-2509, July 2005.

[110] H. L. Van-Trees, *Optimum Array Processing: Part IV of Detection, Estimation, and Modulation Theory*, John Wiley & Sons, Inc., NY, 2002.

[111] W. Weichselberger, M. Herdin, H. Ozcelik, E. Bonek, E., "A stochastic MIMO channel model with joint correlation of both link ends," *IEEE Transactions on Wireless Communications*, vol.5, no.1, pp. 90-100, Jan. 2006.

[112] WiFi Alliance, http://www.wi-fi.org/, retrieved on 25 Jan. 2008.

[113] WiMax Forum, http://www.wimaxforum.org/home/, retrieved on 25 Jan. 2008.

[114] WINNER-Wireless World Initiative New Radio, https://www.ist-winner.org/, retrieved on 25 Jan. 2008.

[115] H. Xu, M. J. Gans, N. Amitay, R. A. Valenzuela, "Experimental verification of MTMR system capacity in controlled propagation environment," *Electronics Letters*, vol.37, no.15, pp.936-937, 19 Jul 2001.

[116] L. Zheng, D. N. C. Tse, "Communication on the Grassmann manifold: a geometric approach to the noncoherent multiple-antenna channel," *IEEE Transactions on Information Theory*, vol.48, no.2, pp.359-383, Feb 2002.

[117] L. Zheng, D. N. C. Tse, "Diversity and multiplexing: a fundamental tradeoff in multiple-antenna channels," *IEEE Transactions on Information Theory*, vol.49, no.5, pp. 1073-1096, May 2003.

[118] V. M. Zolotarev, "On Real Improvements of Central Limit Theorems", *Proceedings of the Mathematical Institute, the USSR Academy of Sciences*, vol. 182, pp. 24-47, Moscow, 1988.

[119] D. Zwillinger, *CRC Standard Mathematical Tables and Formulae*, 31st Edition, CRC Press LLC, 1996.